



SHIELDING REQUIREMENTS FOR PARTICLE BED PROPULSION SYSTEMS

S.J. Gruneisen

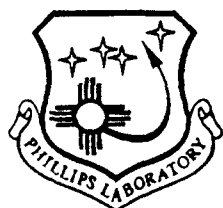
August 1991

Final Report

DTIC
ELECTE
SEP 19 1991
S B D

APPROVED FOR PUBLIC RELEASE; DISTRIBUTION UNLIMITED.

91-10768



PHILLIPS LABORATORY
Propulsion Directorate
AIR FORCE SYSTEMS COMMAND
EDWARDS AIR FORCE BASE CA 93523-5000

9 1 2 16 089

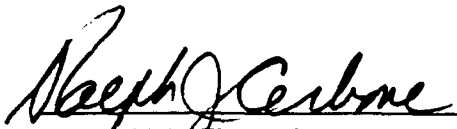
NOTICE

When U. S. Government drawings, specifications, or other data are used for any purpose other than a definitely related Government procurement operation, the fact that the Government may have formulated, furnished, or in any way supplied the said drawings, specifications, or other data, is not to be regarded by implication or otherwise, or in any way licensing the holder or any other person or corporation, or conveying any rights or permission to manufacture, use or sell any patented invention that may be related thereto.

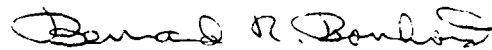
FOREWORD

This Special Report was submitted on completion of this phase of JON: 305800R7 by the OL-AC PL/RAS Branch, at the Phillips Laboratory (AFSC), Edwards AFB CA. PL Project Manager was David R. Perkins

This report has been reviewed and is approved for release and distribution in accordance with the distribution statement on the cover and on the DD Form 298.

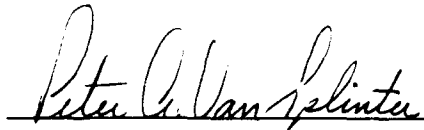


RALPH J. CERBONE.
Visiting Senior Scientist

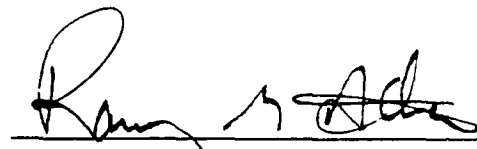


BERNARD R. BORNHORST
Chief, Space Propulsion Branch

FOR THE COMMANDER



PETER A. VAN SPLINTER
Director
Applications Engineering Division



RANNEY ADAMS
Public Affairs Officer

REPORT DOCUMENTATION PAGE			Form Approved OMB No. 0704-0188	
Public reporting burden for this collection of information is estimated to average 1 hour per response, including the time for reviewing instructions, searching existing data sources, gathering and maintaining the data needed, and completing and reviewing the collection of information. Send comments regarding this burden estimate or any other aspect of this collection of information, including suggestions for reducing this burden, to Washington Headquarters Services, Directorate for Information Operations and Reports, 1215 Jefferson Davis Highway, Suite 1204, Arlington, VA 22202-4302, and to the Office of Management and Budget, Paperwork Reduction Project (0704-0188), Washington, DC 20503.				
1. AGENCY USE ONLY (Leave blank)	2. REPORT DATE Jun 91	3. REPORT TYPE AND DATES COVERED Special May 90 to Mar 91		
4. TITLE AND SUBTITLE SHIELDING REQUIREMENTS FOR PARTICLE BED PROPULSION SYSTEMS		5. FUNDING NUMBERS PE - 62302F PR - 3058 TA - 00R7		
6. AUTHOR(S) S.J. Gruneisen				
7. PERFORMING ORGANIZATION NAME(S) AND ADDRESS(ES) Phillips Laboratory (AFSC) ** OL-AC PL/RAS Edwards AFB CA 93523-5000		8. PERFORMING ORGANIZATION REPORT NUMBER PL-TR-91-3018		
9. SPONSORING/MONITORING AGENCY NAME(S) AND ADDRESS(ES)		10. SPONSORING/MONITORING AGENCY REPORT NUMBER		
11. SUPPLEMENTARY NOTES ** OLAC Phillips Laboratory formerly known as the Astronautics Laboratory COSATI Codes: 18-06, 21-06				
12a. DISTRIBUTION/AVAILABILITY STATEMENT Approved for Public Release. Distribution is Unlimited.		12b. DISTRIBUTION CODE		
13. ABSTRACT (Maximum 200 words) Nuclear Thermal Propulsion systems present unique challenges in reliability and safety. Due to the radiation incident upon all components of the propulsion system, shielding must be used to keep nuclear heating in the materials within limits; in addition, electronic control systems must be protected. This report analyzes the nuclear heating due to the radiation and the shielding required to meet the established criteria while also minimizing the shield mass. Heating rates were determined in a 2000 MWt Particle Bed Reactor (PBR) system for all materials in the interstage region, between the reactor vessel and the propellant tank, with special emphasis on meeting the silicon dose criteria. Using a Lithium Hydride/Tungsten shield, the optimum shield design was found to be: 50 cm LiH/2 cm W on the axial reflector in the reactor vessel and 50 cm LiH/2 cm W in a "collar" extension of the inside shield outside of the pressure vessel. Within these parameters, the radiation doses in all of the components in the interstage and lower tank regions would be within acceptable limits for mission requirements.				
14. SUBJECT TERMS Particle Bed Reactor; Particle Bed Reactor propulsion system.			15. NUMBER OF PAGES 86	
			16. PRICE CODE	
17. SECURITY CLASSIFICATION OF REPORT UNCLASSIFIED	18. SECURITY CLASSIFICATION OF THIS PAGE UNCLASSIFIED	19. SECURITY CLASSIFICATION OF ABSTRACT UNCLASSIFIED	20. LIMITATION OF ABSTRACT SAR	

Table of Contents

Introduction.....	1
Methodology.....	5
Shield Design, Modeling and Optimization.....	9
Results.....	14
Final Design.....	23
Summary and Conclusions.....	23
References.....	27
Appendix (Graphs).....	29



Accession For	
NTIS GRA&I	<input checked="" type="checkbox"/>
DTIC TAB	<input type="checkbox"/>
Unannounced	<input type="checkbox"/>
Justification	
By	
Distribution/	
Availability Codes	
Dist	Avail and/or Special
A-1	

List of Figures

Figure #1: PBR Fuel Element.....	2
Figure #2: PBR Fuel Element.....	3
Figure #3: PBR Fuel Particle.....	4
Figure #4: Calculational Procedure.....	7
Figure #5: PBR System Diagram.....	10
Figure #6: 400 MWt PBR.....	13
Figure #7: 2000 MWt PBR.....	15
Figure #8: 2000 MWt with External Shield.....	16
Figure #9: 2000 MWt with Collar and External Shield.....	20
Figure #10: 2000 MWt with Collar Shield.....	21
Figure #11: 2000 MWt Final Design.....	22
Figure #12: Cone Tank.....	24
Figure #13: Collar Shields with Support.....	25

List of Tables

Table #1: Heating in a 400 MWt LiH moderated PBR.....	11
Table #2: Heating in a 400 MWt Be moderated PBR.....	12
Table #3: Heating in a 2000 MWt PBR with External Shield.....	18
Table #4: Heating in a 2000 MWt PBR wiht Collar Shield.....	19

Acknowledgements

I would like to acknowledge all those who helped with this report, with special thanks to Dr. R. J. Cerbone of Brookhaven National Laboratory. I would also like to thank Dr. Franklin Mead of the Astronautics Lab for making this project possible. Lastly, I would also like to thank C. Leakeas, L.Cox , and R. Nachtrieb for their all-around help during the project.

INTRODUCTION

The direct heating of a propellant by a nuclear reactor space propulsion system offers improved characteristics over traditional chemical rockets. Traditional rockets have a large thrust with a low specific impulse, which is unsuited for the long distance space missions of the future. A rocket which uses nuclear energy to directly heat its propellant, a Nuclear Thermal Rocket (NTR), can achieve large thrust along with a high I_{sp} . These characteristics make an NTR an ideal propulsion system for long range space missions.

The major drawback of an NTR is the inherent radiation that accompanies any nuclear device. Furthermore, during these long space voyages, the manned spacecraft would be subjected to large radiation fields in space from which it must be shielded. Therefore, the problem of shielding, without severe weight penalties, for both biological and mechanical systems, becomes as important as the actual workings of the system. If adequate shielding can be provided, then an NTR can be operated as safely as any conventional chemical rocket.

One type of NTR is the Particle Bed Reactor (PBR). The PBR core consists of 19 (100-400 MWt) or 37 (1000-2000 MWt) fuel elements arranged in a hexagonal pattern and surrounded by a moderator. Each fuel element is made up of an annular shaped fuel bed contained between two coaxial porous cylinders, called frits. The propellant, cryogenic hydrogen, after flowing through the moderator, flows radially through the fuel element; from the outer, "cold" frit, through the fuel bed where it is heated, through the inner, "hot" frit, and into the duct formed by the hot frit where it then flows out to the nozzle (Figures 1 and 2). The fuel particles themselves are roughly 500 microns in diameter, and consist of a central fuel kernel, a layer of pyrolytic graphite, and an outer coating of zirconium carbide (Figure 3) (for a more complete description, Reference 1).

Two types of PBR were considered in this report, the 400 MWt and the 2000 MWt reactors. The 400 MWt PBR is designed for use as an Orbital Transfer Vehicle. In this report it is used as a baseline from which to gather information on different shield types. The 2000 MWt PBR is designed for use on a manned mission to Mars. This study focused on the shielding requirements for materials in a 2000MWt PBR propulsion system for a Mars type mission.

The project's purpose was to design a shield for a PBR system that would adequately protect critical materials in the system. Heating rate calculations were iterated with different shield types and configurations until a shield was found that met all given criteria and was as light as possible. This project was undertaken due to the need for accurate predictions of the

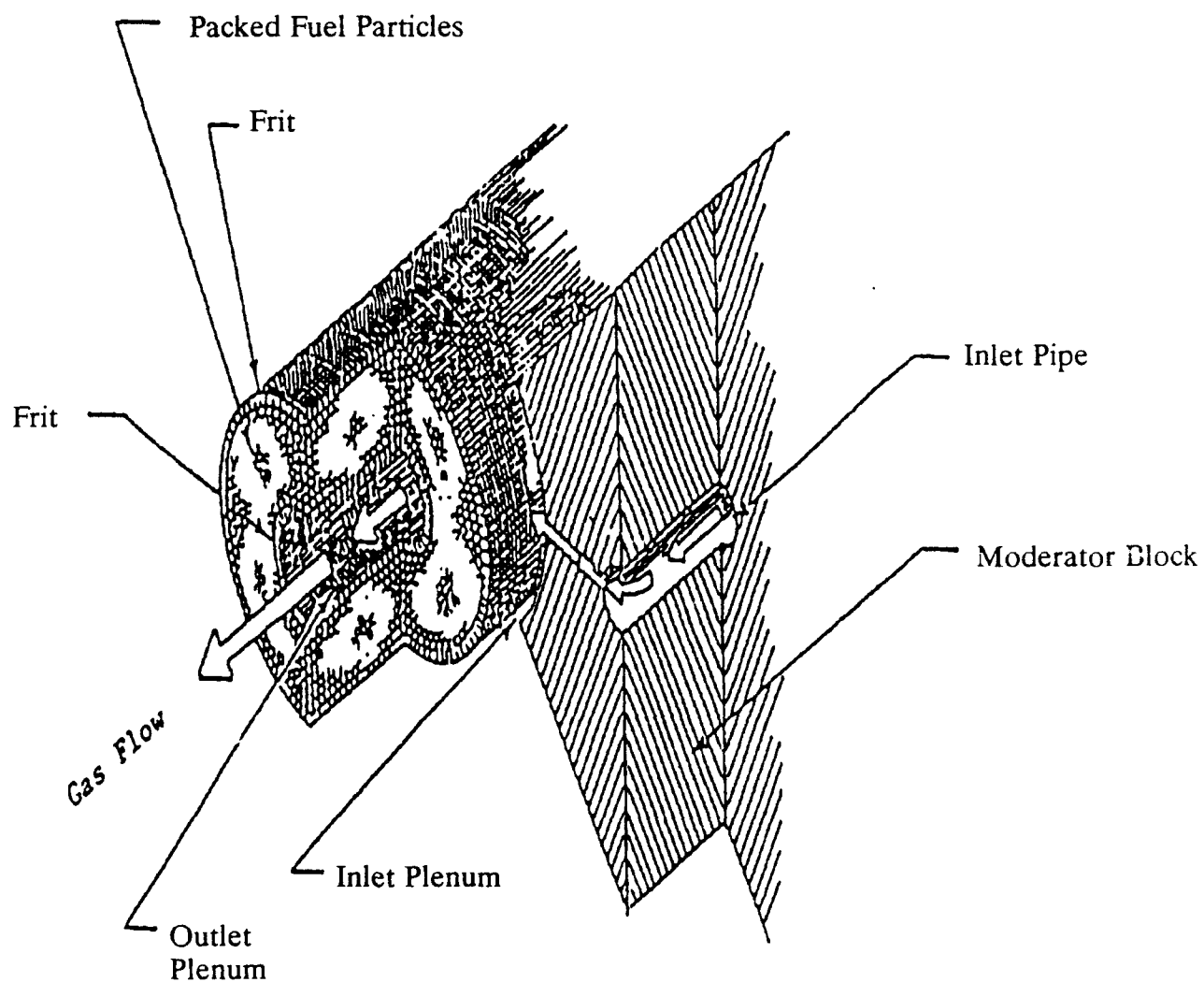


Figure 1. PBR Fuel Element (side view)

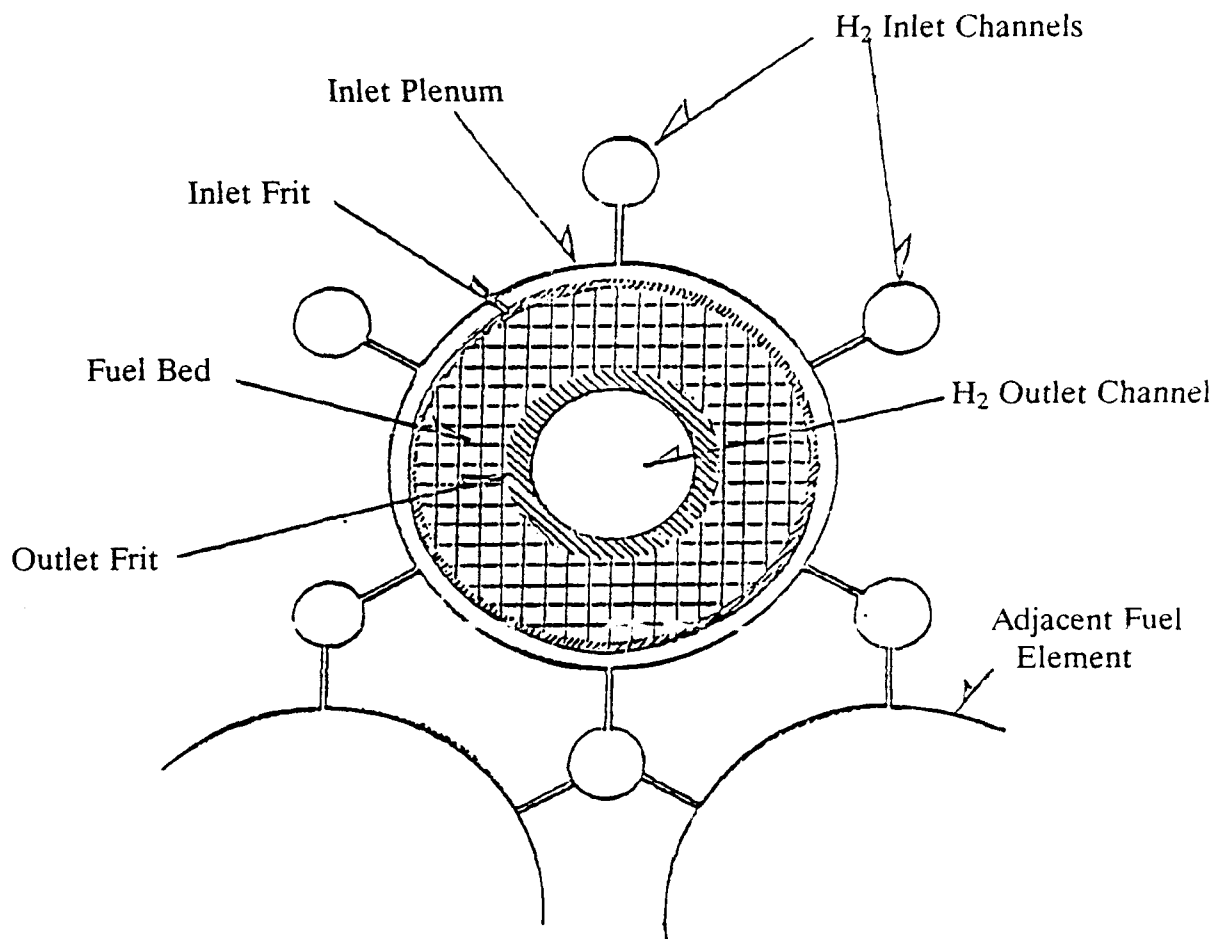


Figure 2. PBR Fuel Element (head-on view)

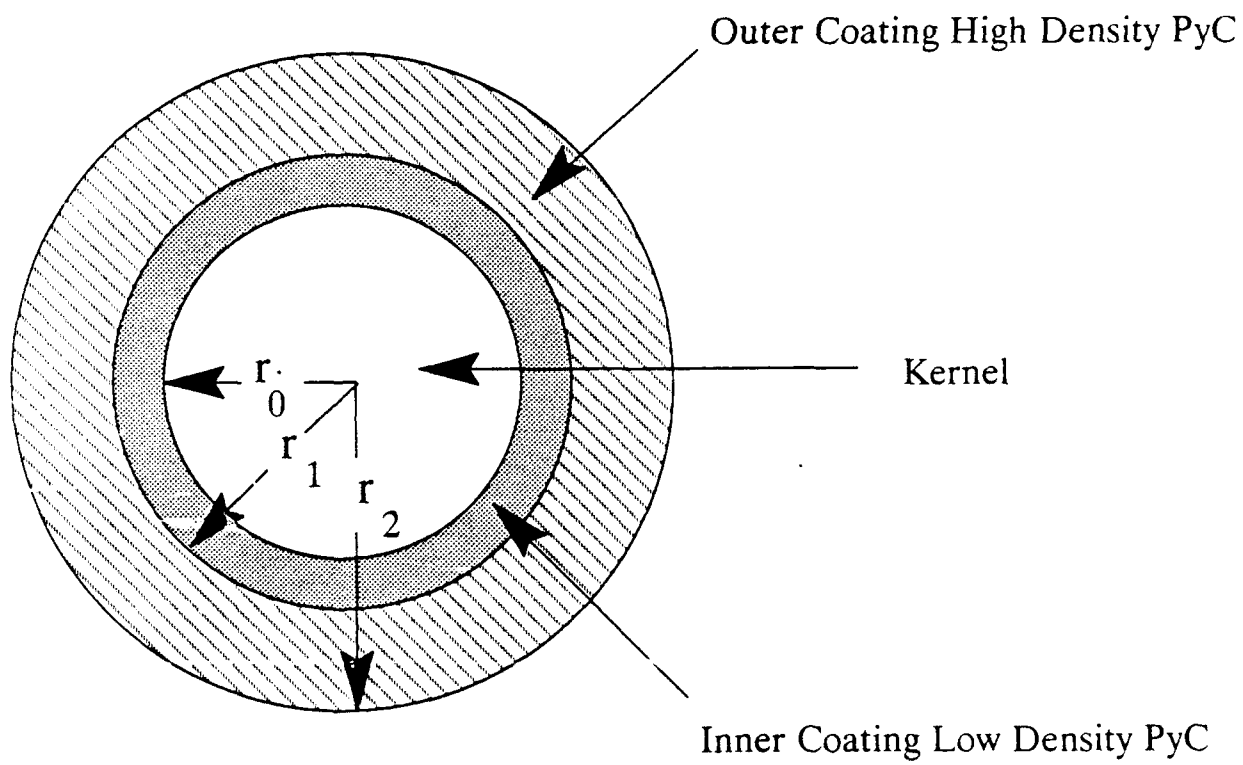


Figure 3. PBR Fuel Particle

radiation environment in a PBR and the need for a working shield design in a PBR.

METHODOLOGY

To determine the radiation environment and subsequent shielding, a solution to the Boltzmann equation is required. The Boltzmann conservation equation,

$$\begin{aligned} \vec{\Omega} \cdot \nabla \Psi(\vec{r}, \vec{\Omega}, E) + \Sigma_T(\vec{r}, E) \Psi(\vec{r}, \vec{\Omega}, E) \\ - \int dE' \int d\Omega' \sum_j f^j(E') v^j \Sigma_f^j(\vec{r}, E') + \Sigma_s(\vec{r}, \vec{\Omega}' \rightarrow \vec{\Omega}, E' \rightarrow E) \Psi(\vec{r}, \vec{\Omega}', E') \\ + Q(\vec{r}, \vec{\Omega}, E), \end{aligned}$$

is a statement of particle conservation, where $\vec{\Omega}$ is the solid angle vector, Ψ is the angular flux density, Σ_s is the macroscopic scattering cross section, Σ_f is the macroscopic fission production cross section, f is the fission spectrum for the j^{th} isotope, and Q is the nonfission source density (Reference 2). The differential part of the equation represents the loss and the integral part represents the production of the particles. This equation is used to calculate the neutron and gamma ray fluxes throughout the system. The difficulty in solving the equation arises from the fact that one side is differential and the other is integral and is therefore unsolvable directly. The accuracy of the flux calculations is tied to how well the geometry (r), energy (E), and angular dependency ($\vec{\Omega}$) of the flux can be represented.

The Boltzmann equation can be approximated to different orders with differing degrees of accuracy in the flux calculations. A zero order representation uses a monoenergetic, isotropic source. A first order approximation uses the multigroup diffusion theory with a first order Legendre expansion (P_1) to represent the scattering with an isotropic source. This first order approximation is good only near the source because diffusion theory breaks down away from the source. A second order representation approximates the scattering with a higher order Legendre expansion (P_n) and uses Gaussian-Quadrature (S_n) to represent the angular distribution in the transport equation. The highest order approximation uses a Monte Carlo approach. This method uses a continuous energy, explicit geometry statistical approach, following the lifetimes of thousands of particles.

This study used the TWODANT (Two-dimensional Diffusion-Accelerated Neutron-particle Transport) computer code to calculate

the heating rates needed to determine the shielding (Reference 3). TWODANT uses the second degree approximation of the Boltzmann equation. All calculations were performed with a third order Legendre expansion (P_3) and a twelfth order Gaussian-Quadrature (S_{12}). The neutron and gamma ray cross sections that were input into TWODANT were obtained from a Los Alamos 42 group library. This library consisted of 30 neutron groups and 12 prompt gamma groups. Delayed gammas were not taken into consideration in this library.

TWODANT was also used to run an eigenvalue (K_{eff}) calculation. For this problem, the code uses a homogenous source (nonfission source term, Q , equals 0) to generate an inhomogenous source ($Q \neq 0$) for use in the heating calculations. This inhomogenous source is calculated using the relationship:

$$\Sigma_f \Phi(r, z) = F(r, z)$$

which relates K_{eff} to the fission distribution. This fission distribution, when multiplied by the fission spectrum, can be used to calculate the inhomogenous source Q ;

$$F(r, z) \chi(E) = Q(r, z, E)$$

The code uses this inhomogenous source in approximating the Boltzmann equation to determine the particle fluxes. These fluxes are used, together with supplied, calculated KERMA factors to determine the heating rates (Figure 4).

KERMA (Kinetic Energy Released in Materials) factors are the response functions of a material to radiation. These functions describe the heating that will take place when a certain type of radiation is incident upon it. These KERMA factors can be used along with the calculated fluxes to find the heating rates from the equation:

$$\text{Heating Rate} = \int \text{KERMA} \times \text{Flux } dE$$

The KERMA factors themselves are equal to some value, K , dependent on energy, times the number density.

$$\text{KERMA} = K(E) \times n \quad (n = \text{number density})$$

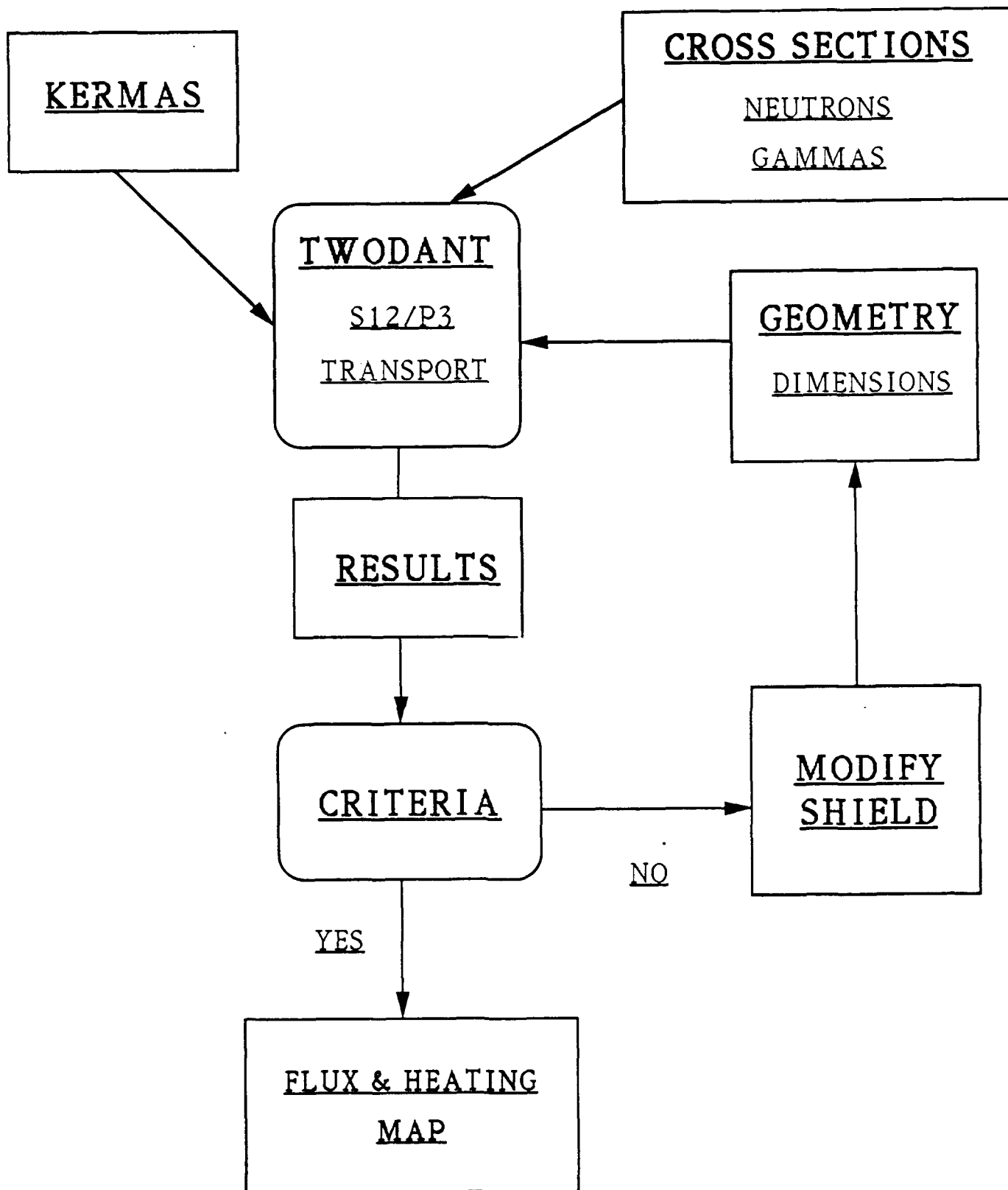


Figure 4: Calculational Procedure

The K's for neutron radiation radiation are given as:

$$K_n(E) = \frac{2A \times \Sigma_s}{(A+1) \times n} [1 - \mu_0(E)] \times E$$

and for gamma radiation argiven as:

$$K_\gamma(E) = \frac{\mu_a(E)}{n} \times E$$

where A is the mass number of the scattering nucleus, Σ_s is the scattering cross section, μ_0 is the average cosine of the scattering angle for neutrons of energy E, n is the number density, μ_a is the linear absorbtion coefficient, and E is the energy of the neutron or gamma ray (Reference 4). The KERMA factors used in this study were from the MACK IV library (Reference 5).

These K's are calculated in [energy \times area/atom], so when multiplied by the number density, [volume⁻¹], the KERMA factors come out to be in units of [energy/length \times atom]. When the flux, [particles/(area \times time)], is integrated with the KERMA, the resultant heating rates are in the units of [power/unit volume]. These KERMA factors, along with the neutron and gamma ray cross sections and system geometry parameters are input into TWODANT, which performs the flux and heating calculations.

Comparison Between Methods

One of the first objectives of this project was to compare TWODANT with FEMP2D, a two-dimensional diffusion code; FEMP2D was the code used to calculate heating rates before TWODANT was installed at the Astro Lab (Reference 6). An early run of the TWODANT code to determine heating in the reactor pressure vessel was compared to a FEMP2D calculation. As seen in Graph #1 (Appendix), near the source, FEMP2D predictions agree reasonably well with TWODANT, but away from the source, diffusion theory breaks down and the particle transport is underpredicted. This is shown in the graph as the FEMP2D curves leveling out to a constant heat rate while the TWODANT curves still fall off as they move away from the source.

The results in this paper will all be presented in this manner. To avoid confusion, a brief explanation of Graph #1 is given. The abscissa is the axial, or vertical along the centerline, distance from the core center. The ordinate is the heating rate as you move up and away from the core horizontal midplane. Each of the curves on a single graph represents the heating rate along a particular radius, r, away from the core

vertical centerline (an exception to this is Graph #1; because all of the rates were taken at the same radius to make comparisons).

SHIELD DESIGN, MODELING AND OPTIMIZATION

The major goal of the project was to determine the shielding for a PBR system using calculated heat rates. To determine the shielding; the system design, the criteria for the materials shielded, and the shield itself must be known. The system design for the PBR is known and can be seen in Figure 5 and the criteria for this study will be shown below.

The criteria that are set for this system were derived from knowledge of the materials and how radiation from neutrons and gamma rays affect them. These criteria are the conservative upper limits at which point the materials begin to fail and performance of the systems begins to degrade. The criteria are:

- For materials in the interstage turbo-pump assembly, valves, and gimbal (Al, C, Ti, and SS); a maximum heating of:
1 W/cc
- For Silicon (electronics) in the interstage region; maximum
neutron fluence: $5.0e+13$ neutrons/cm²
gamma dose: $5.0e+5$ Rads

Two types of shield were studied, a lithium hydride/tungsten combination and the BATH (Boron Aluminum Titanium Hydride) shield, which was used in the NERVA project. The LiH/W shield is composed of a thin layer of tungsten with a thicker amount of lithium hydride on top of it. The dense tungsten attenuates the gamma radiation very well as well as having an absorption cross section for thermal neutrons. Lithium hydride has a large scattering cross section for fast neutrons and it also has an absorption cross section for thermal neutrons. A combination of these materials provides good shielding for the radiation from the PBR (Reference 7).

The BATH shield is a solid mixture of boron, aluminum, titanium, and hydrogen. The denser aluminum and titanium attenuate the gamma radiation while the boron and hydrogen act as absorbers and scatterers for the neutrons, thus attenuating the neutron flux. This BATH material also provides a good shield for PBR radiation (Reference 8).

At the beginning of the project, a 400 MWt PBR was selected as a reference. This 400 MWt reactor can be used to power an Orbital Transfer Vehicle (OTV). The initial calculations for this project were run using this type of PBR. These initial results were used to compare with the earlier FEMP2D results and were also used to compare the two shield types. The results of the TWODANT/FEMP2D comparison have already been shown.

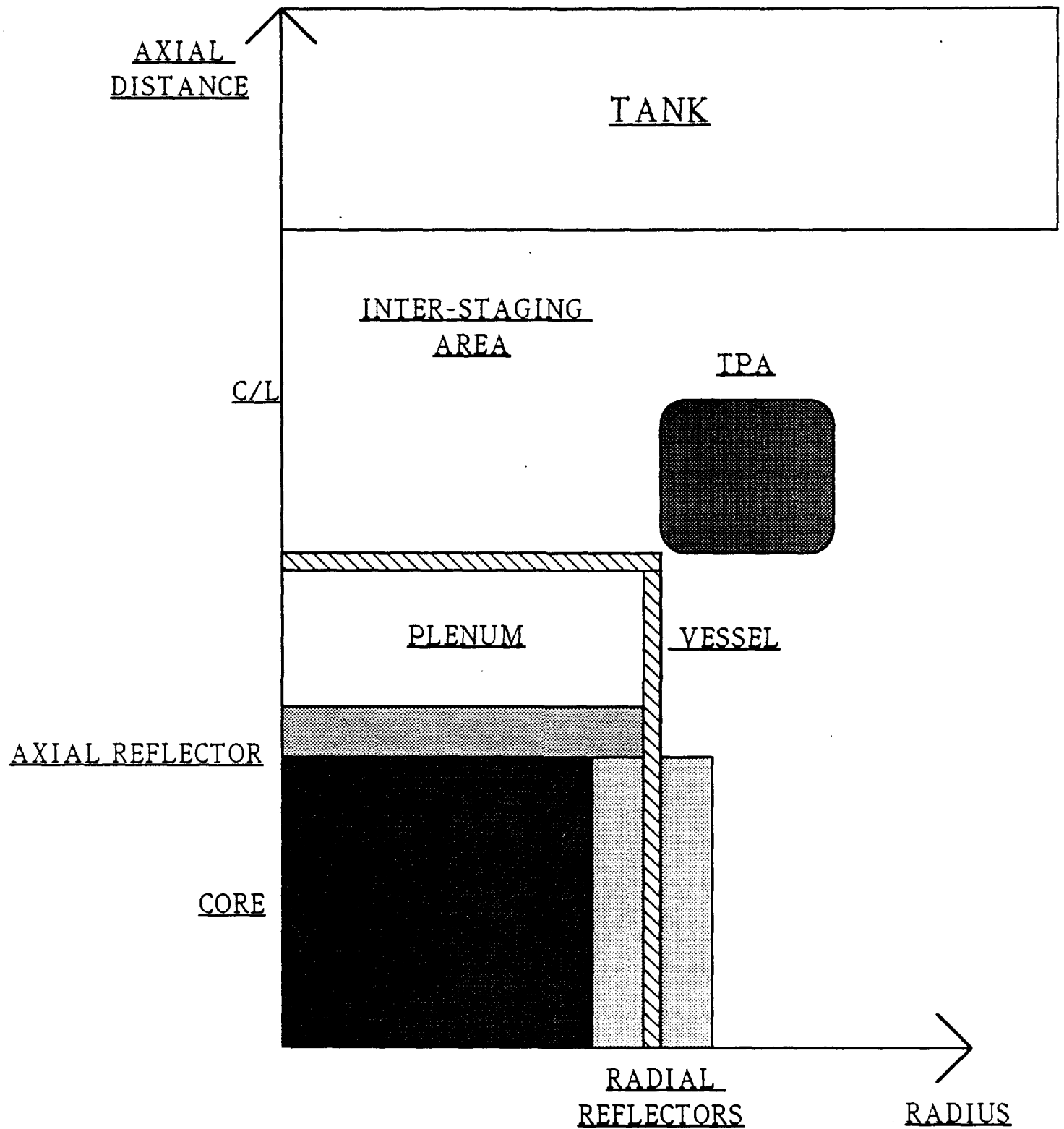


Figure 5: Upper Region of PBR

The 400 MWt PBR was also calculated with two different moderators. The two types are lithium hydride and beryllium. The lithium hydride, due to its better moderating qualities, allows for a more compact (height=44 cm, diameter=45.5 cm), higher power density core; but the moderator requires cooling at higher temperatures. Beryllium, on the other hand, can operate at higher temperatures but operates at a lower power density than the LiH and therefore is larger in size (height=60 cm, diameter=60 cm).

The initial calculations with the 400MWt PBR were made with both moderators and both types of shield. The total shield thicknesses were 22 cm; 22 cm of BATH or 20 cm of LiH and 2 cm of W. The heating rates and doses calculated for the 400MWt reactor were taken from the area above the shields (the plenum) and are shown in the following tables.

Table 1:
Heating in a 400MWt Lithium Hydride moderated PBR.

Shield Material:	None	LiH/W	BATH
	Heating Rates [W/cc]	Heating Rates [W/cc]	Heating Rates [W/cc]
Hydrogen	11.5	0.09	0.38
Carbon	48	2.2	8.3
Aluminum	80	3.6	14.5
Titanium	335	4.8	36
Stainless Steel	500	13.0	91
	Dose [Rad]	Dose [Rad]	Dose [Rad]
Silicon	8.6e+9	2.65e+5	4.4e+5

Table 2:
Heating in a 400MWt Beryllium moderated PBR.

Shield Material:	None	LiH/W	BATH
	Heating Rates [W/cc]	Heating Rates [W/cc]	Heating Rates [W/cc]
Hydrogen	6.5	0.13	0.26
Carbon	27	4.8	7.3
Aluminum	46	10.6	13.2
Titanium	345	12.4	31
Stainless Steel	320	21.5	80
	Dose [Rad]	Dose [Rad]	Dose [Rad]
Silicon	4.9e+9	1.36e+5	3.6e+5

The plenum region for these measurements can be seen on Figure 6. The total dose to Silicon was calculated by multiplying the heat rate by a Rad/(W/cc) conversion factor, then multiplying that by the total time which the reactor will operate. The total time used was two hours. This time is applicable to both the OTV and Mars Mission reactors, and takes into account the longest time that the reactor would operate. These values were taken from graphs 2-37. The highest values of the heating rates are the values that were used in the comparisons.

These results show clearly that for this type of radiation environment, the Lithium Hydride/Tungsten is the better shield. Although not always strongly superior, in the cases of the hydrogen and silicon, the LiH/W provides much better shielding than the BATH material.

In addition to these initial shield comparisons, something else was discovered from these calculations. The results from the first run with a shield on the axial reflector showed unexpected results. It appeared that the heating at the outer radii was greater than at inner radii above a certain axial distance. These results showed that some of the radiation coming out of the reactor on the sides either went through the shield partially or missed the shield totally. This meant that the TPA, which extends out from the reactor pressure vessel (RPV), would see unshielded radiation.

Once these results had been obtained, the major thrust of this research changed from a 400MWt OTV type PBR to a 2000MWt Mars Mission type PBR. It was decided to focus on the beryllium moderated core due to the temperature requirements of this type of

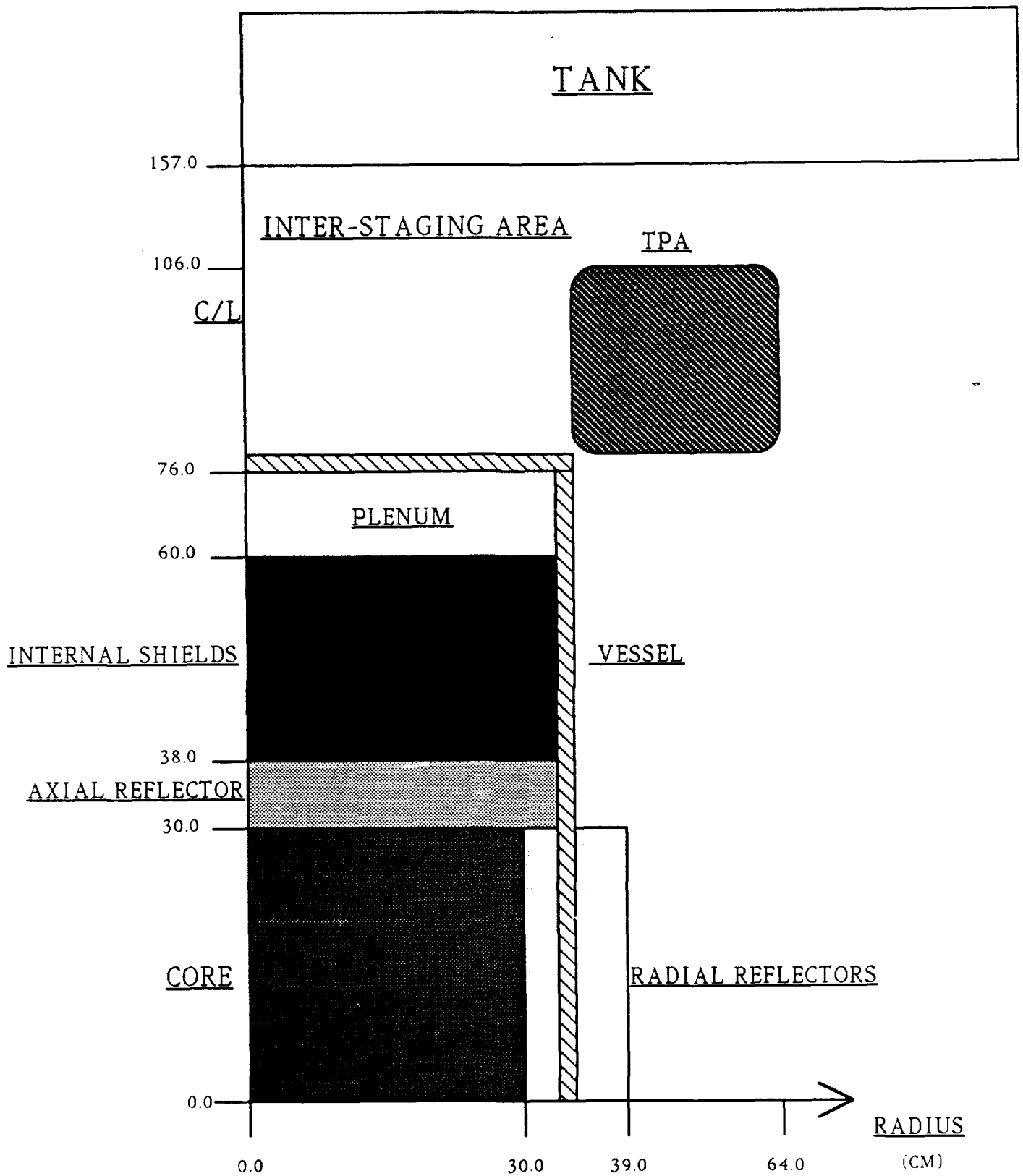


Figure 6: Upper Region of 400 MWT PBR

mission. The actual physical changes, from 400 to 2000Mwt, in the reactor are a size increase from a height and diameter length of 60 cm to a height and diameter length of 87 cm, an increase in the number of fuel elements from 19 to 37, and the removal of the radial reflectors. A diagram of this reactor can be seen in Figure 7.

To model this new configuration in TWODANT, a new nonhomogeneous source had to be calculated. This was done using the K_{eff} eigenvalue, problem in the code. Once this new heterogeneous source had been calculated, heating rate calculations were ready to be performed.

After these calculations were made, the results had to be examined to see if they fell within the criteria. If the results did not meet the criteria then corresponding modifications to the shield dimensions and reactor geometry were made; and new calculations were made (Figure 2).

When the results met the criteria, after several iterations, the next step was to minimize the shield mass by rearranging the shield configuration while maintaining the total shield thickness. Most of this reconfiguration came from moving some of the outer shield to the inner shield (smaller radius).

The 2000 Mwt reactor was shielded in the same way as the 400 Mwt, with the shield inside the RPV. In the initial calculations, it became apparent that the unshielded radiation reaching the TPA would have to be shielded somehow. The options for shielding the TPA were to use a large external shield on top of the RPV that extended out past the TPA, a "collar" shield that was an extension of the internal shield outside of the RPV, or actually moving the TPA in, so it would be above the inner shield. The first shield investigated was the large external shield on the RPV.

Once the shield was selected, iterations to calculate the shield thicknesses were needed until heating rates fell within the criteria. The first calculations were run with a 20 cm LiH/2 cm W shield on the inside and the same size shield outside, on top of the RPV. In the succeeding calculations both the inner and outer shields were varied to meet the shielding criteria while minimizing the total mass as much as possible, which means placing as much shielding inside the vessel, due to the resulting smaller radius of the shield.

RESULTS

The shield consisting of 35 cm LiH/2 cm W inside the vessel and 20 cm LiH/2 cm W on top of the vessel (Figure 8) was adequate, so that all of the heating criteria were met. At this point the neutron and gamma fluxes were examined to determine if the silicon dose and neutron fluence were within the criteria. It was at this

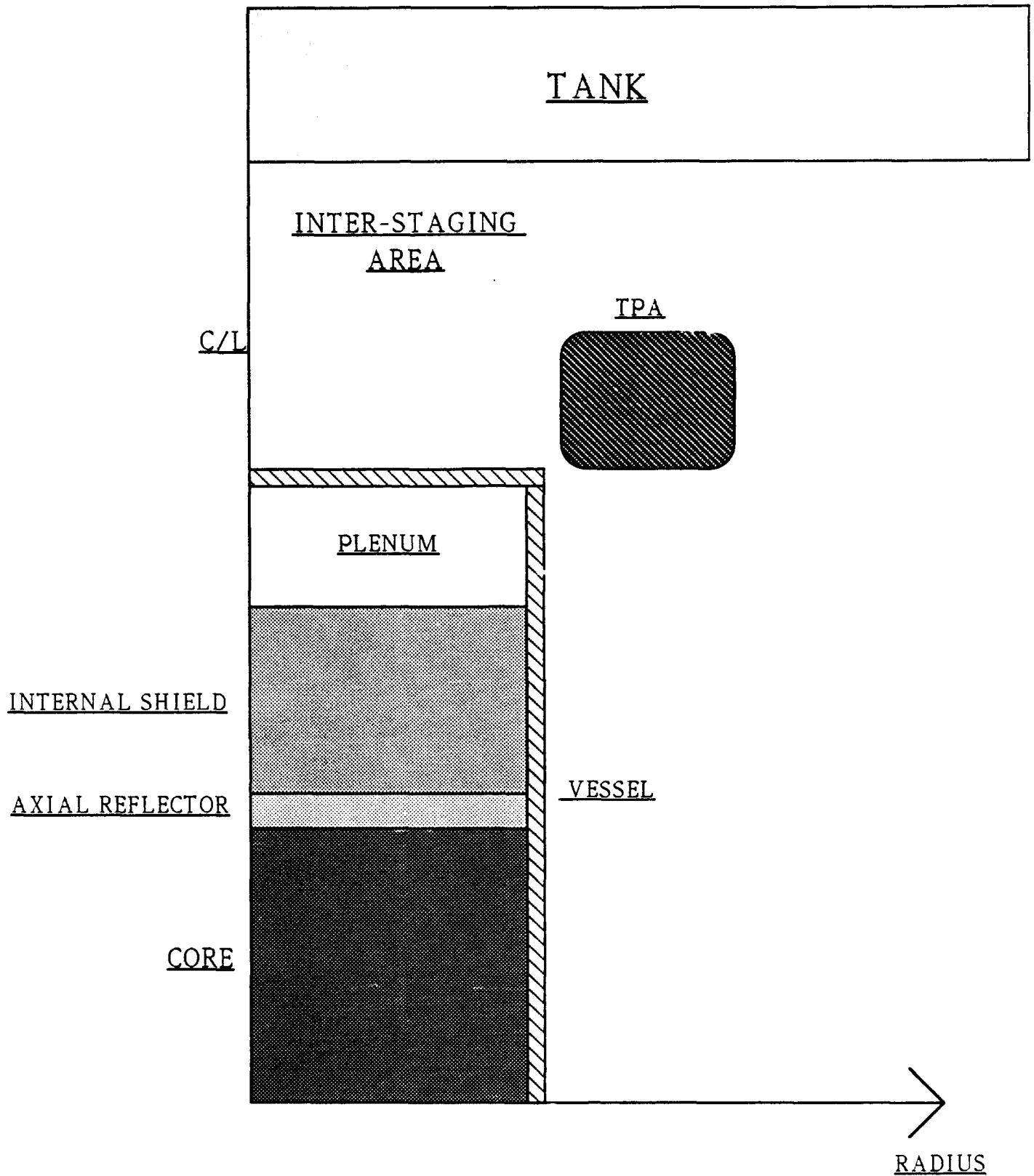


Figure 7: Upper Region of 2000MWt PBR

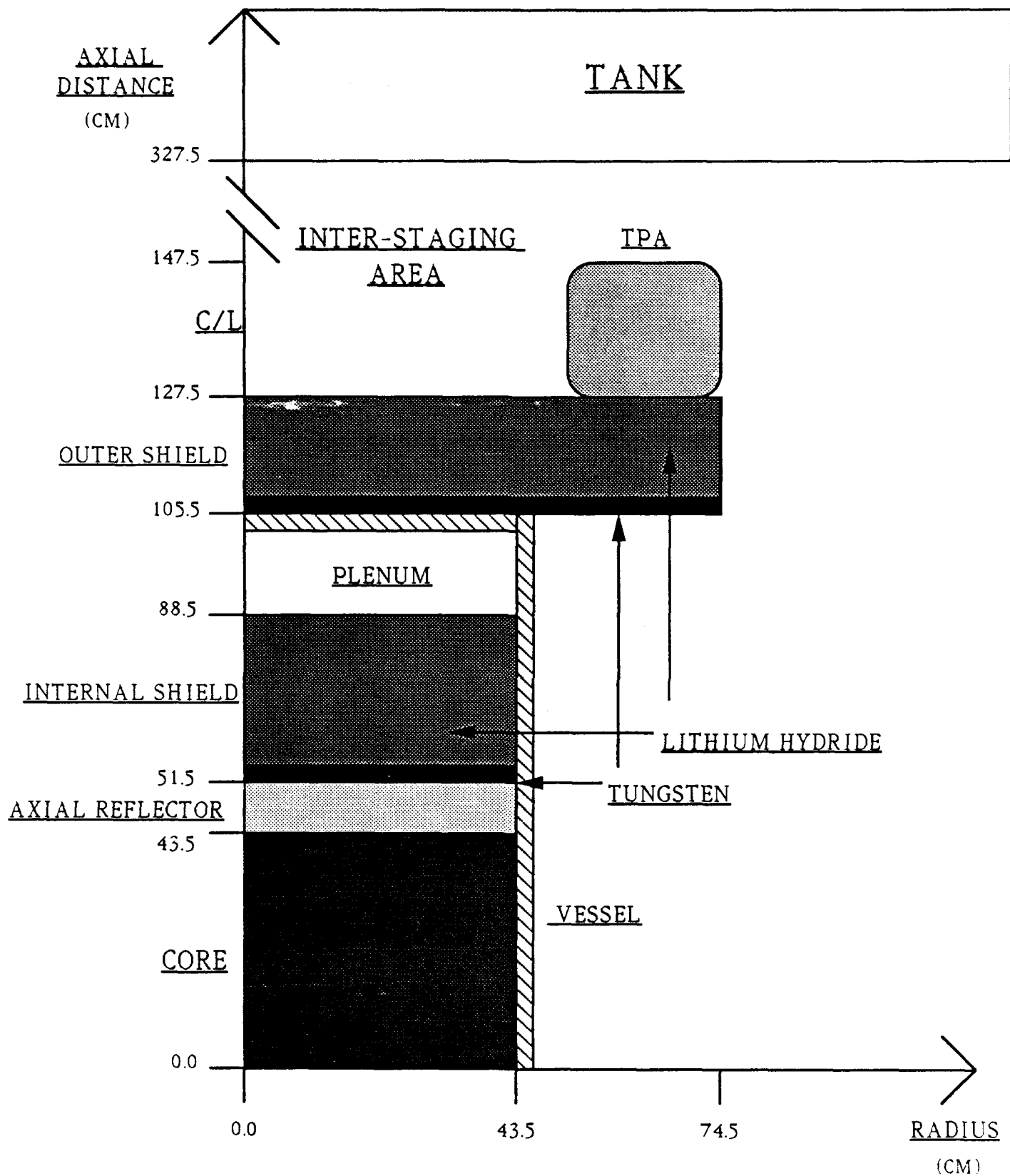


Figure 8: Upper Region of 2000MWt PBR with External Shield

time that the discovery of a problem with the calculation was found. The neutron fluxes showed gross oscillations high in the interstage region, near the tank, where the behavior should have been smooth $1/r_2$ (Graph #52). Several explanations for this anomaly include; back scattering of neutrons from the tank, side scattering from the TPA, or problems with the code in dealing with the geometry selected.

Each of the possible sources of error were systematically examined to determine the true cause of the problem. First the tank was removed from the geometry; but the oscillations were still present in the neutron fluxes. Next, the TPA was removed; and again, there were still oscillations. With these possible scattering sources removed, it was determined that the problem was in the calculation itself.

The problem is the code's inability to deal with the large void areas in the interstage region. At these distances from the source of the neutrons (core) and the lack of any scattering material in the void, the code had difficulty in predicting the particles behavior in this void region (Reference 7). This effect is called "ray effects" and is observed in S_n calculations in low scattering with highly localized sources. To offset this, a very low density carbon gas (10^{-5}g/cm^3) was put into the void to give some scattering while not affecting the true heating rates. This attempt to rectify the problem worked slightly, but not enough to offset the huge oscillations.

The next probable solution to the problem was to eliminate the large shield extending out into the void. This extended shield could be causing problems with the Gaussian Quadrature representation of the angular distribution of the particles. The oscillations could be caused by ray effects due to the line of sight from the core to the edge of the shield exceeding an allowed value in the quadrature representation (Reference 7). The calculations can break down and give erroneous results to regions beyond this point. However, results for regions below this point have been checked to be satisfactory. The collar shield helped in regions near the TPA, but not in the tank area.

Due to this inadequacy of the calculations, results for the heating in the lower tank could not be examined at this time. The heating and doses for a 2000MWt PBR with an inner shield of 35 cm LiH/2 cm W and an outer extended shield of 20 cm LiH/2 cm W are:

Table 3:
Heating in a 2000MWt PBR with an extended type shield.

	Heating Rates [W/cc]
Hydrogen (plenum)	0.035
Carbon (TPA)	0.17
Aluminum (TPA)	0.32
Titanium (TPA)	0.41
Stainless Steel (TPA)	2.3
Dose/Fluence [Rad]/[n/cm ²]:	
Silicon (TPA/void)	2.4e+4/2.2e+13

The neutron fluence to the silicon is the integral over time of the fast neutron flux in the void region. All of the heating rates here meet the criteria, except for Stainless Steel (Graphs #'s 38-44). Stainless Steel is consistently overheated and the amount of shielding necessary to bring heat rate within the criteria is huge. It is likely that instead of using a huge shield, stainless steel will not be used in the turbo-pump assembly.

Collar Shield

The next design option studied was a "collar" shield. This required an inside shield with an extension of this shield, the same size or smaller, outside the RPV; with or without another shield on the top of the RPV (Figures 9 and 10). Initially, the collar shield was just moved down next to the inner shield while leaving the portion of the top shield directly on top of the RPV intact (Figure 9). Later, the top shield was removed and the inner shield was extended to try to lower the total mass of the shields (Figure 10).

The geometrical model was then changed to fit this configuration and the calculations were run with these shields. After running the calculations for the system with both collar and upper outer shields, optimization of shield mass trials were also run to find the smallest shield size possible. The final collar type shield system, which met all criteria and was as small as possible was a system with an inner shield of 50 cm LiH/2 cm W and a collar of 50 cm LiH/2 cm W (Inner/Collar) (Figure 11). The results from these calculations are:

Table 4:
Heating in a 2000MWt PBR with a Collar type shield.

Shield:	Inner/Collar
	Heating Rates [W/cc]
Hydrogen (plenum)	0.03
Carbon (TPA)	0.33
Aluminum (TPA)	0.70
Titanium (TPA)	0.80
Stainless Steel (TPA)	7.5
	Dose/Fluence [Rad]/[n/cm ²]
Silicon (TPA/void)	1.2e+4/1.8e+13

These results were gathered from graphs 45-51.

Shield Masses

The next major design feature of the shields, after meeting the criteria, is the total shield mass. The whole project was to design the lightest shield possible that could still meet the design criteria. One way to reduce the shield mass was to have the shield in direct contact with the reactor. Other studies have used a "shadow" shield located away from the reactor with a larger radius to shield the same solid angle from the source. Placing the shield as close to the core itself means a smaller radius and, therefore, a smaller mass. As long as cooling from the propellant is provided, the shield can be very close to the core.

Through successive iterations, the minimum shield mass for each shield type was achieved. The shield masses for these shields are:

- For the case with the 35 cm LiH/2 cm W inner shield and 20 cm LiH/2 cm W outer, fully extended top shield (Figure 8):
Mass = 1359 kg

- For the case with the 50 cm LiH/2 cm W inner shield and 50 cm LiH/2 cm W collar shield (Figure 11):
Mass = 955 kg

Although the masses of these shield seem large, varying from roughly 1-1.5 metric tons, they will in fact not be the major weight source in the propulsion system. The mass of the PBR itself is about 4 tons. Therefore, the shield mass is small when compared to the reactor mass and would be even smaller when compared to the mass of the whole system.

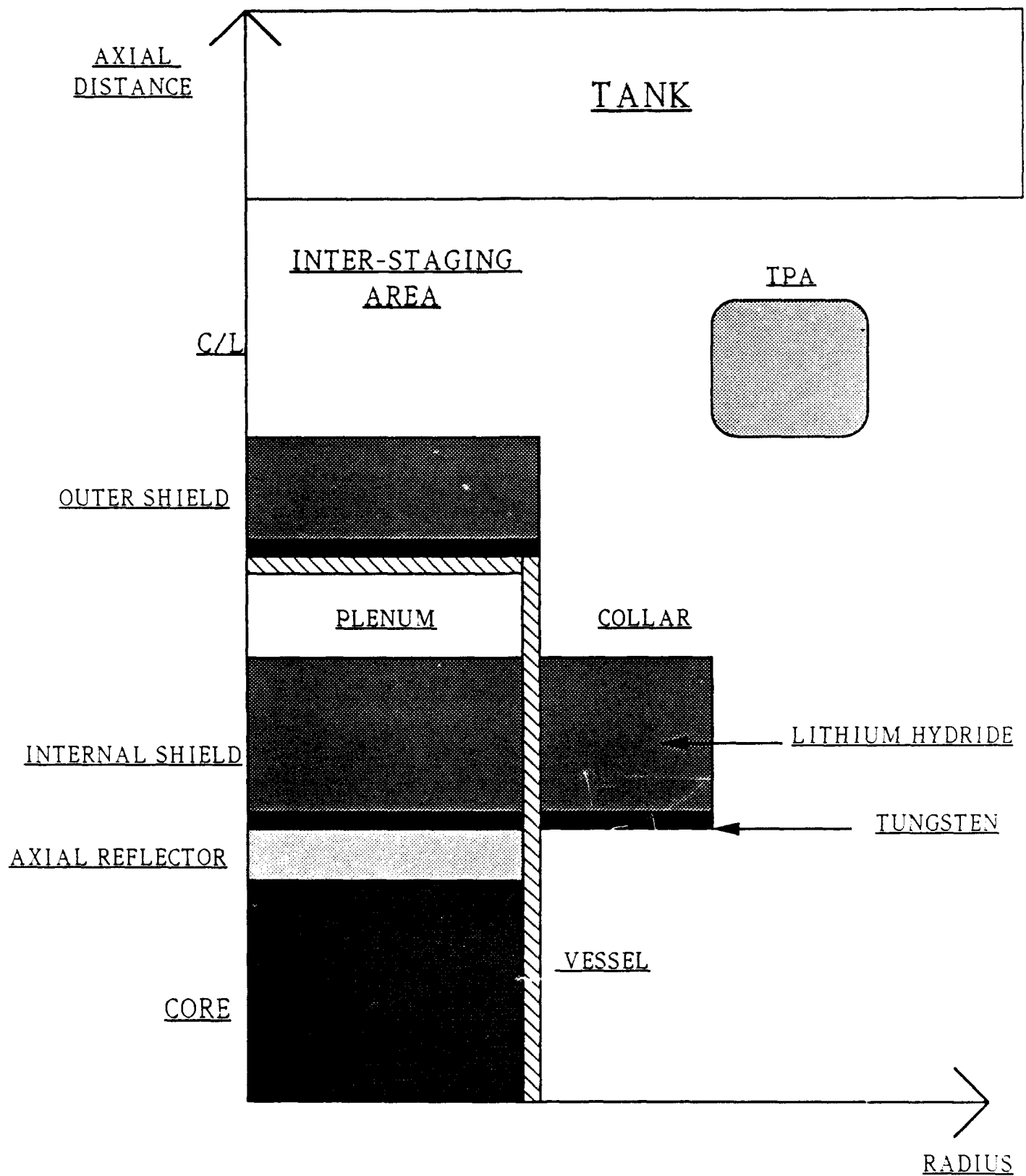


Figure 9: 2000MWt PBR with Collar and External Shield

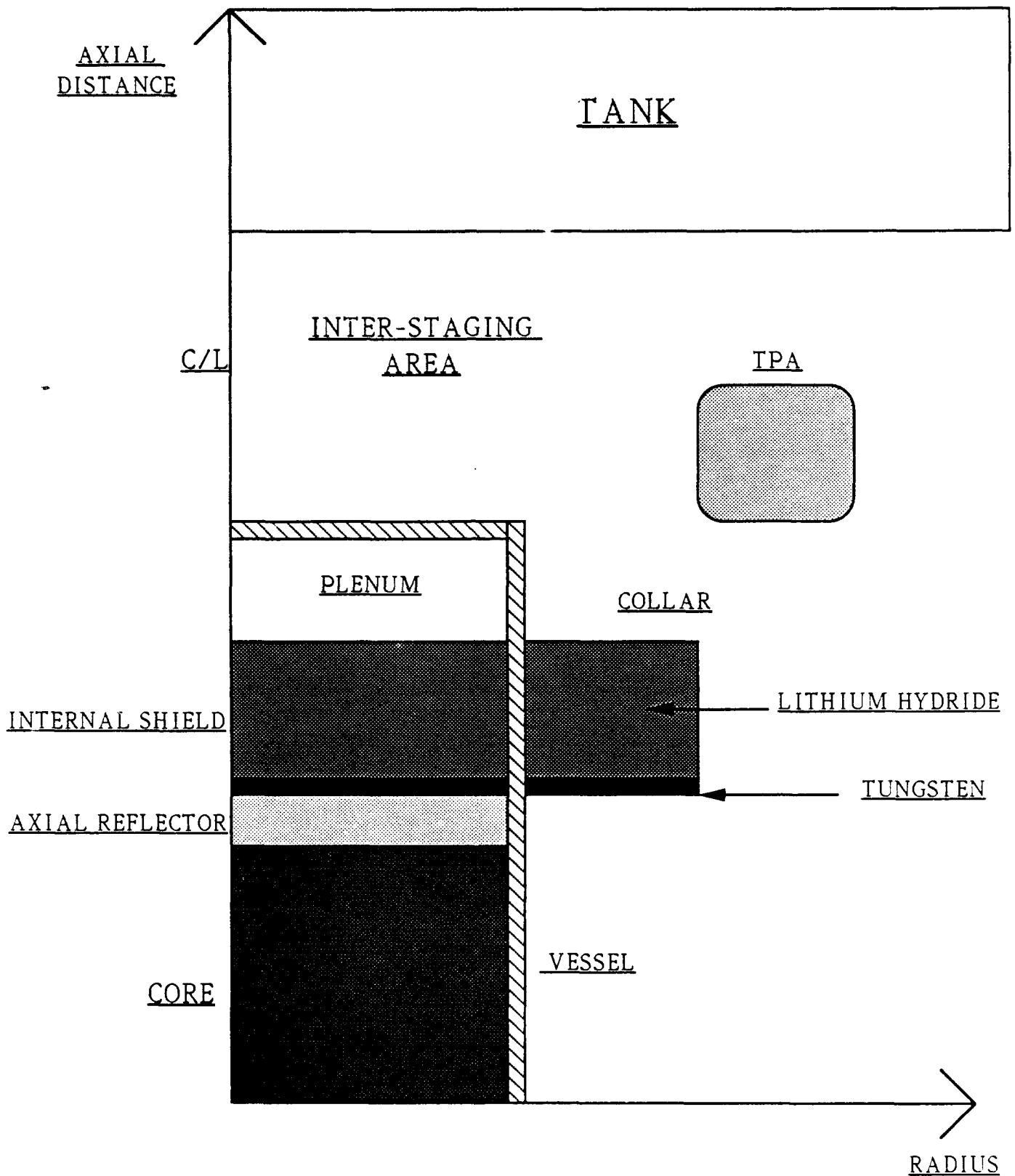


Figure 10: 2000MWt PBR with Collar Shield

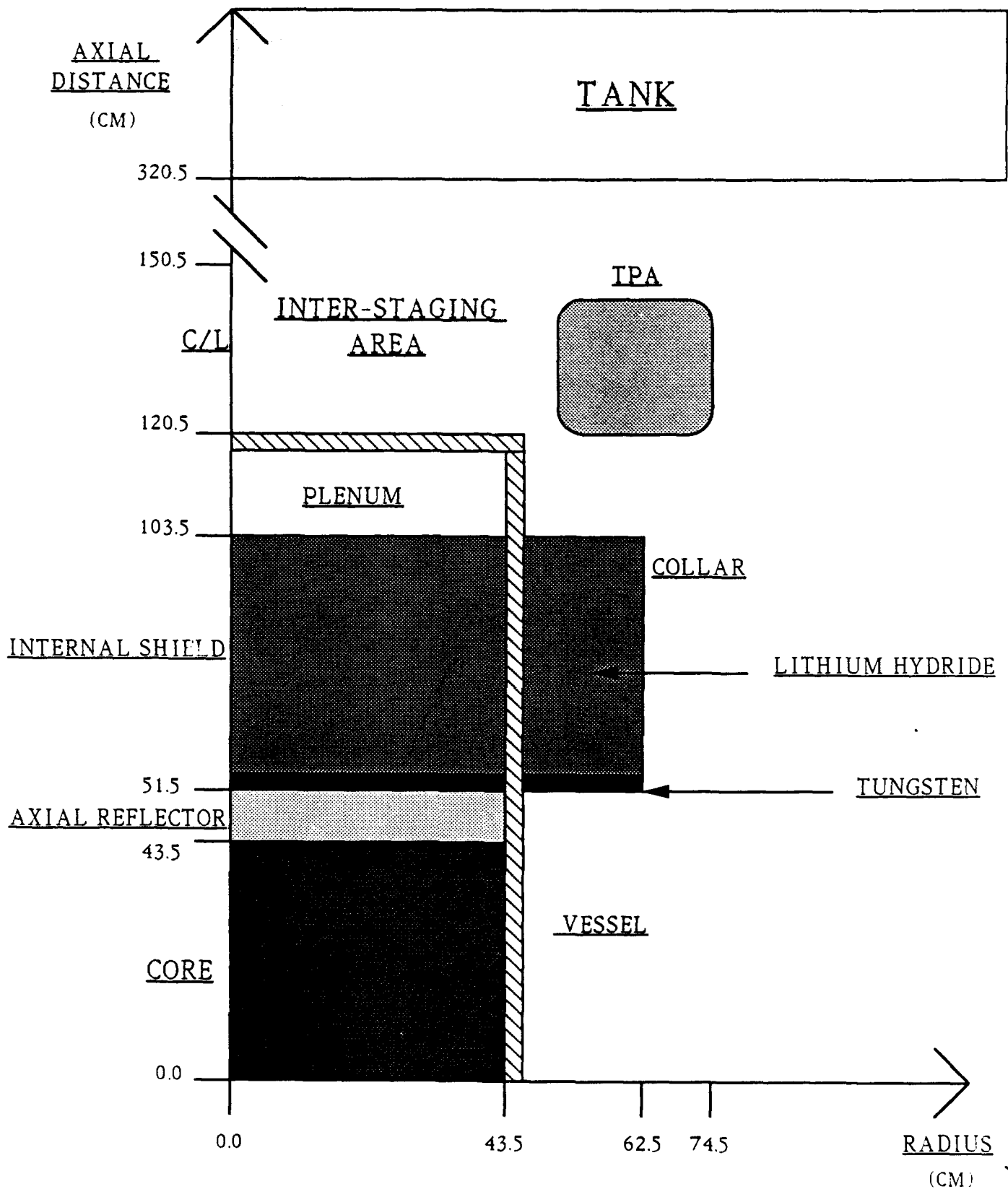


Figure 11: 2000MWt PBR Final Design

These shields represent the shielding needed to adequately shield materials in the interstage region. They do not, however, show any radial shielding effects. Radial shield requirements will depend on mission needs.

FINAL DESIGN

The many design iterations performed have shown that there is a minimum shield amount necessary to keep heating to acceptable limits. The optimum optimum minimum shield configuration to meet the criteria is 2 cm of tungsten folled by 50 cm of lithium hydride placed on top of the axial reflector with a collar outside the vessel, as shown in Figure 11. At a weight of only 955 kg, this is the lightest shield examined that gave the needed shielding.

SUMMARY AND CONCLUSIONS

This study has shown that is possible to adequately shield the critical components in the propulsion system. It was also found that the shield could be minimized to a small fraction of the system weight. The study also showed that many shield designs can adequately shield the system as needed. Although this study focused on the lightest shield possible, if other shield requirements are made, there are other designs that have different characteristics which could be better suited to the new requirements.

Recommendations

The shielding design for a nuclear propulsion device is a very important part of the design process; if the design is inadequate then too much exposure to the incident radiation will cause the materials or systems to fail. Therefore, the adequacy of the design tools for the shield need to be evaluated. The code used in this study needs to be benchmarked against a more accurate method, such as MCNP, a Monte Carlo method code.

Since the actual system design is not complete, certain system changes could aid in reducing heating in the materials. If the Turbo-Pump assembly could be moved directly above the reactor vessel, then the need for extending shields would be removed. Stainless Steel should not be used in the TPA due to its high heating rate and subsequent need for immense shields. If the propellant tank itself were shaped like a cone with the point aimed at the reactor (see Figure 12), then this would reduce the surface area exposed to direct radiation.

The collar design has some problems of its own. Support of the collar on the outside of the RPV will be needed. One idea would be to have the collar supported by a radial shield which is supported by the core support plate (Figure 13); this assumes the use of a radial shield.

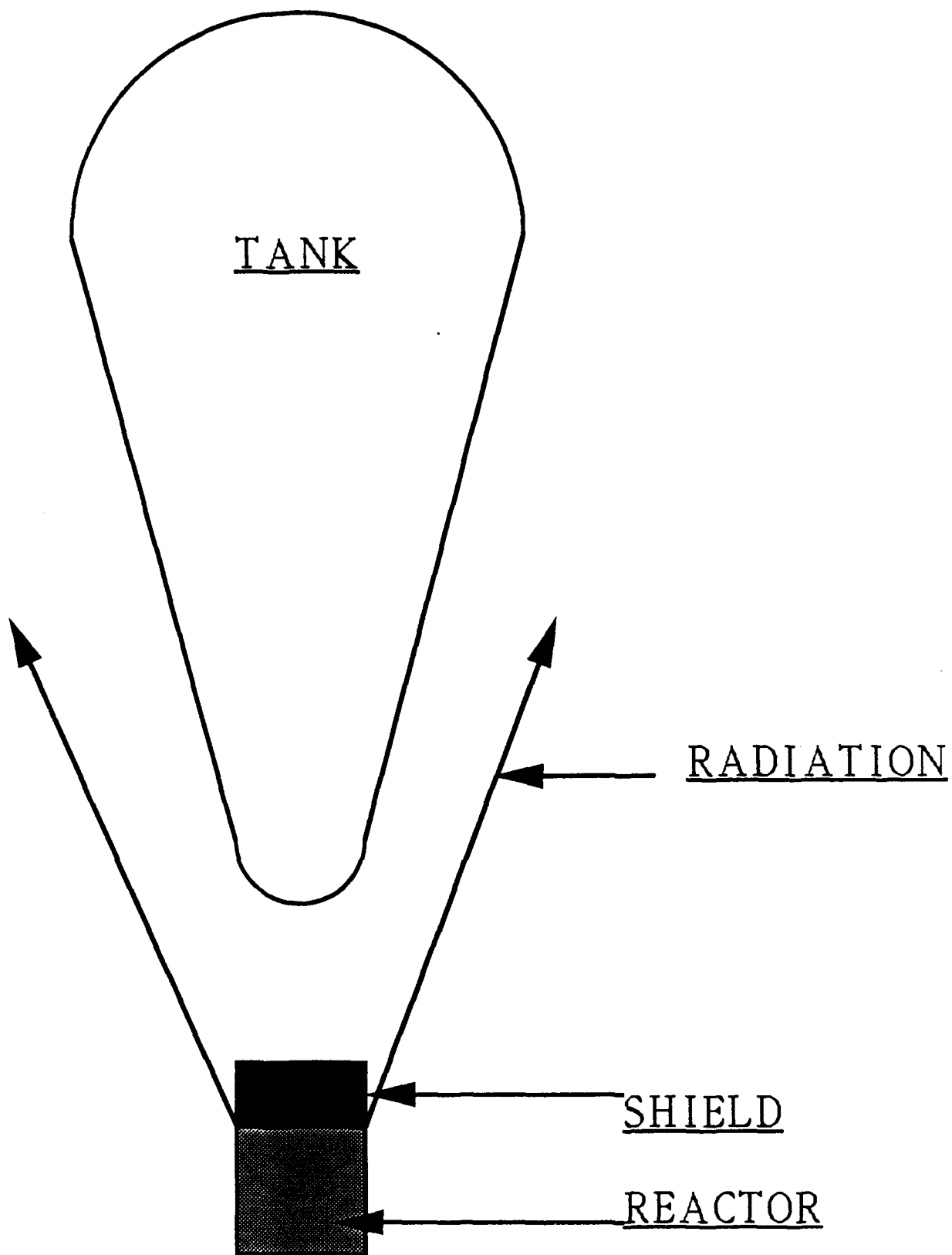


Figure 12: Cone Tank

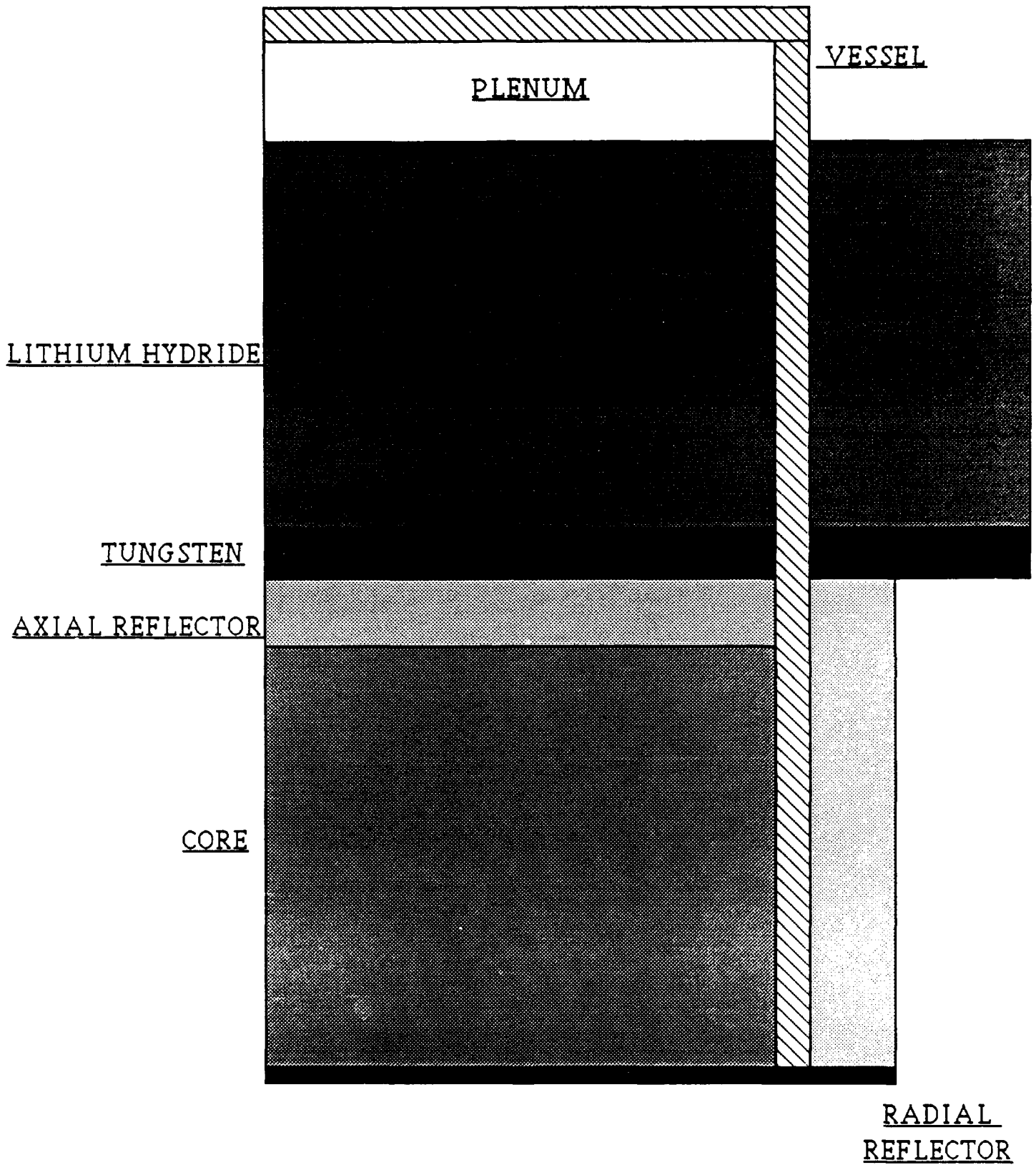


Figure 13: Collar Shield with Support

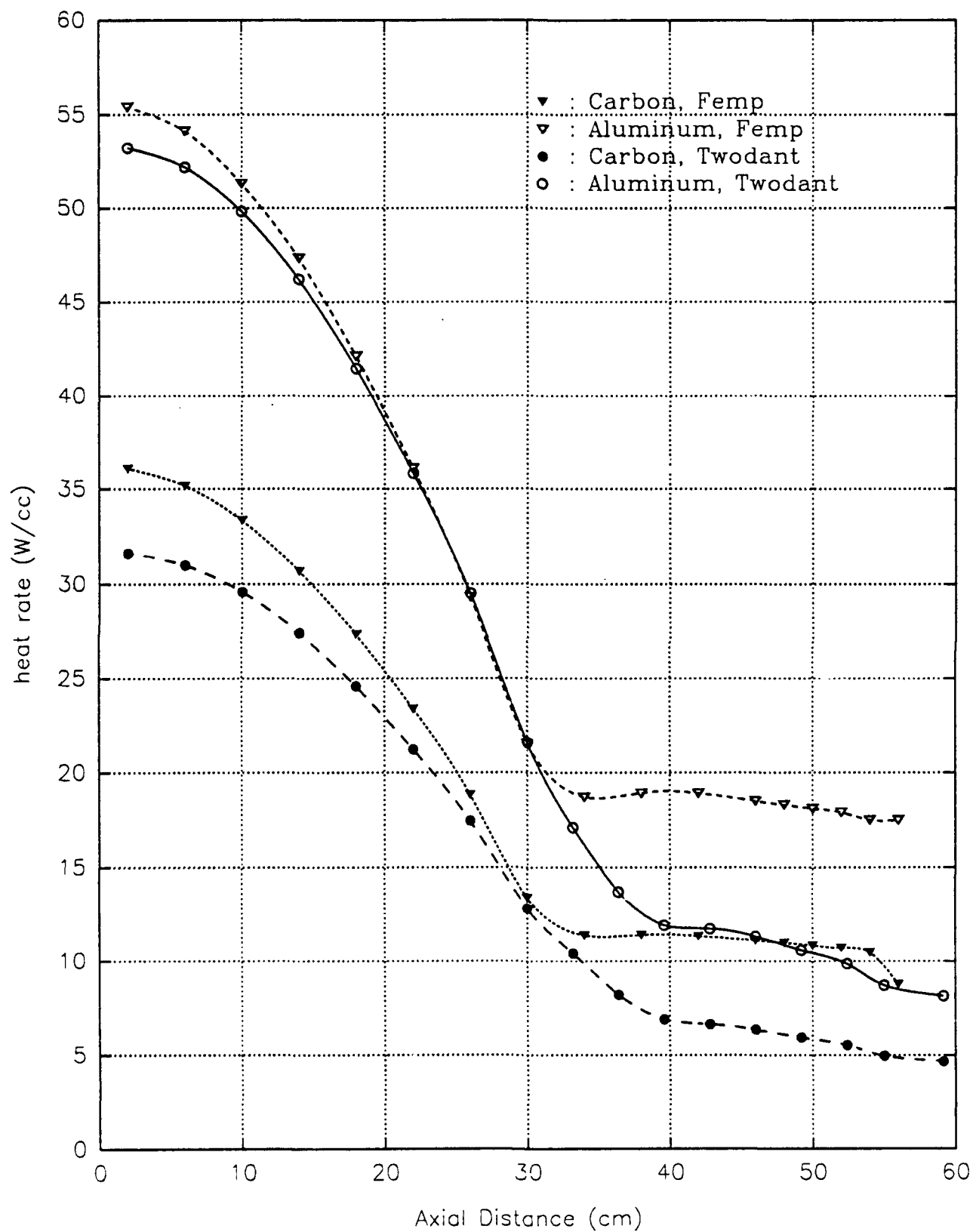
This study was initiated to study nuclear heating to help in shield design. A further, ongoing goal of this study is to parameterize the heating rates in the interstage region. If heating in materials can be predicted by simple, known equations, then future designers will not have to look at nuclear heating in general, but will be able to accurately predict what will happen to any material they might wish to use.

REFERENCES

- (1) R. L. Miller, "Heating Rates in a High Energy Propulsion System (HEPS) Orbital Transfer Vehicle (OTV)," AL-TR-89-056, October 1989.
- (2) A. Henry, Nuclear Reactor Analysis, The MIT Press, Cambridge, MA, 1975, Chapter 8.
- (3) R. O'Dell, F. Brinkley, D. Marr, and R. Alcouffe, "Revised Users Manuel for TWODANT," Los Alamos National Lab, Los Alamos, NM, December 1989.
- (4) S. Glasstone and A. Sesonske, Nuclear Reactor Engineering, Van Nostrand Reinhold Co., 3rd Ed., 1981, Chapters 1 and 2.
- (5) Y. Gohar and M. Abdou, "MACKLIB-IV, a Library of Nuclear Response Functions Generated with the MACK-IV Computer Program from ENDF/B-IV," ANL/FPP/TM-106, 1978.
- (6) A. Chilton, J. Shultis, and R. Faw, Principles of Radiation Shielding, Prentice-Hall Inc., Englewood, NJ, 1984, Chapter 3.
- (7) Private conversations with Dr. R. J. Cerbone, Brookhaven National Lab.

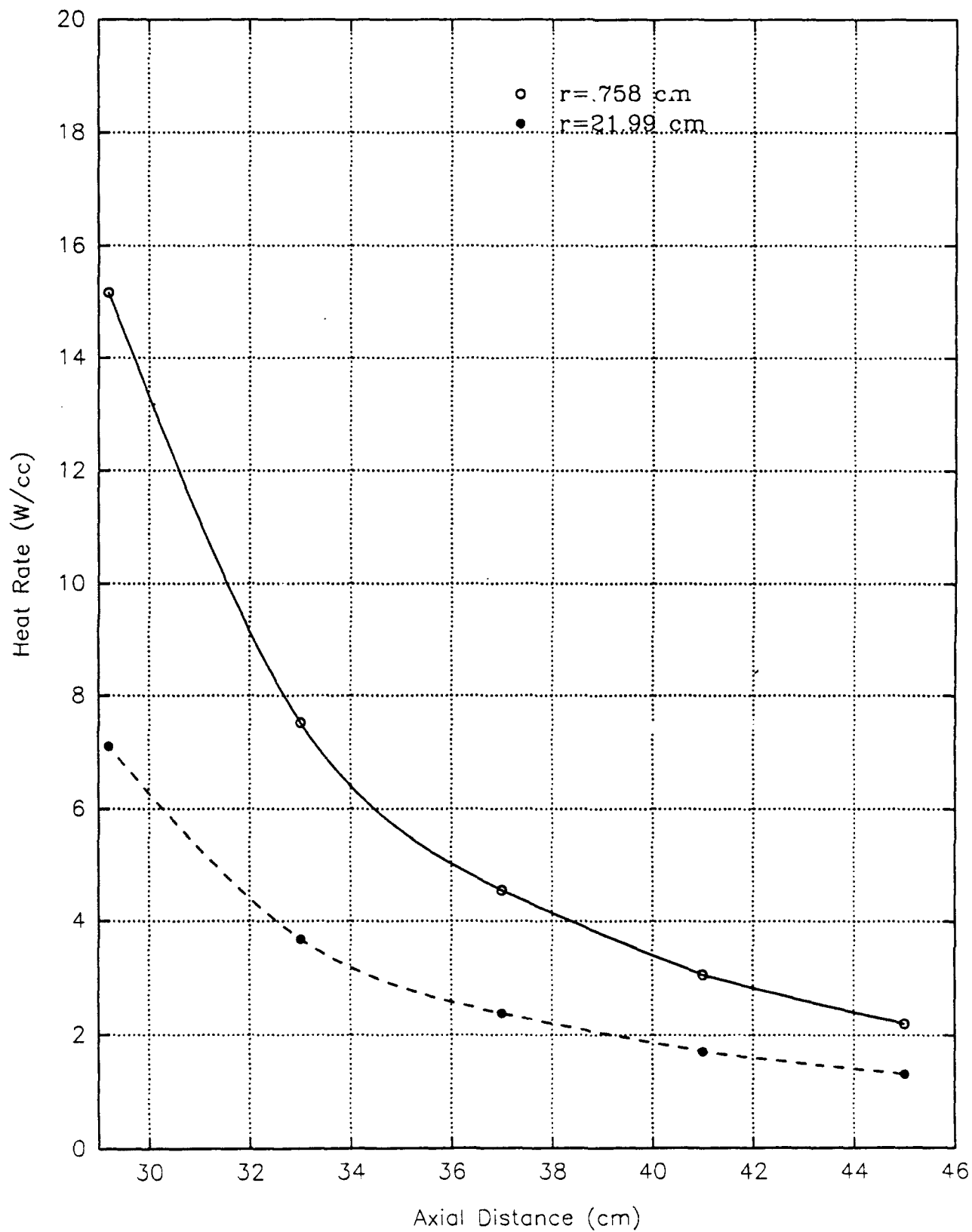
APPENDIX
(Graphs #'s 1-52)

Comparison of Aluminum and Carbon heating rates
in the pressure vessel calculated from TWODANT and FEM2D



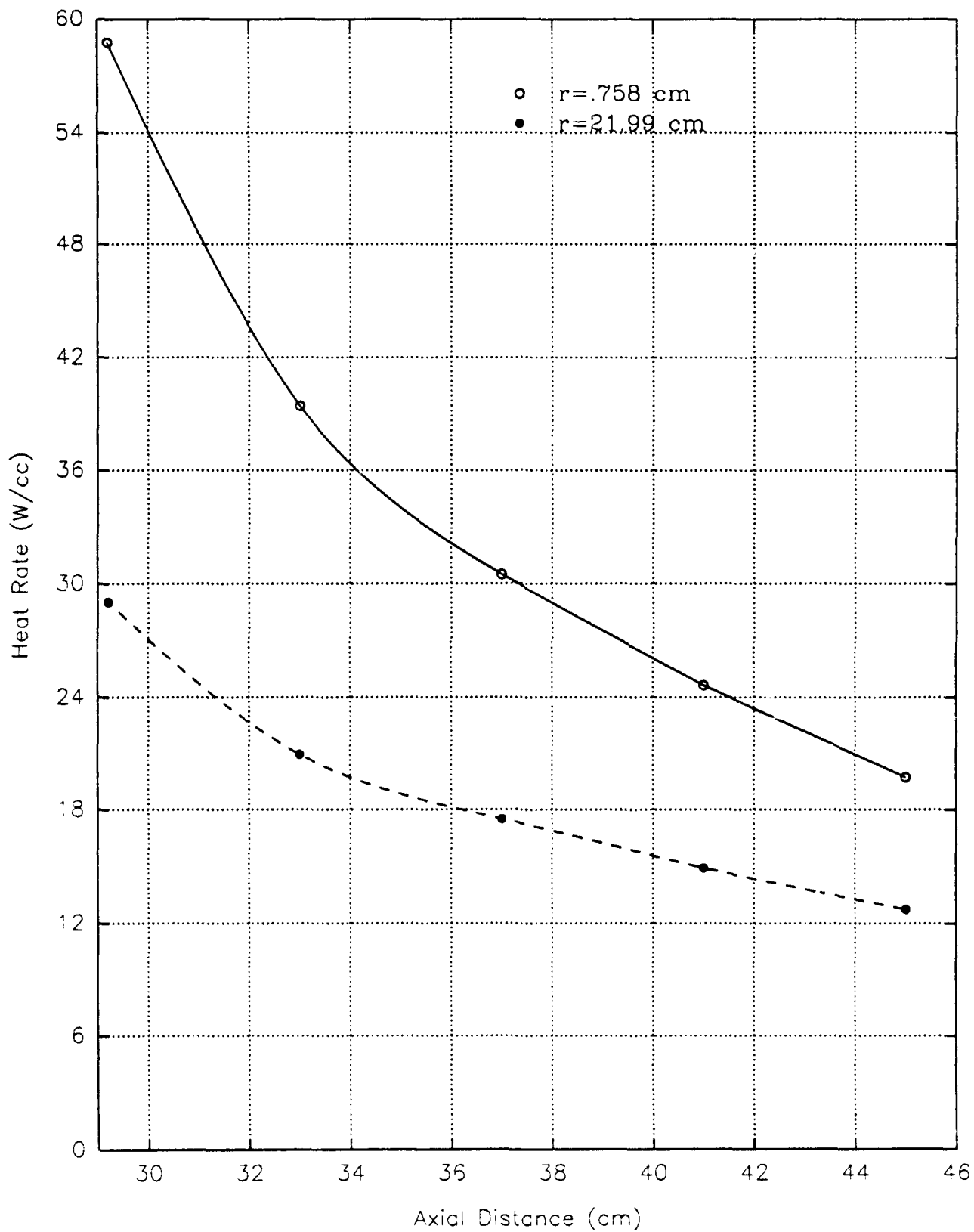
Graph #1

Hydrogen heating in the plenum region of a lithium hydride
moderated 400 MWt PBR with no shielding.



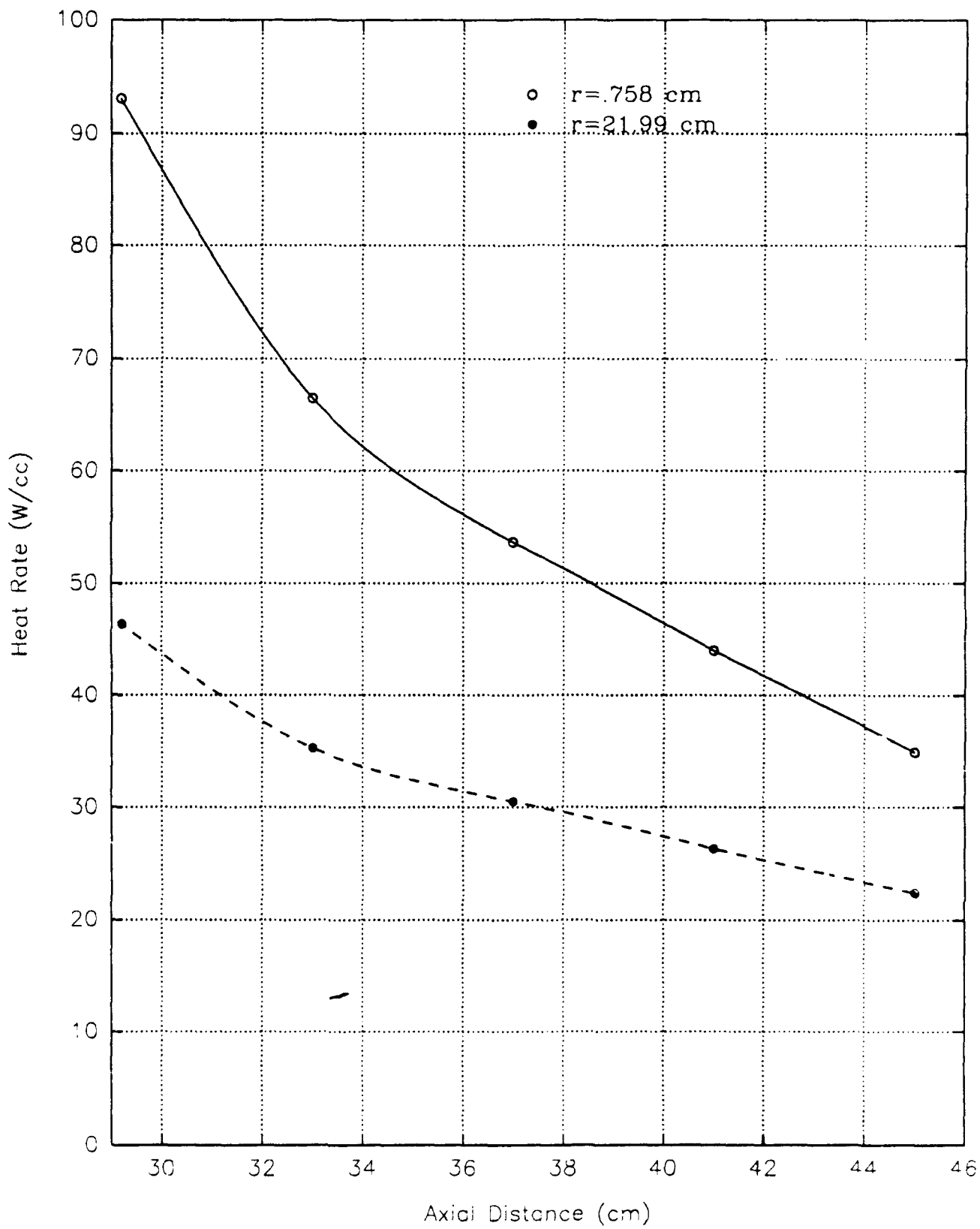
Graph #2

Carbon heating in the plenum region of a lithium hydride
moderated 400 MWt PBR with no shielding.



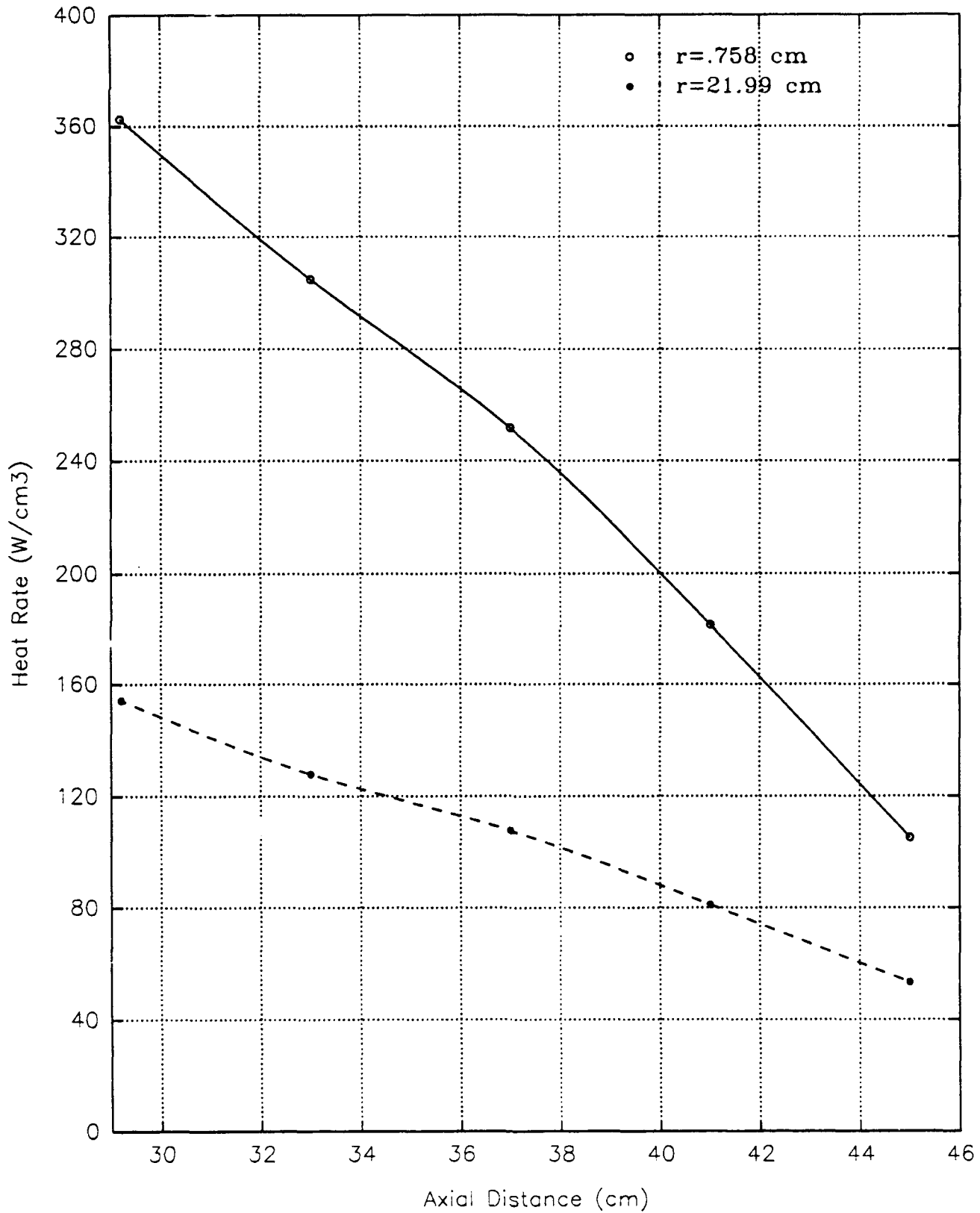
Graph #3

Aluminum heating in the plenum region of a lithium hydride
moderated 400 MWt PBR with no shielding.



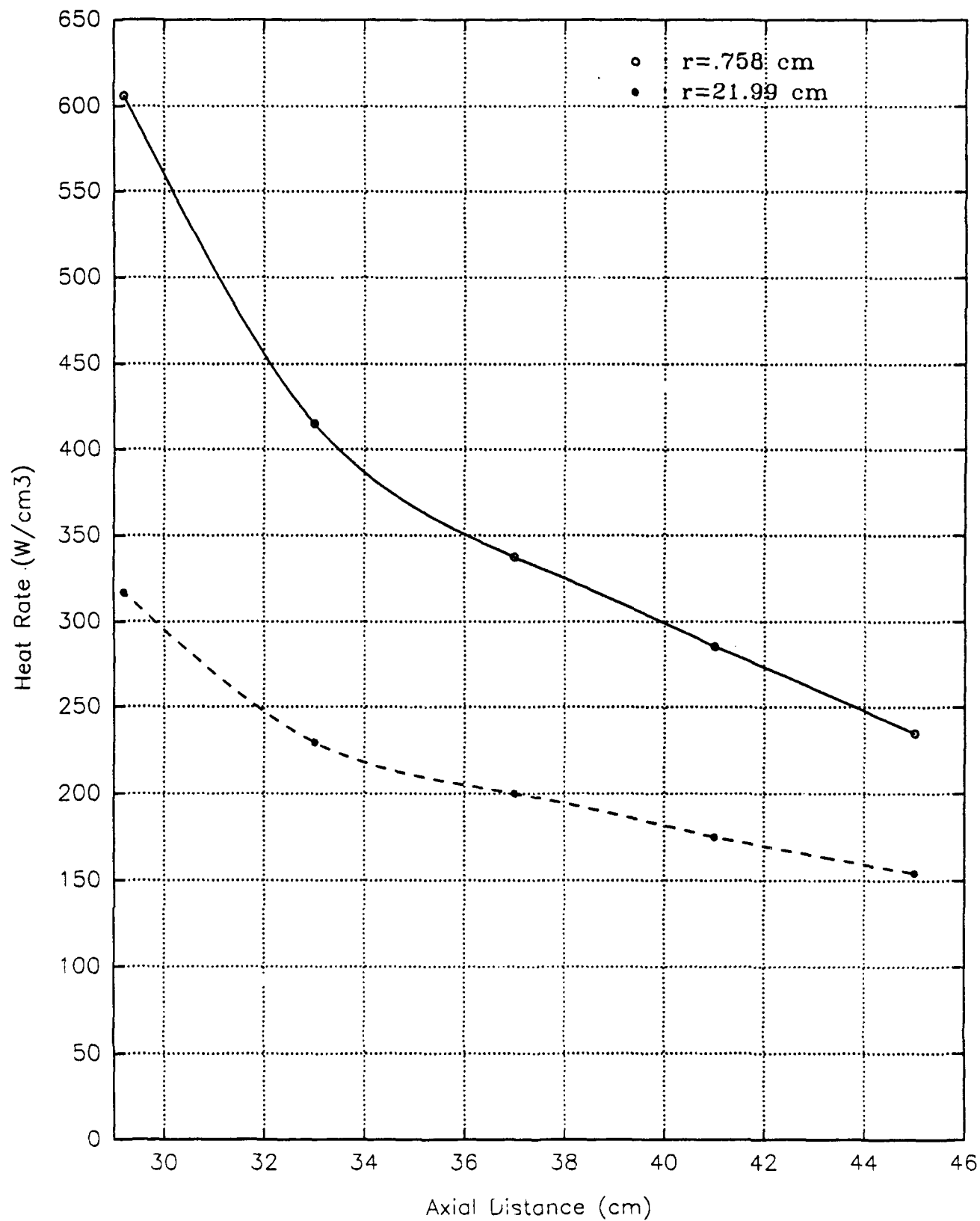
Graph #4

Titanium heating in the plenum region of a lithium hydride
moderated 400 MWt PBR with no shielding



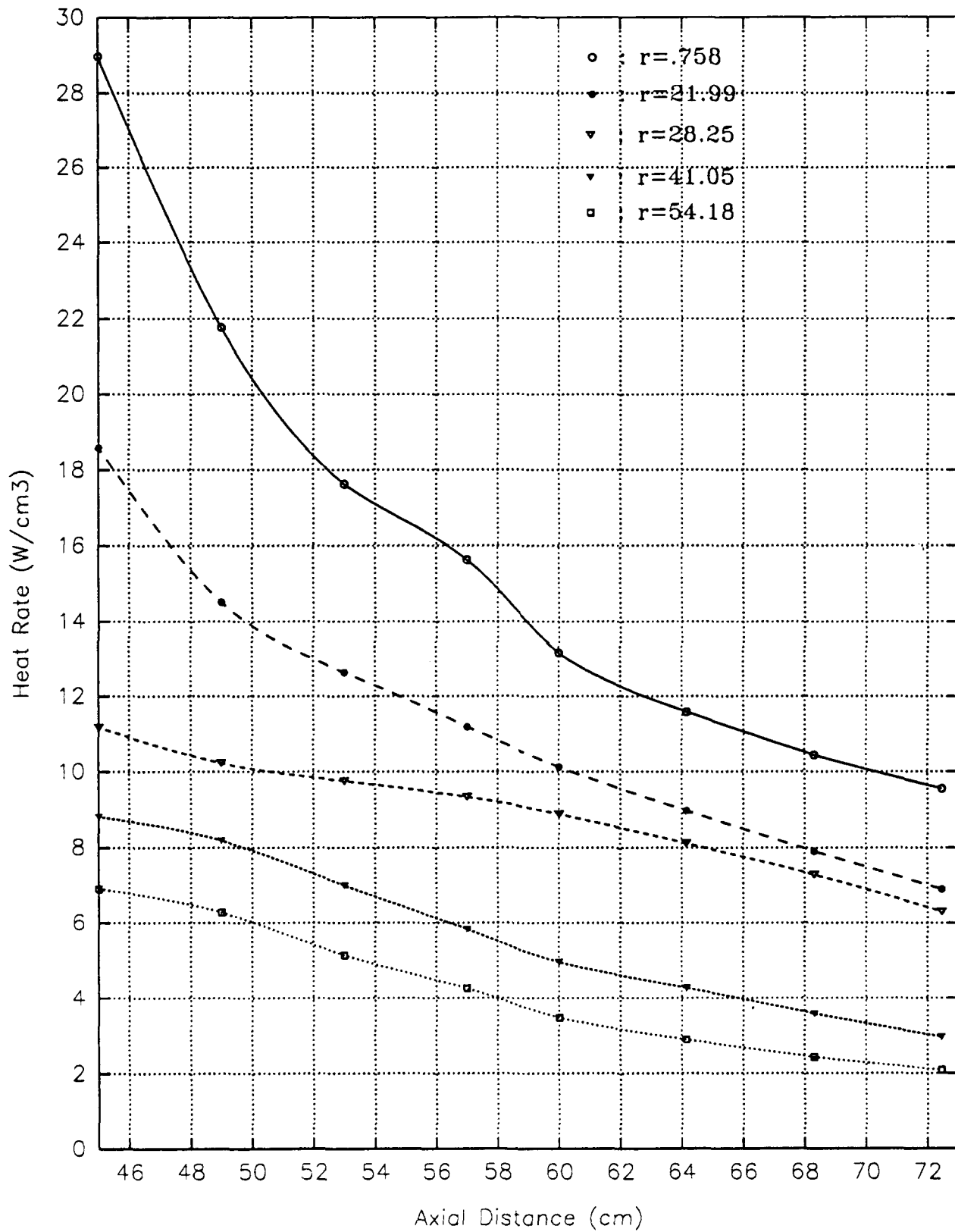
Graph #5

Stainless Steel heating in the plenum region of a lithium hydride
moderated 400 MWt PBR with no shielding



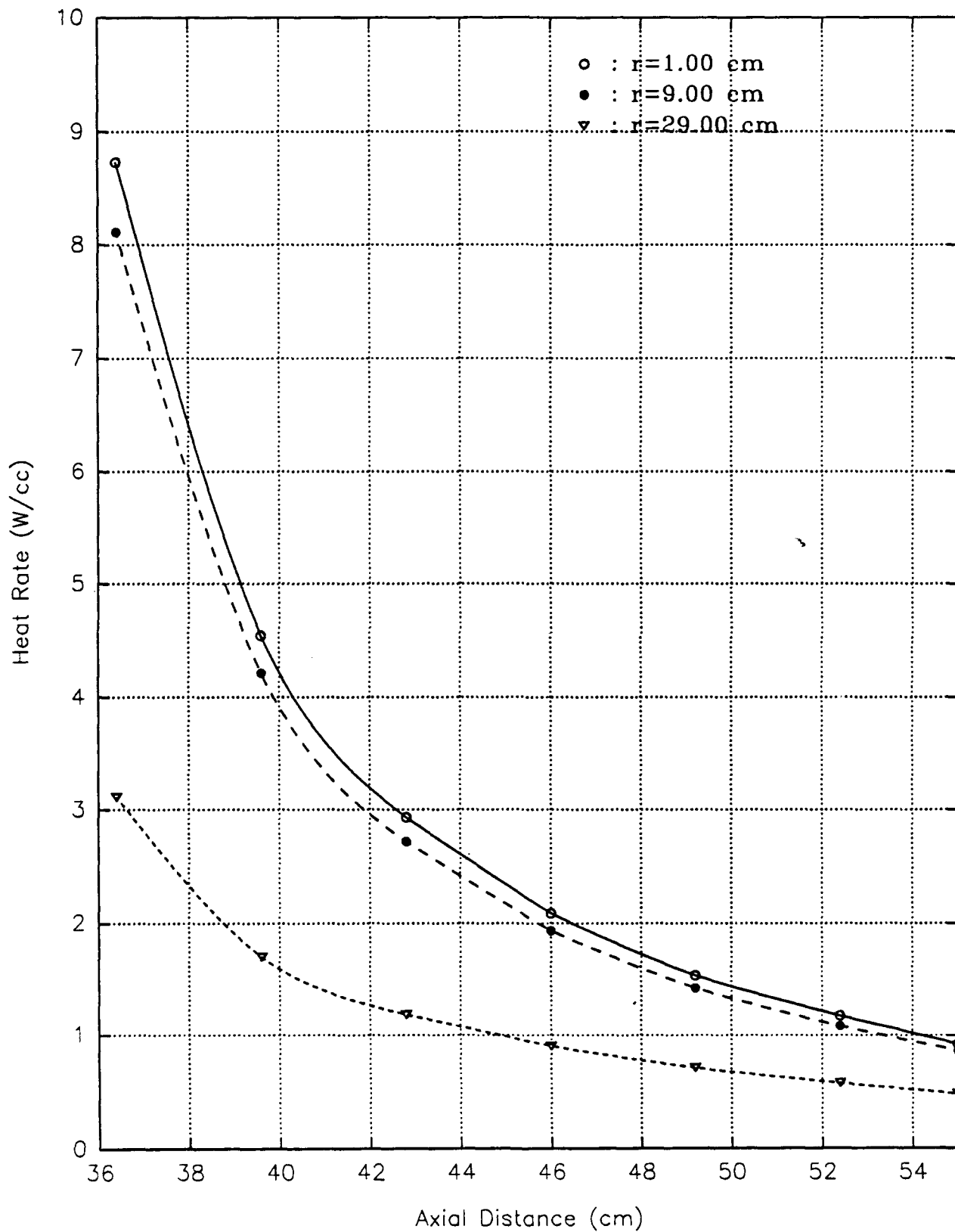
Graph #6

Silicon heating in the TPA region of a lithium hydride
moderated 400 MWt PBR with no shielding



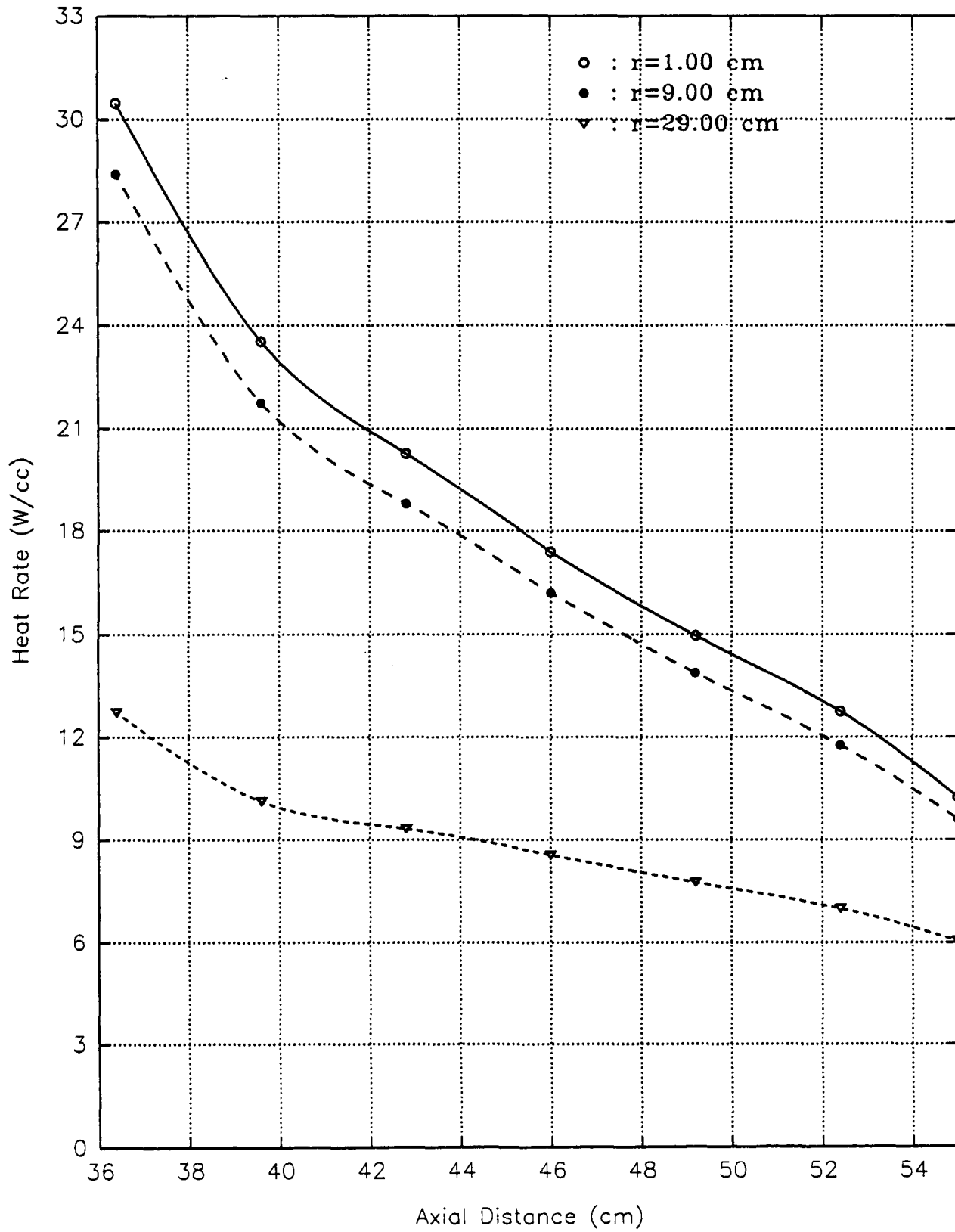
Graph #7

Hydrogen heating in the plenum region of a beryllium
moderated 400 MWt PBR with no shielding



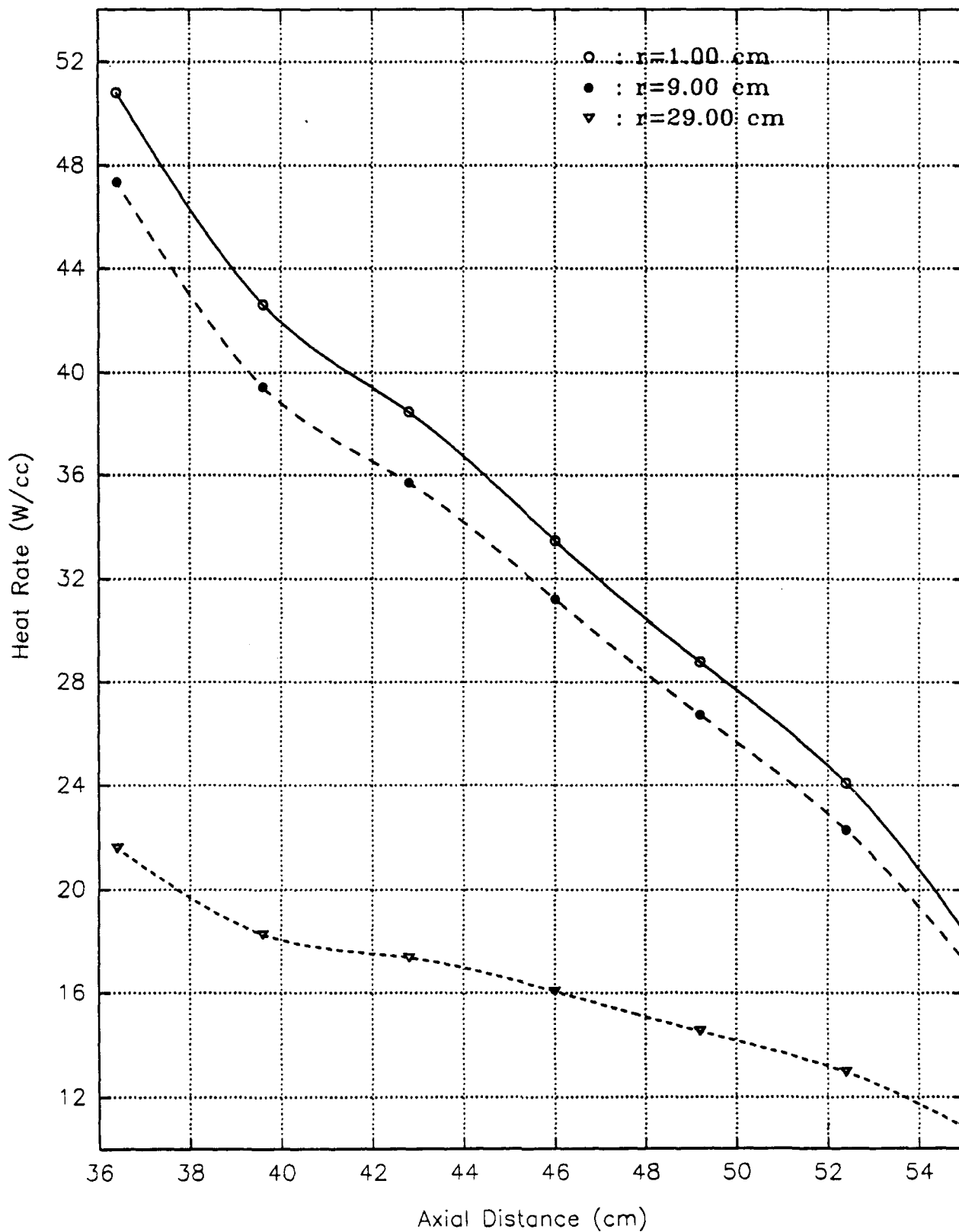
Graph #8

Carbon heating in the plenum region of a beryllium
moderated 400 MWt PBR with no shielding



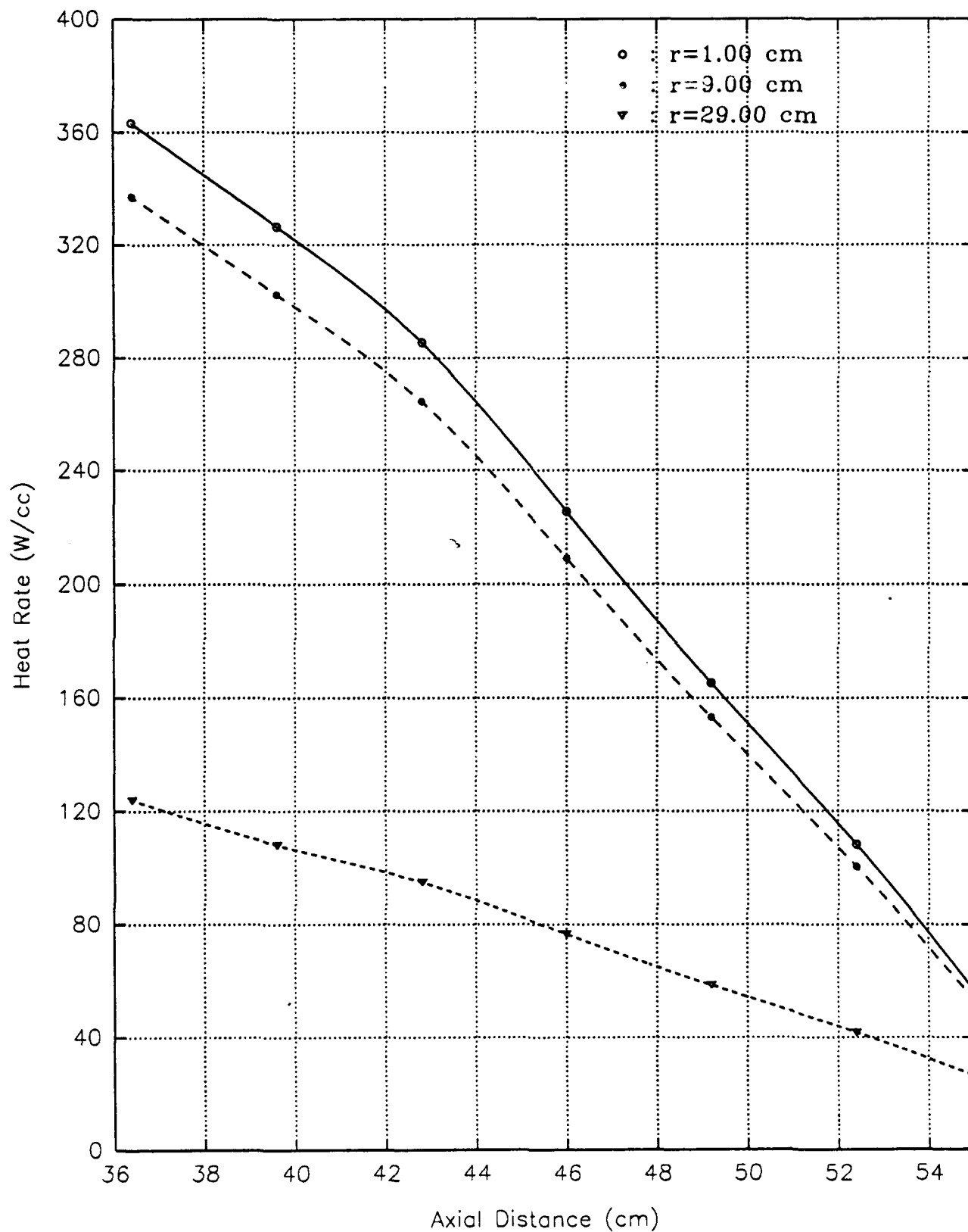
Graph #9

Aluminum heating in the plenum region of a beryllium
moderated 400 MWt PBR with no shielding



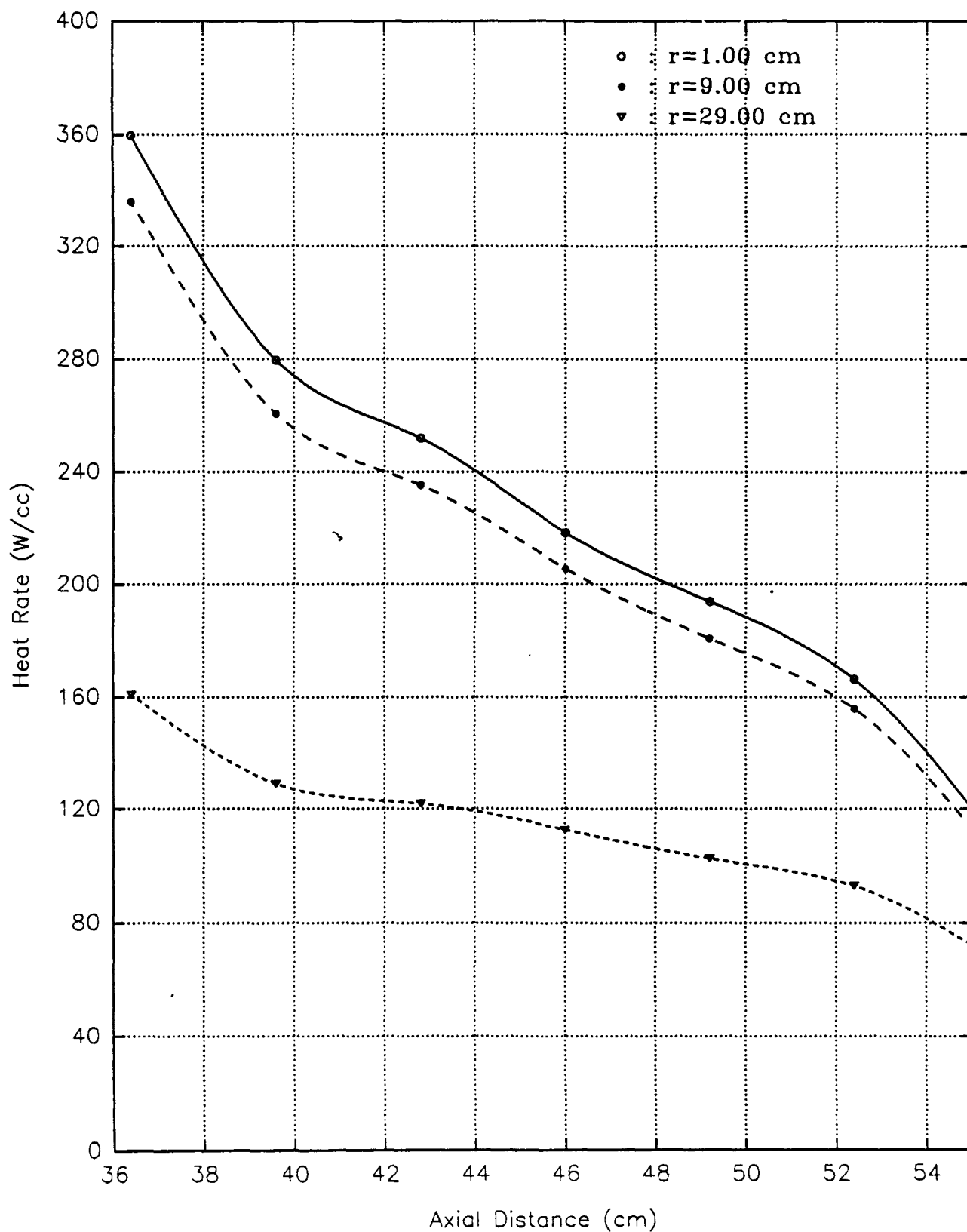
Graph #10

Titanium heating in the plenum region of a beryllium
moderated 400 MWt PBR with no shielding



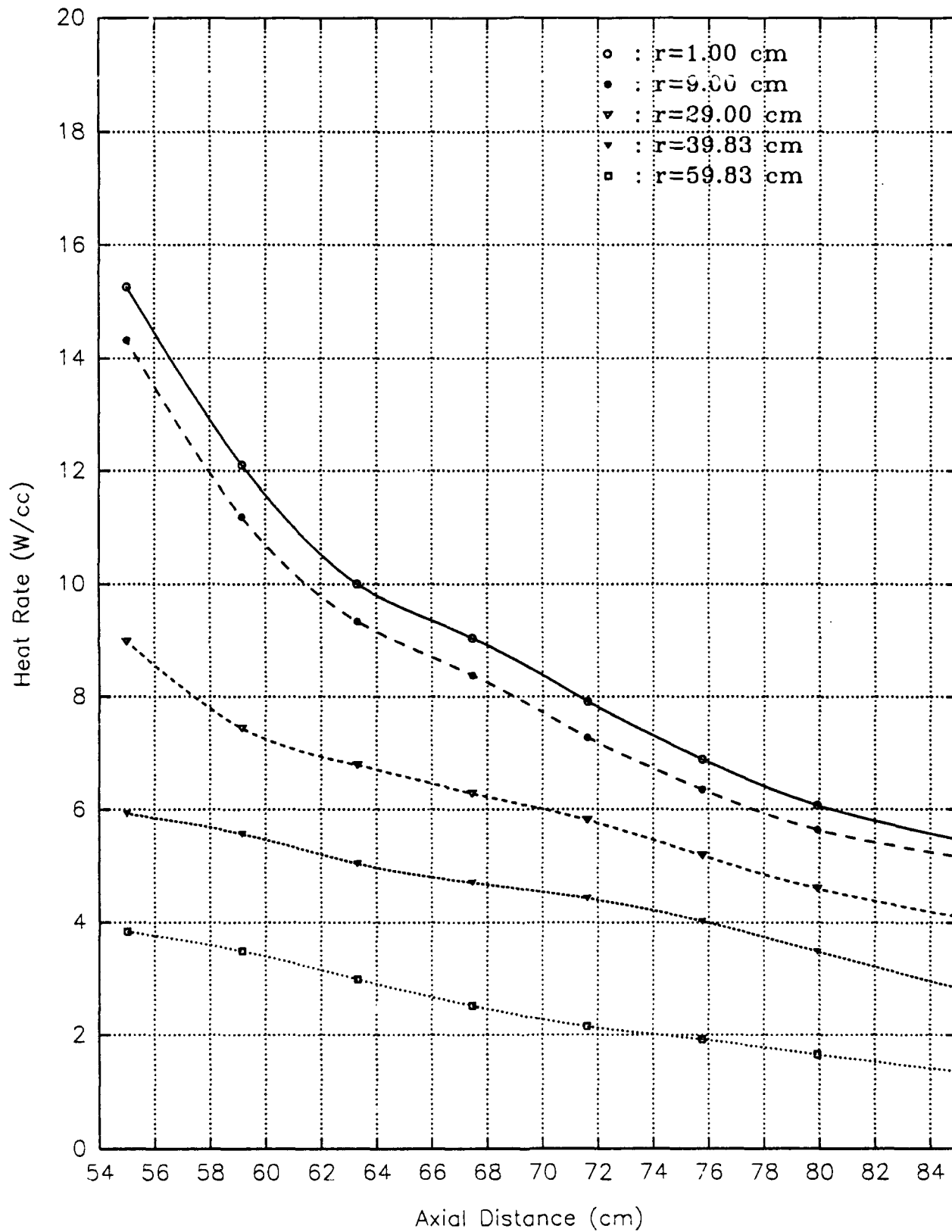
Graph #11

Stainless Steel heating in the plenum region of a beryllium
moderated 400 MWt PBR with no shielding



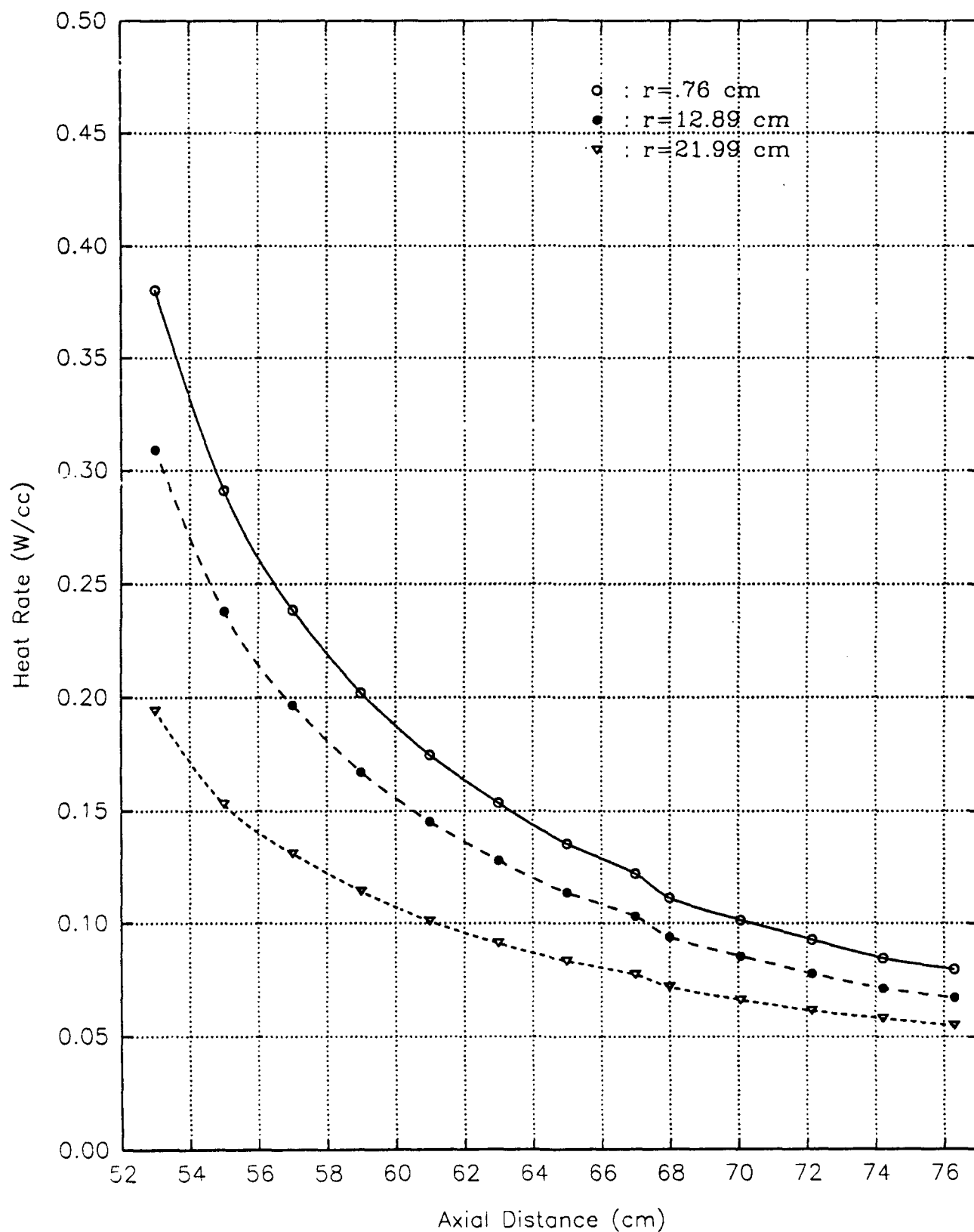
Graph #12

Silicon heating in the TPA/void region of a beryllium
moderated 400 MWt PBR with no shielding



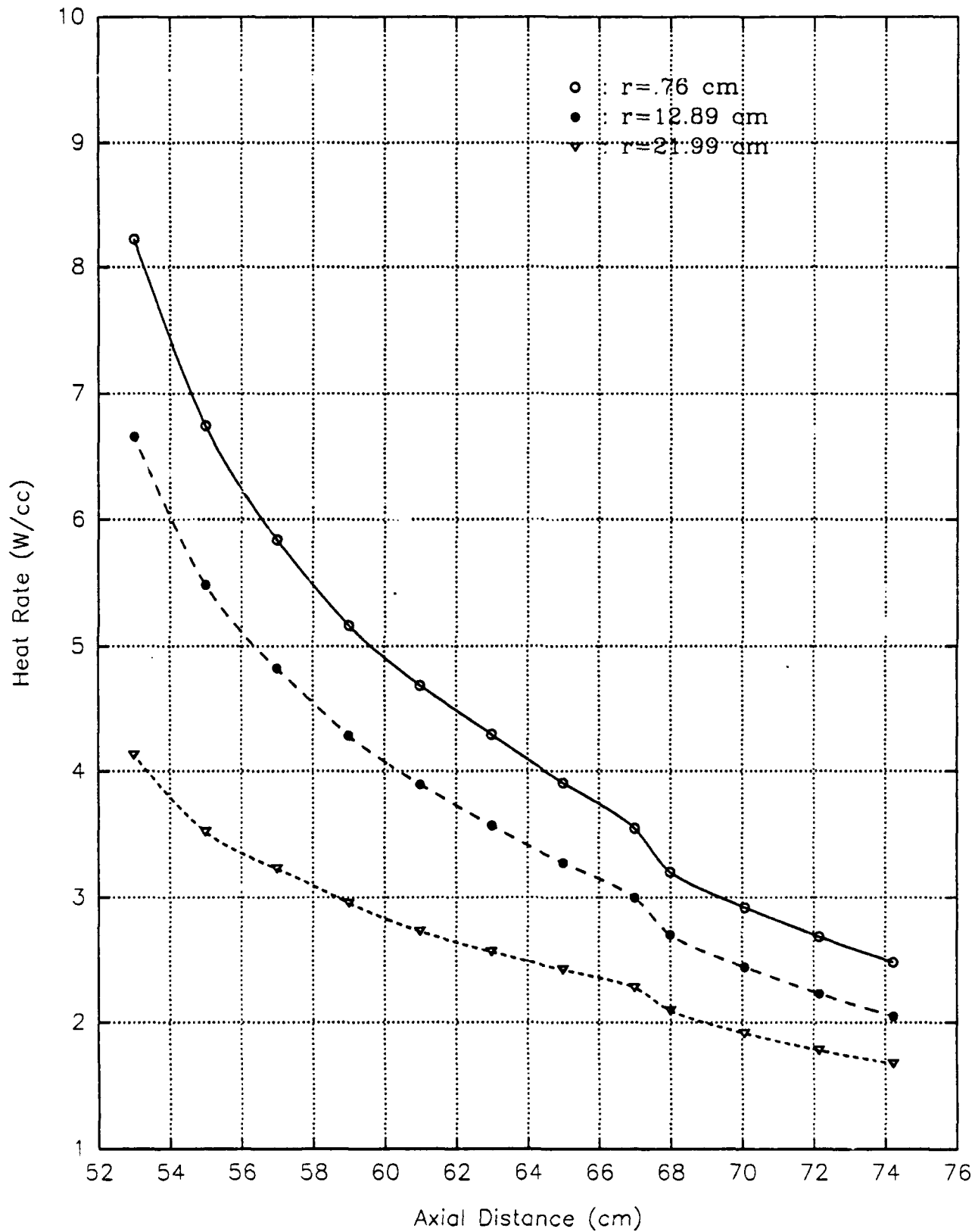
Graph #13

Hydrogen heating in the plenum region of a lithium hydride
moderated 400 MWt PBR with a BATH shield



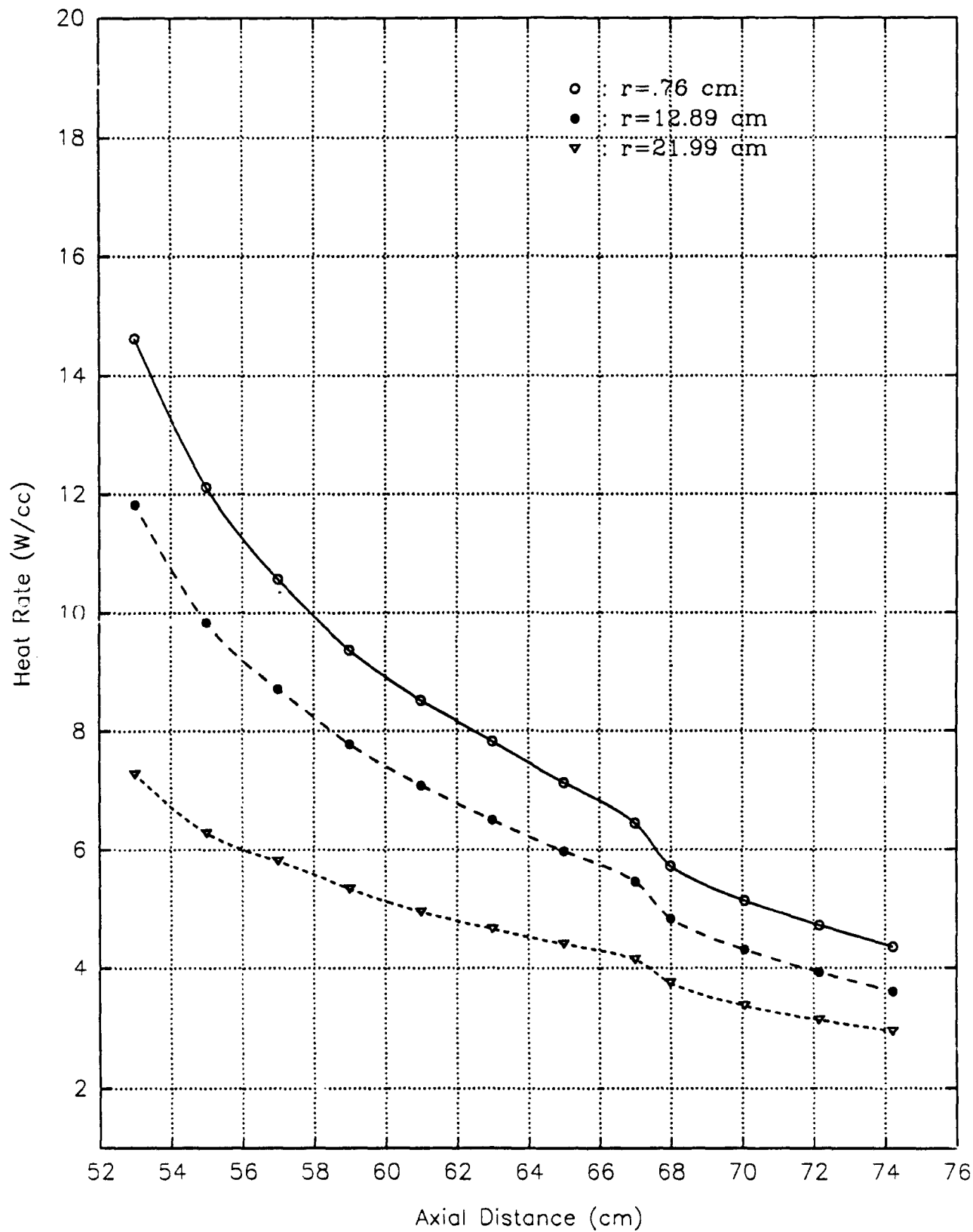
Graph #14

Carbon heating in the plenum region of a lithium hydride
moderated 400 MWt PBR with a BATH shield



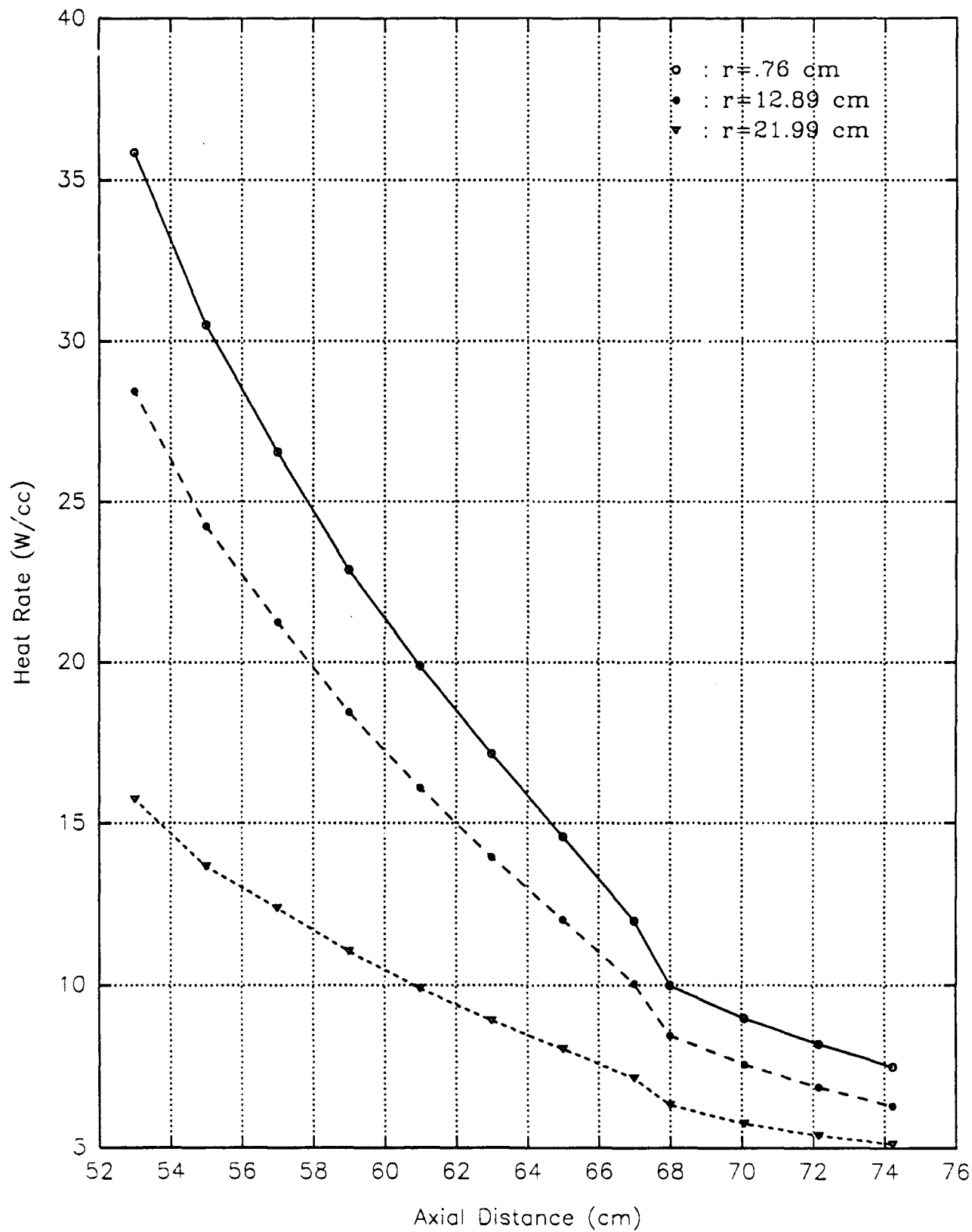
Graph #15

Aluminum heating in theplenum region of a lithium hydride
moderated 400 MWt PBR with a BATH shield



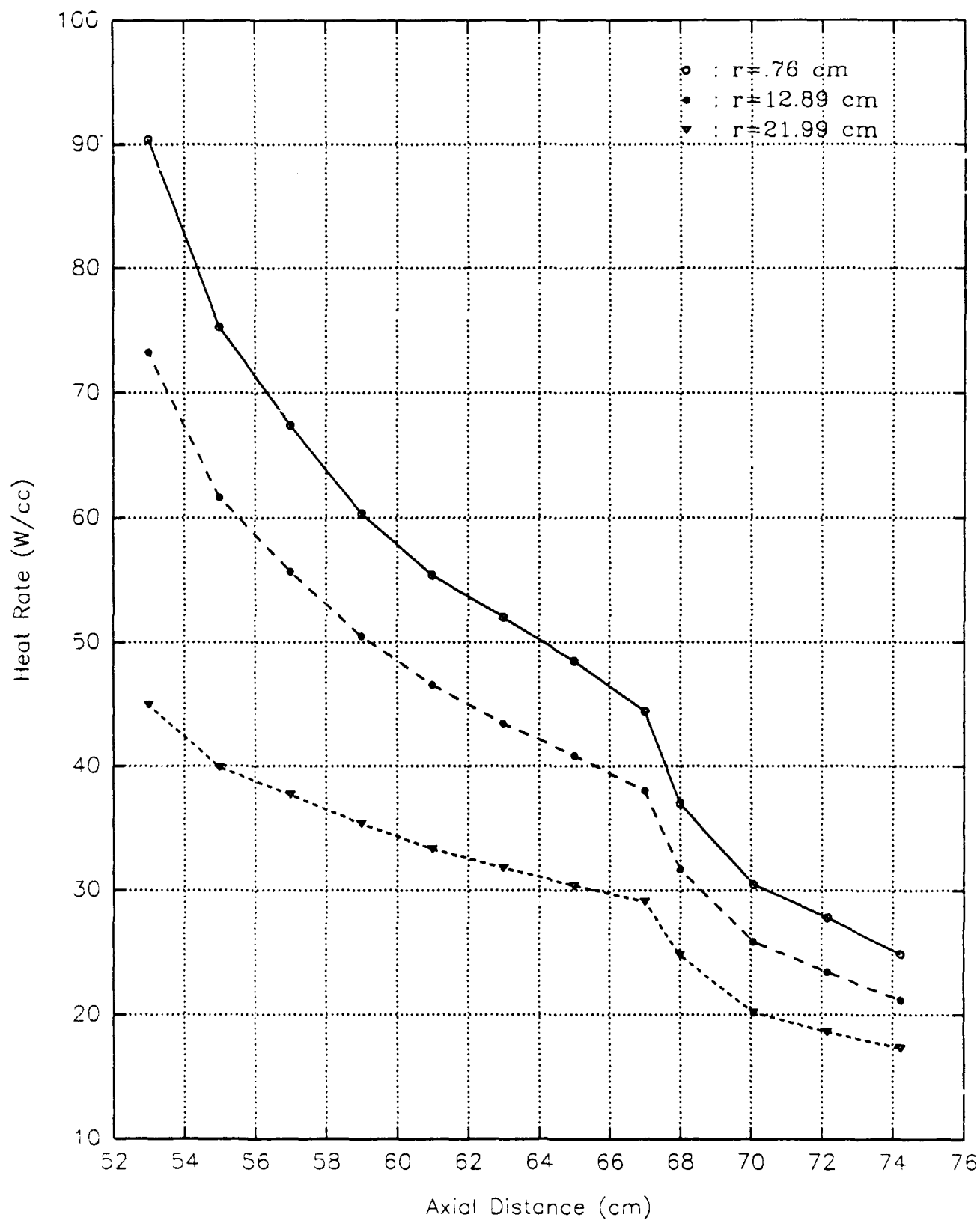
Graph #16

Titanium heating in the plenum region of a lithium hydride
moderated 400 MWt PBR with a BATH shield



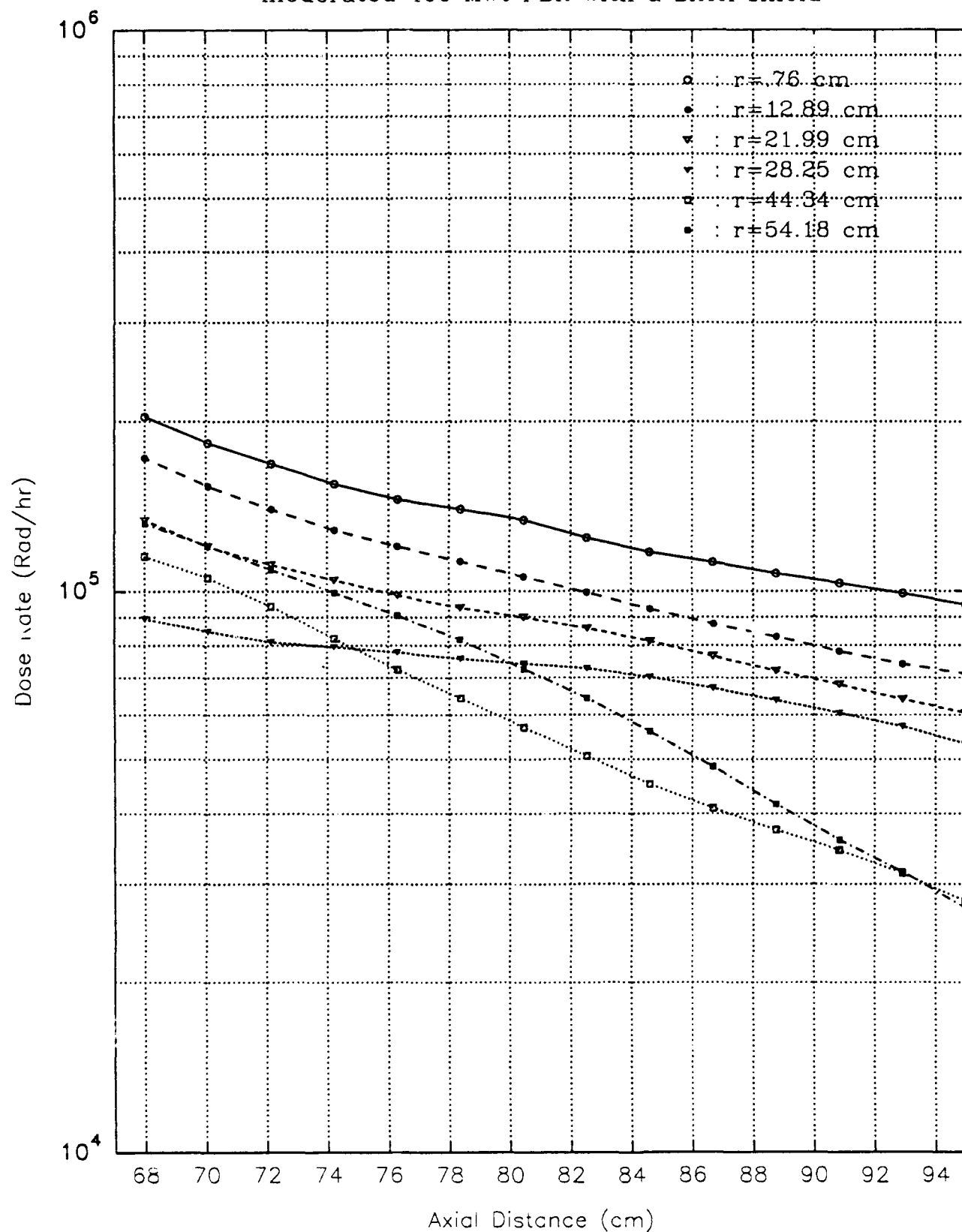
Graph #17

Stainless Steel heating in the plenum region of a lithium hydride
moderated 400 MWt PBR with a BATH shield



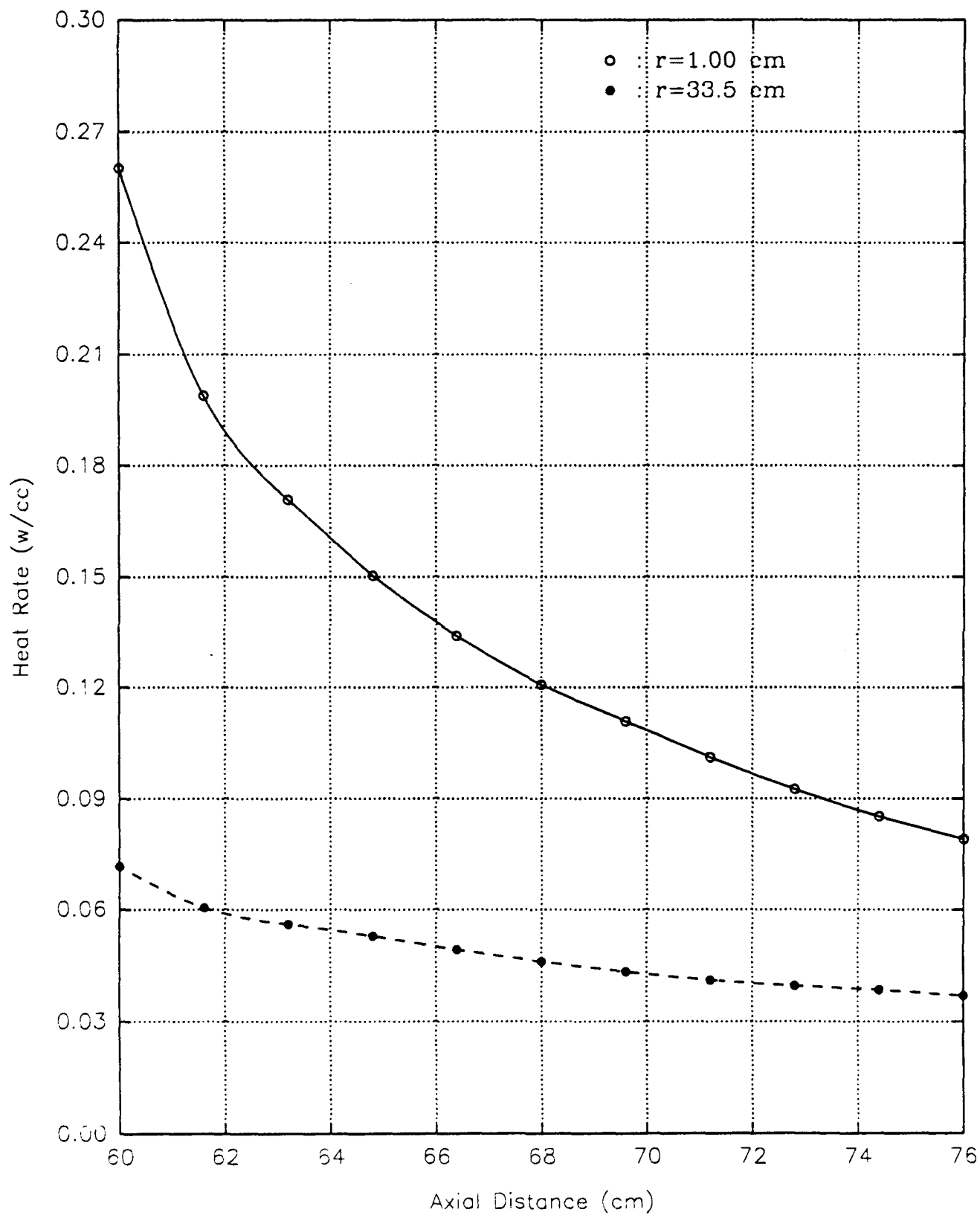
Graph #18

Silicon doses in the TPA/void region of a lithium hydride
moderated 400 MWt PBR with a BATH shield



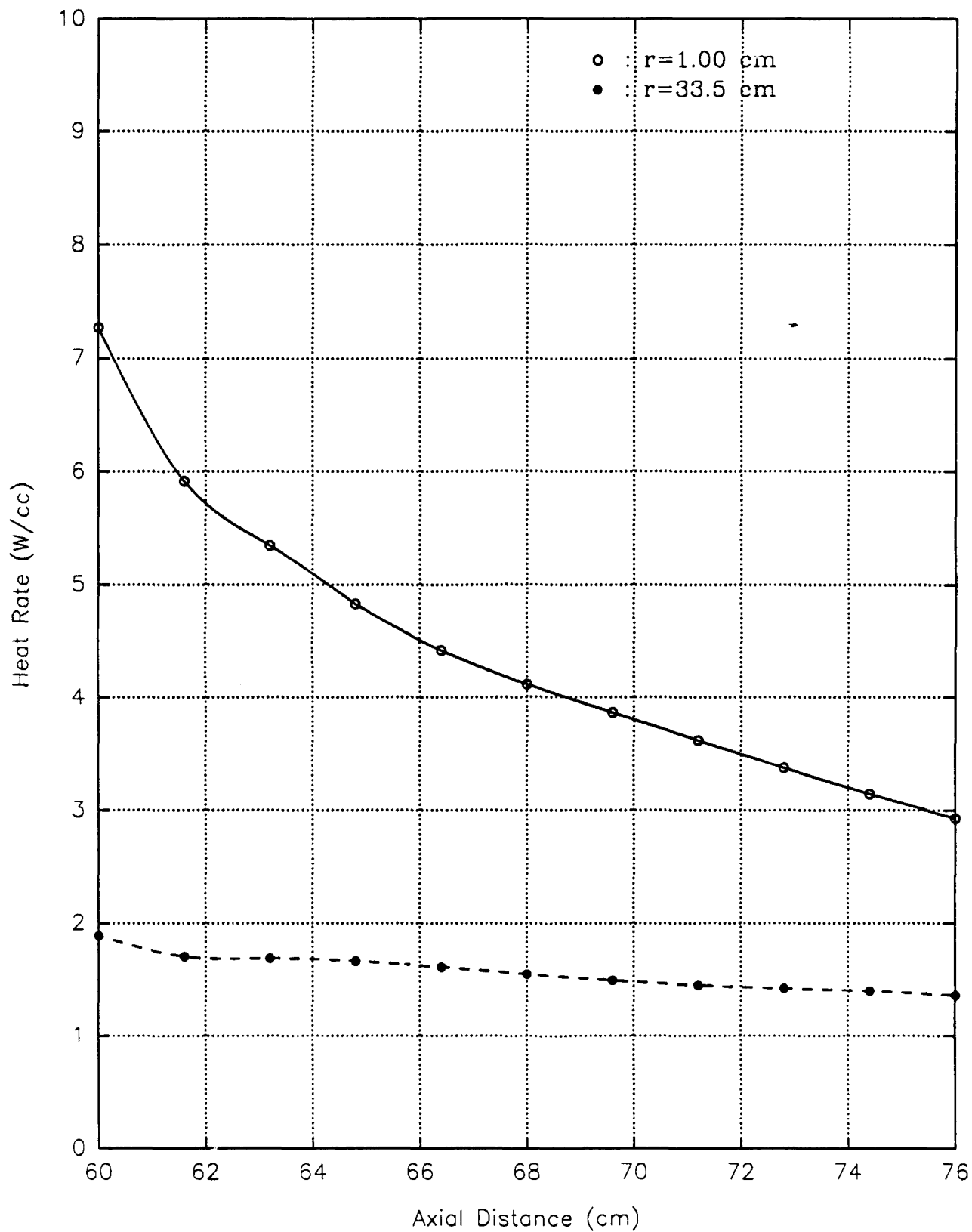
Graph #19

Hydrogen heating in the plenum region of a beryllium
moderated 400 MWt PBR with a BATH shield



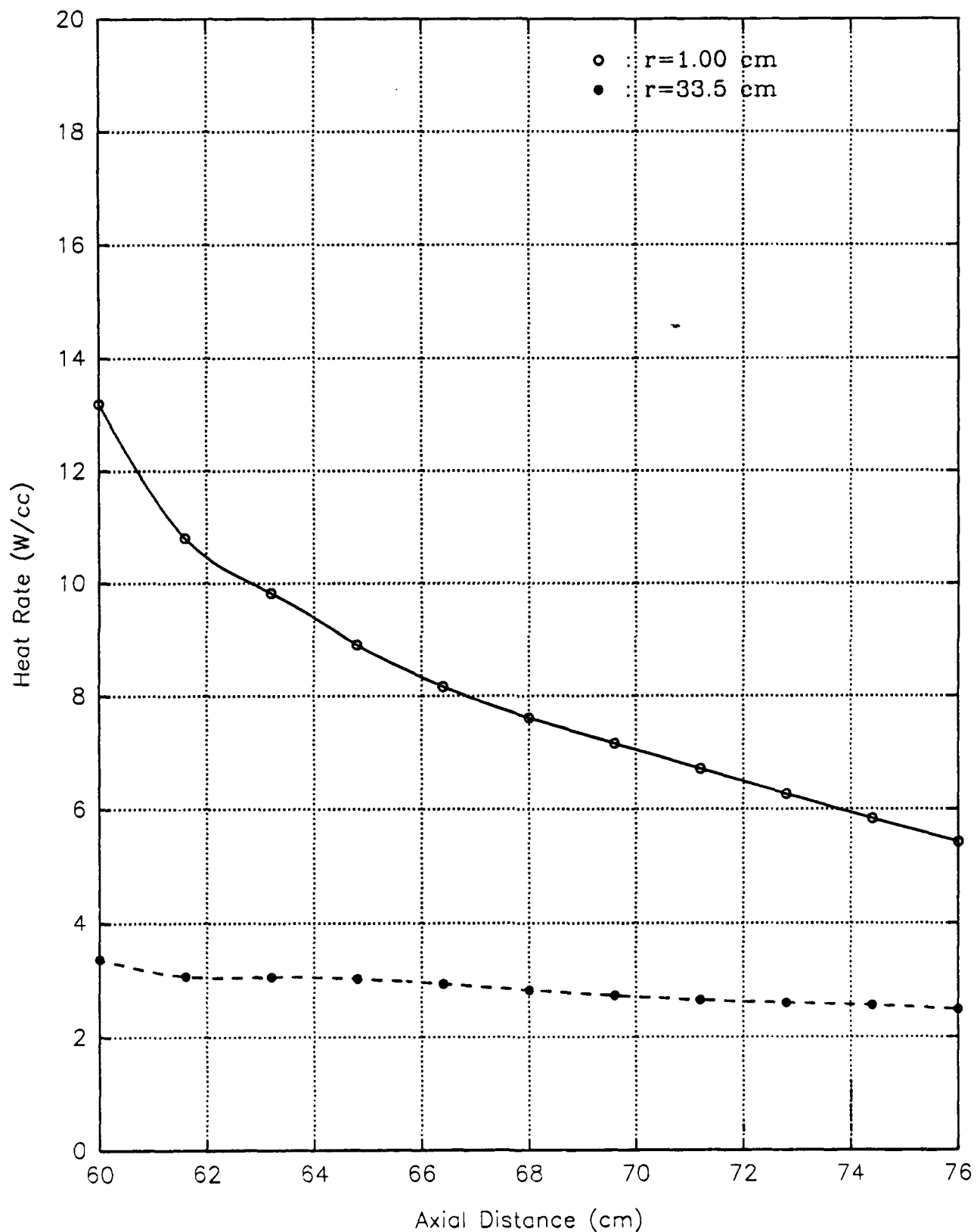
Graph #20

Carbon heating in the plenum region of a beryllium
moderated 400 MWt PBR with a BATH shield



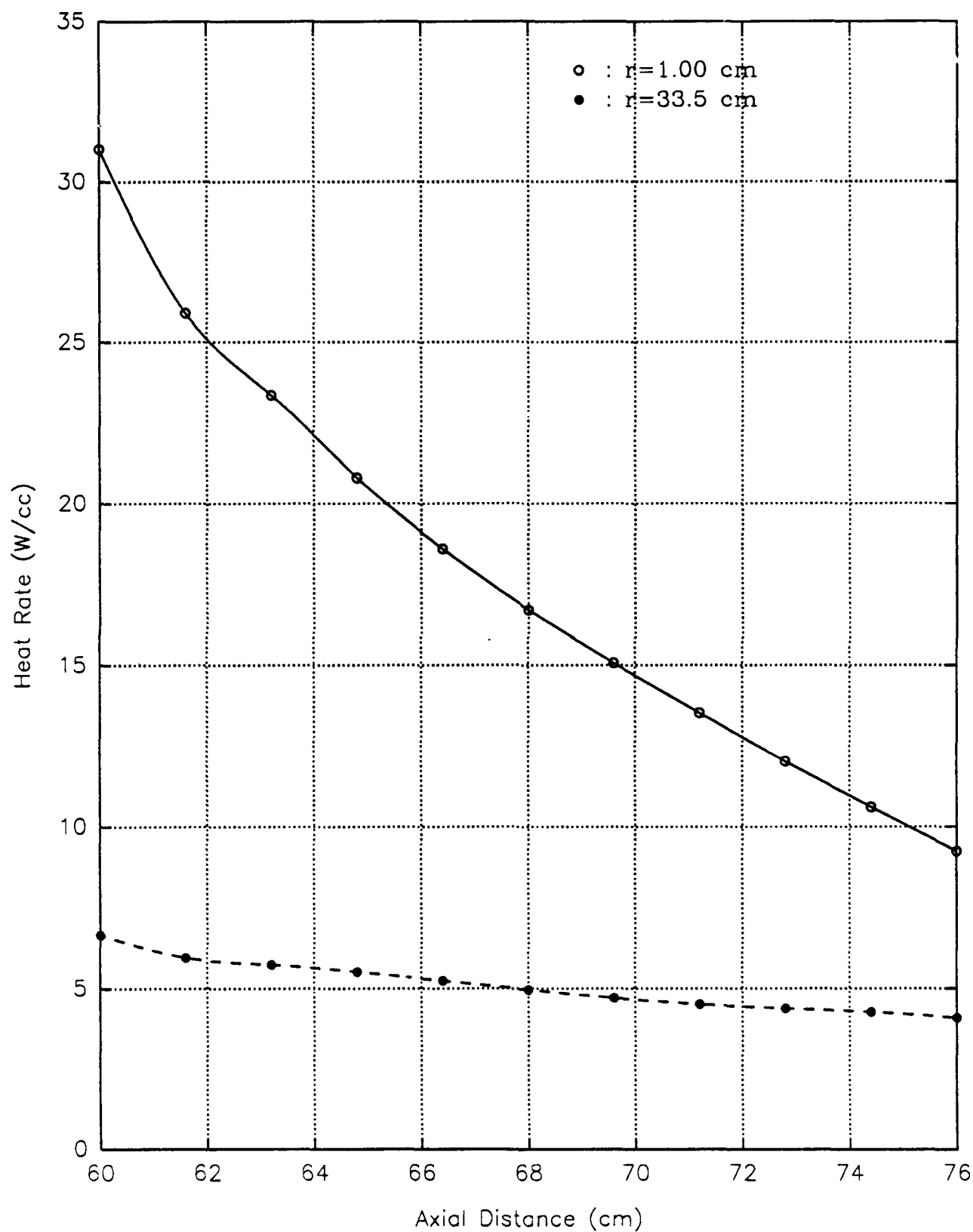
Graph #21

Aluminum heating in the plenum region of a beryllium
moderated 400 MWt PBR with a BATH shield



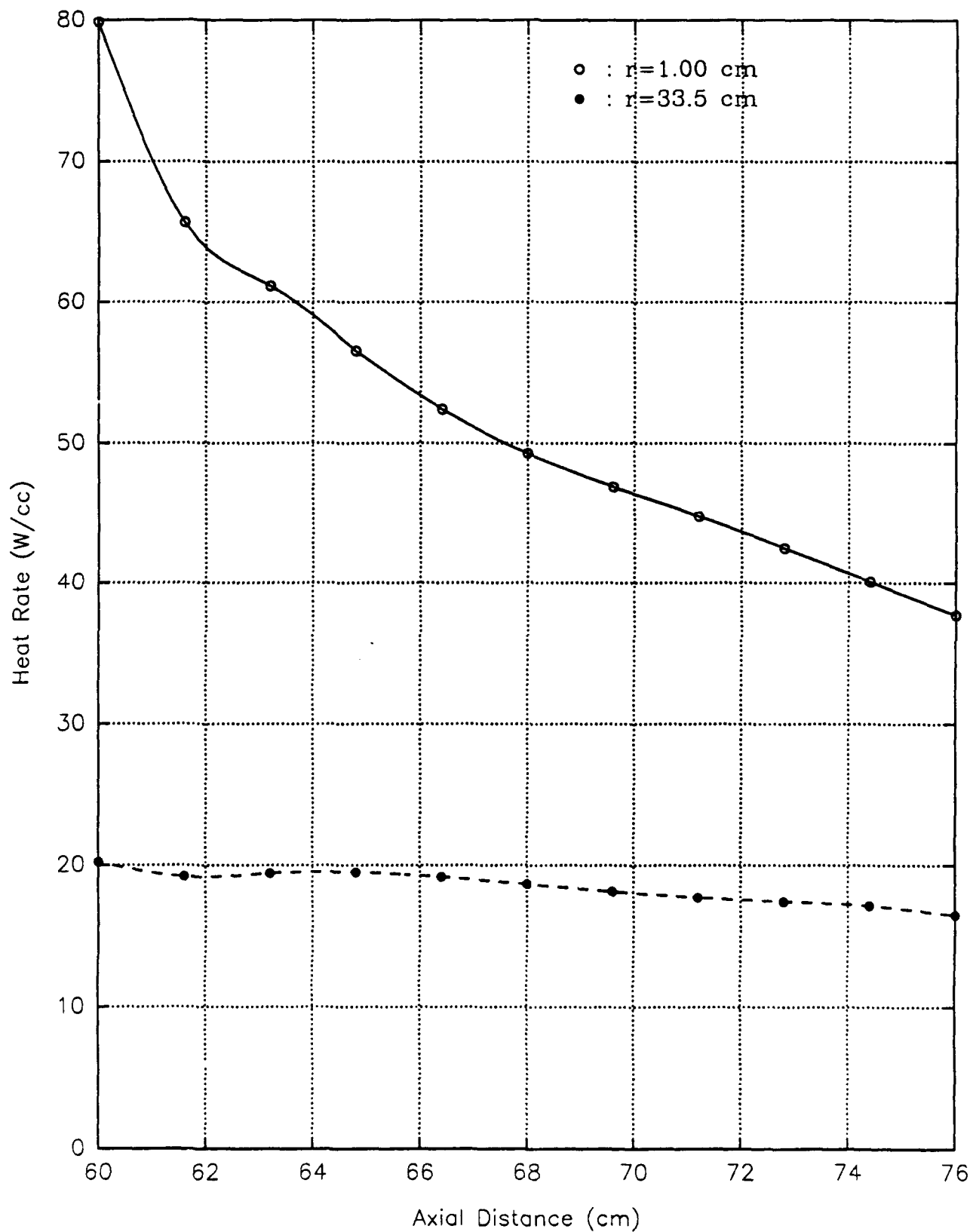
Graph #22

Titanium heating in the plenum region of a beryllium
moderated 400MWt PBR with a BATH shield



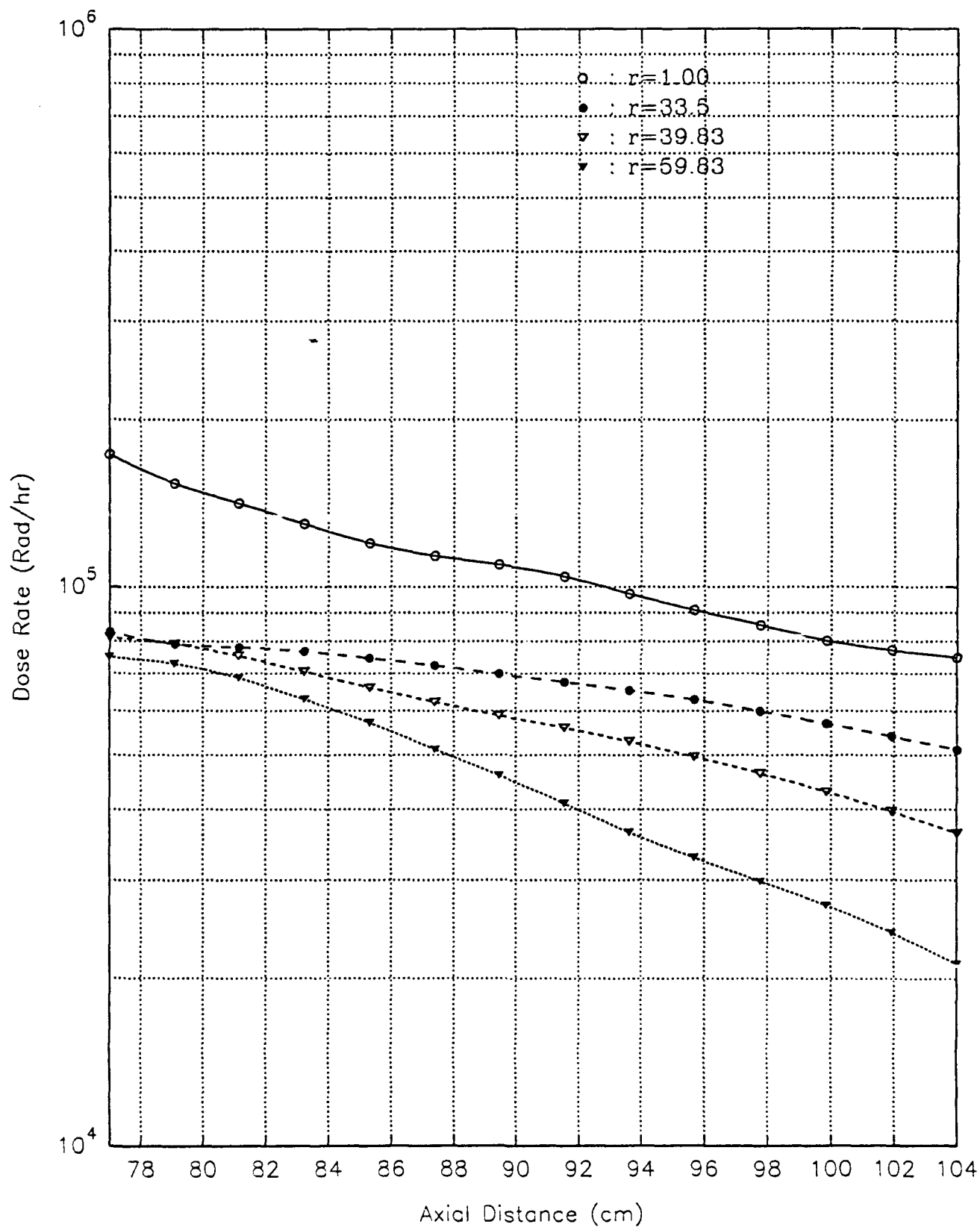
Graph #23

Stainless Steel heating in the plenum region of a beryllium
moderated 400MWt PBR with a BATH shield



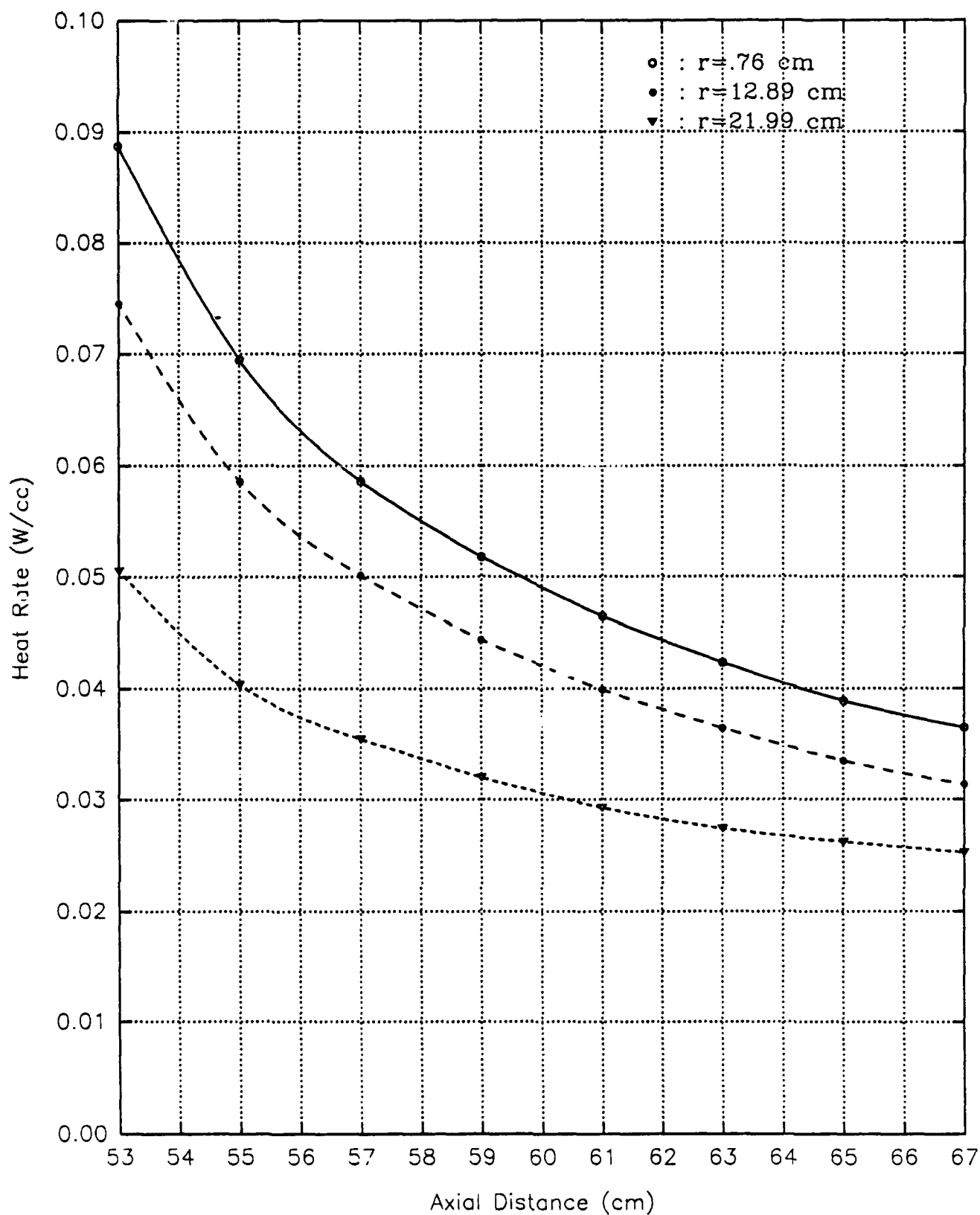
Graph #24

Silicon doses in the TPA/void region of a beryllium
moderated 400MWt PBR with a BATH shield



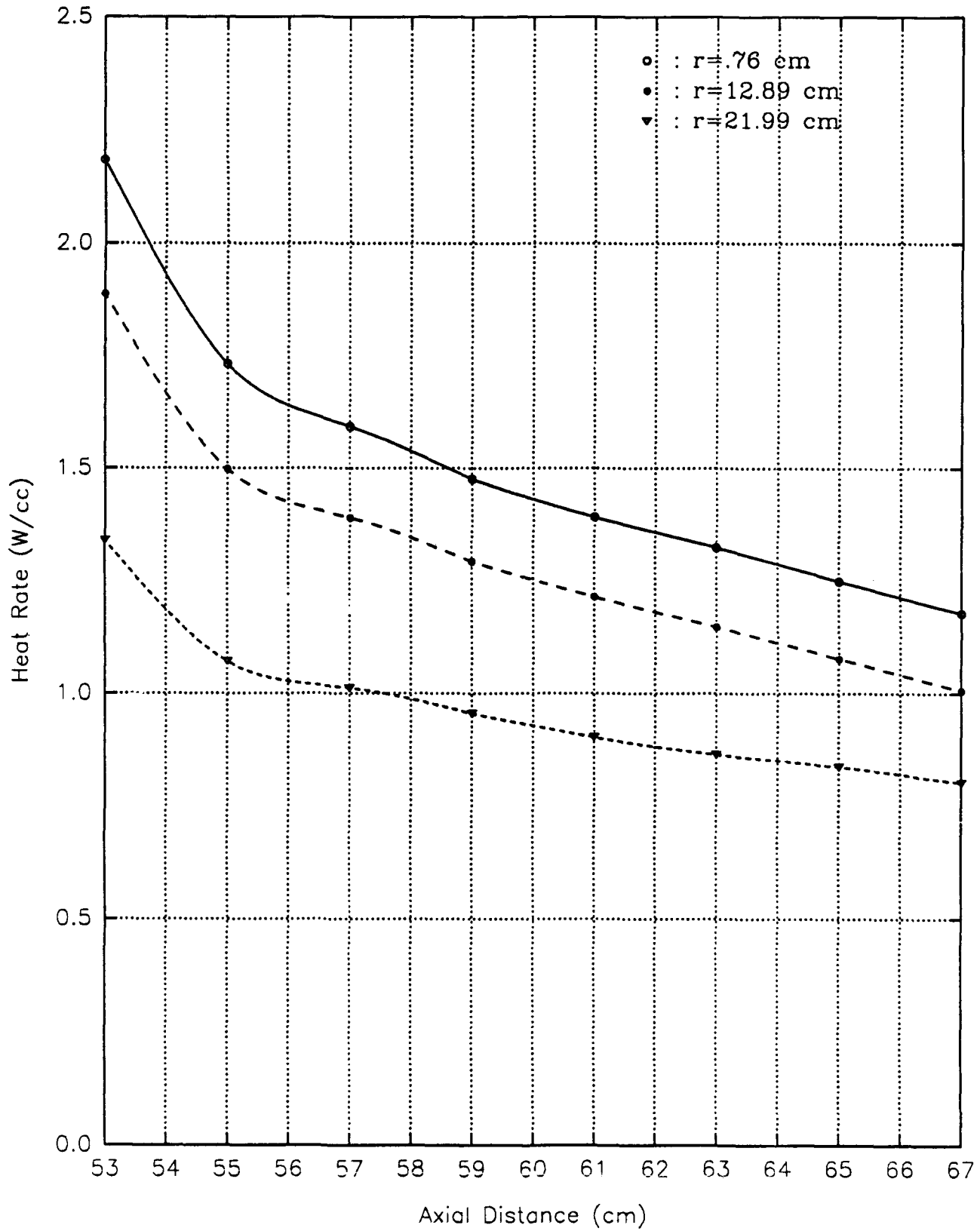
Graph #25

Hydrogen heating in the plenum region of a lithium hydride
moderated 400 MWt PBR with a lithium hydride/tungsten shield



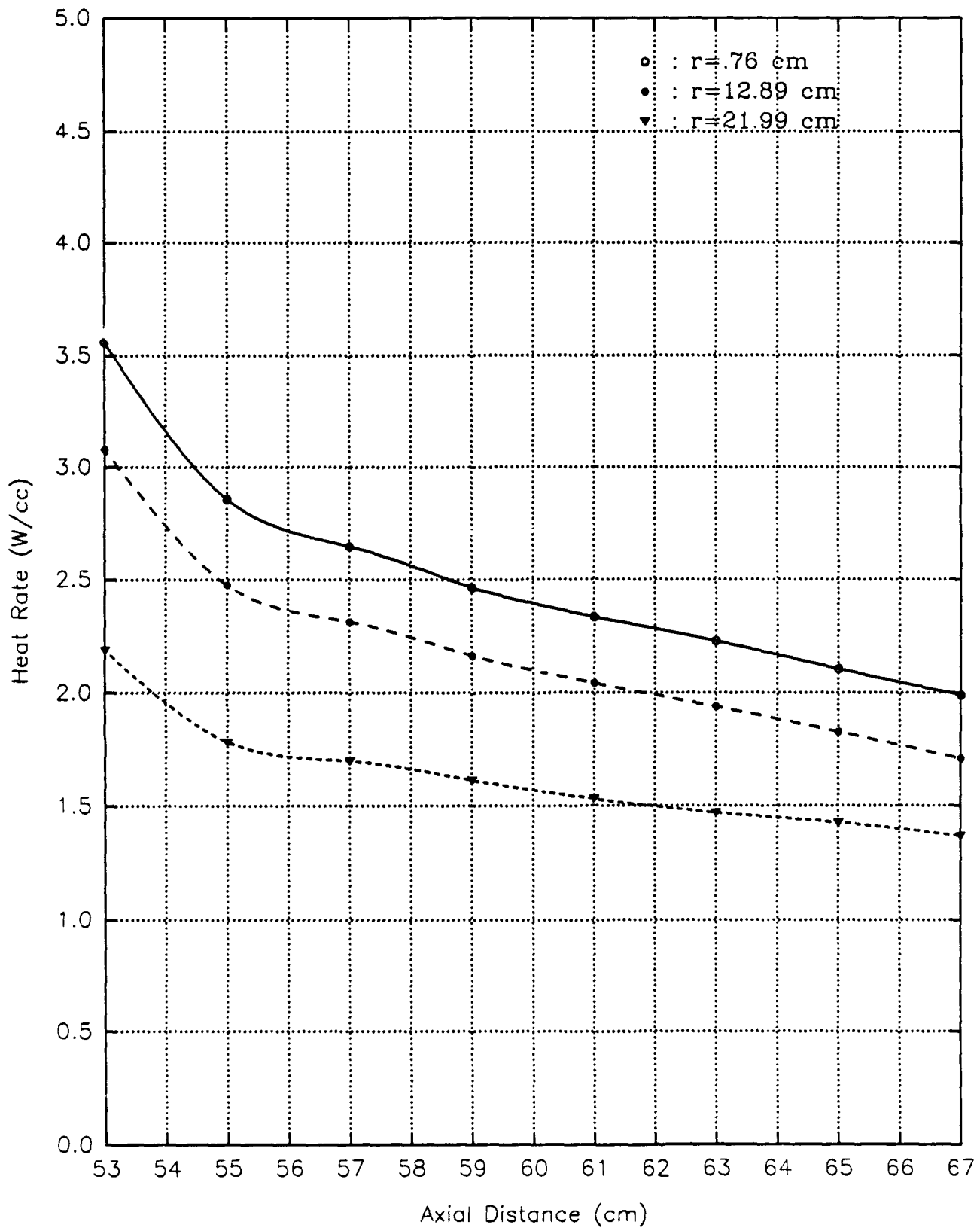
Graph #26

Carbon heating in the plenum region of a lithium hydride
moderated 400 MWt PBR with a lithium hydride/tungsten shield



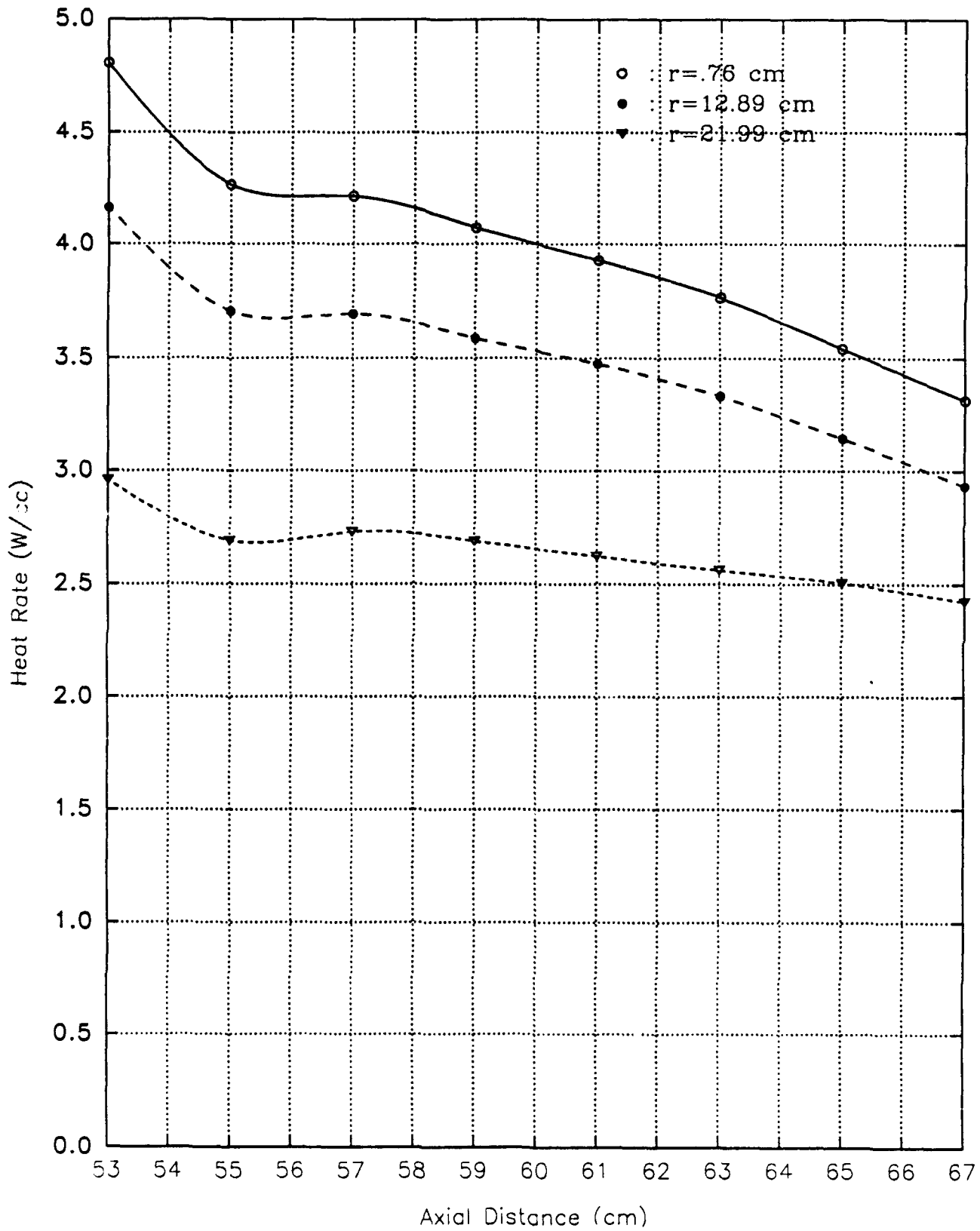
Graph #27

Aluminum heating in the plenum region of a lithium hydride
moderated 400 MWt PBR with a lithium hydride/tungsten shield



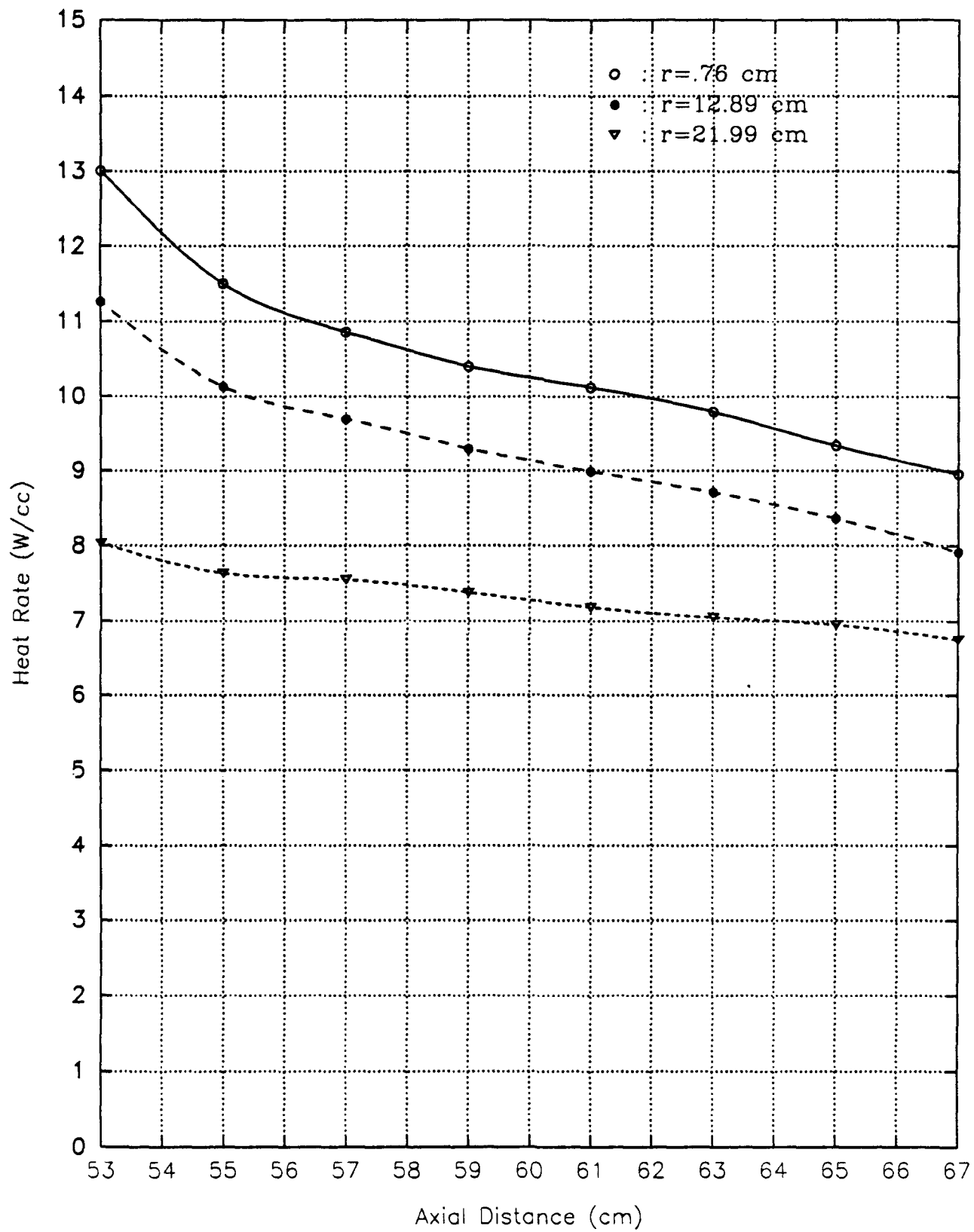
Graph #28

Titanium heating in the plenum region of a lithium hydride
moderated 400 MWt PBR with a lithium hydride/tungsten shield



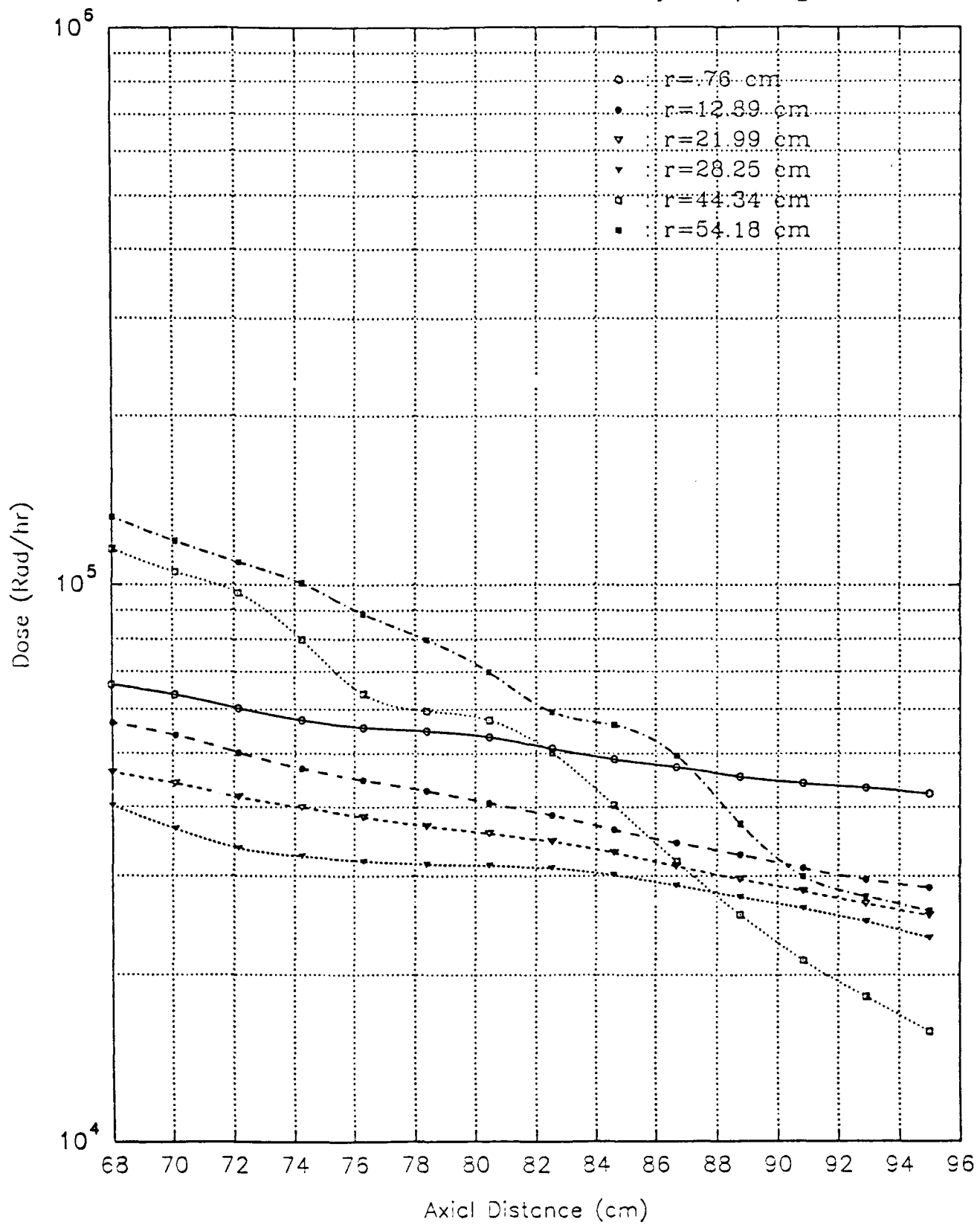
Graph #29

Stainless Steel heating in the plenum region of a lithium hydride
moderated 400 MWt PBR with a lithium hydride/tungsten shield



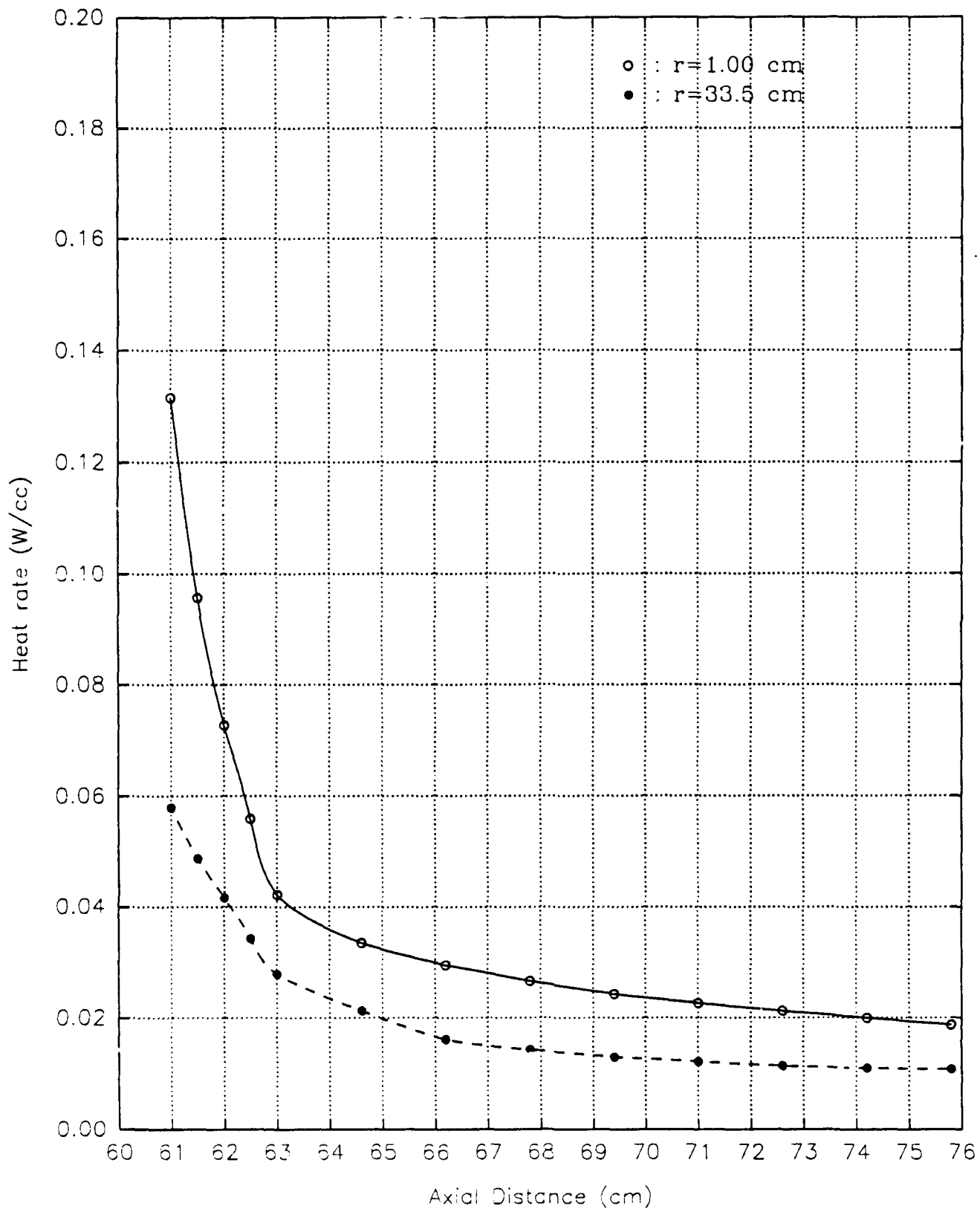
Graph #30

Silicon doses in the TPA/void region of a lithium hydride
moderated 400 MWt PBR with a lithium hydride/tungsten shield



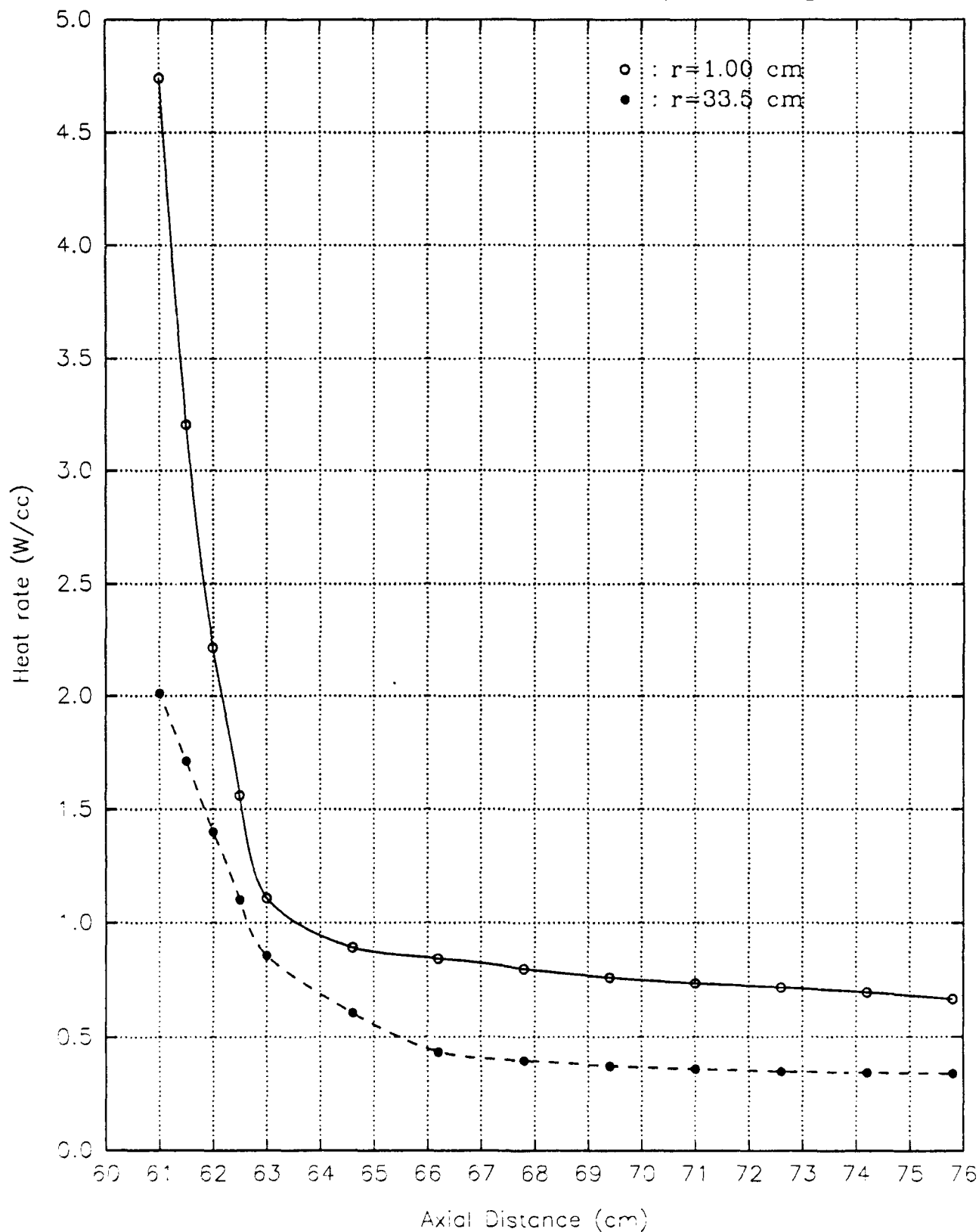
Graph #31

Hydrogen heating in the plenum region of a beryllium
moderated 400 MWt PBR with a lithium hydride/tungsten shield



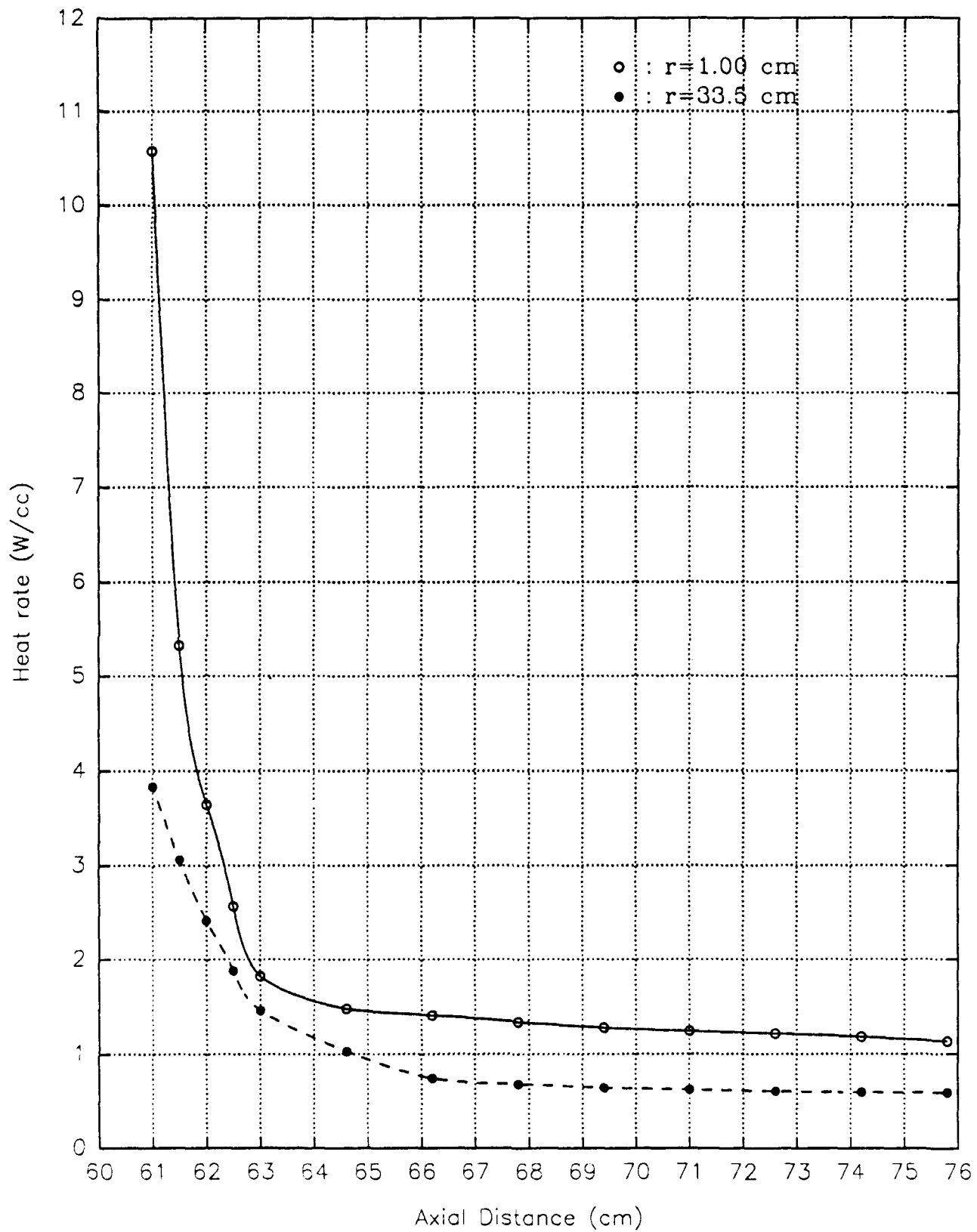
Graph #32

Carbon heating in the plenum region of a beryllium
moderated 400 MWt PBR with a lithium hydride/tungsten shield



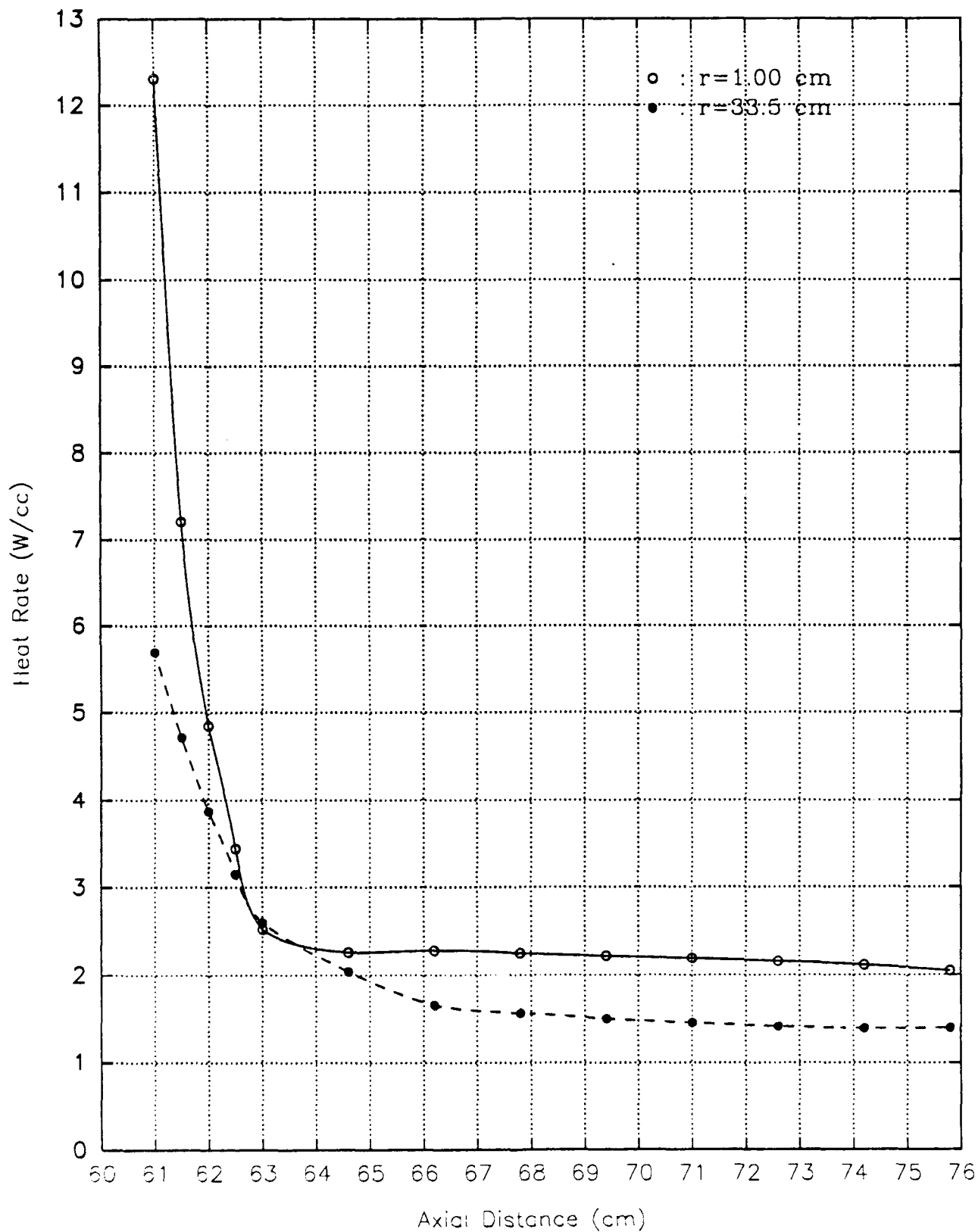
Graph #33

Aluminum heating in the plenum region of a beryllium
moderated 400 MWt PBR with a lithium hydride/tungsten shield



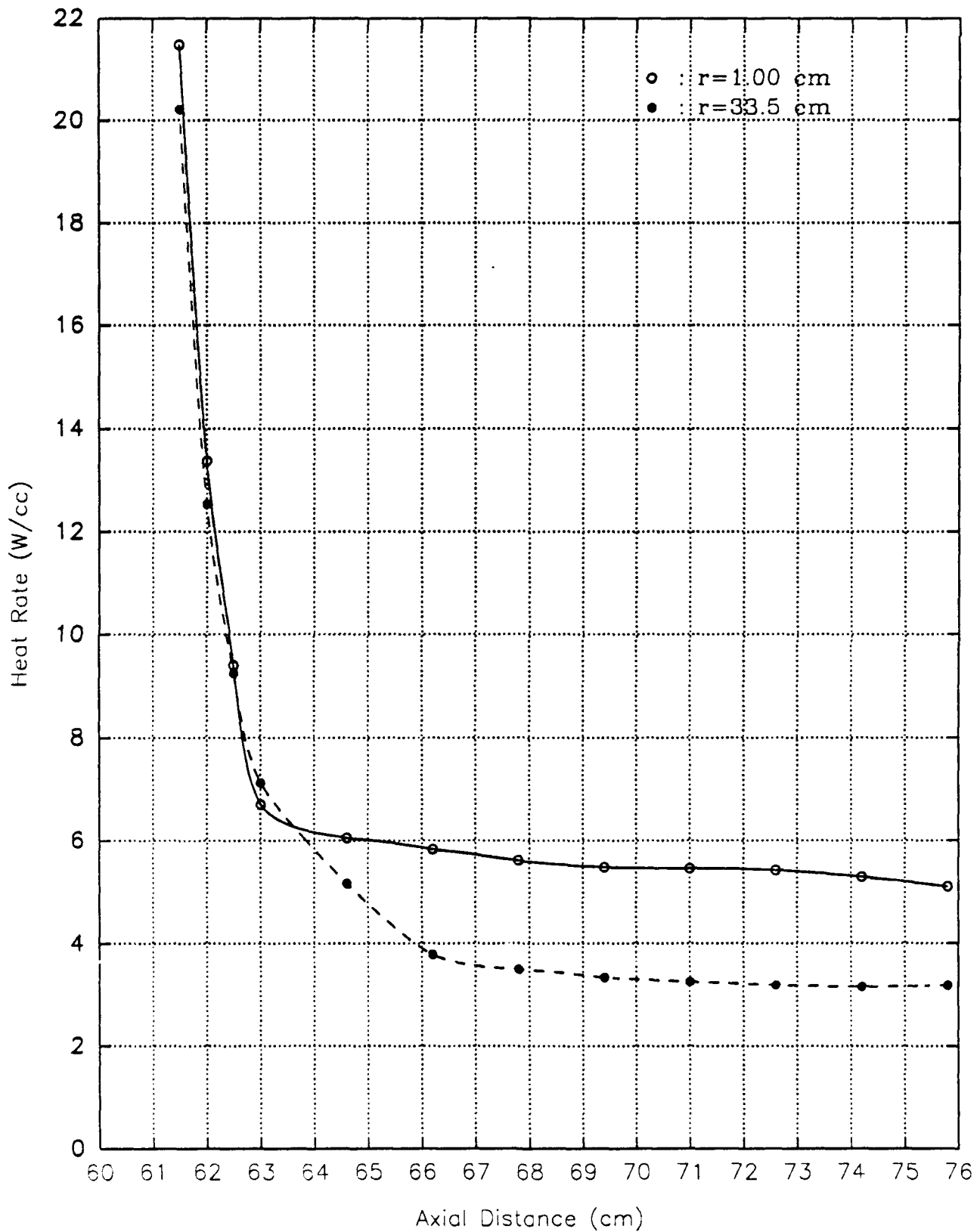
Graph #34

Titanium heating in the plenum region of a beryllium
moderated 400 MWt PBR with a lithium hydride/tungsten shield



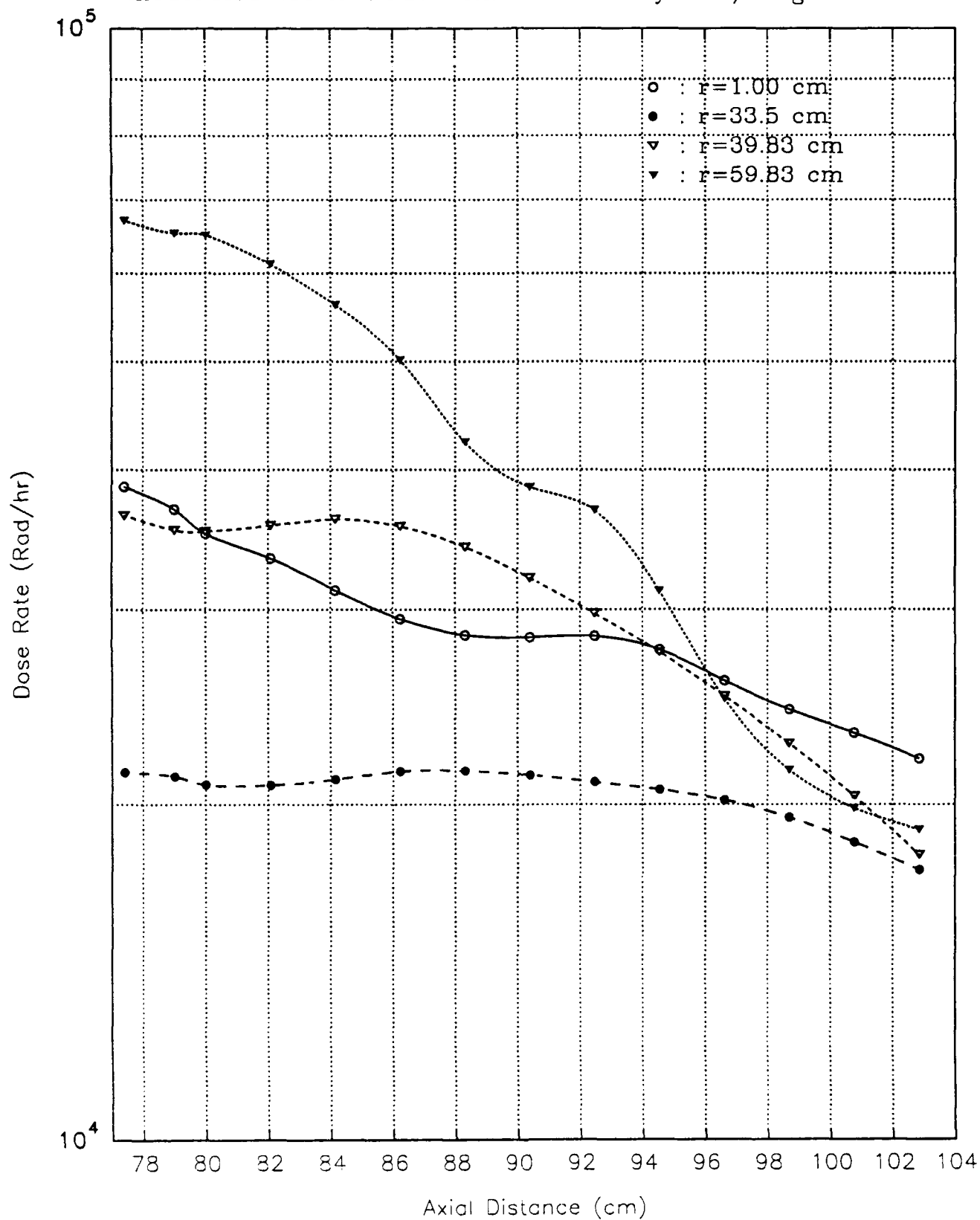
Graph #35

Stainless Steel heating in the plenum region of a beryllium
moderated 400 MWt PBR with a lithium hydride/tungsten shield



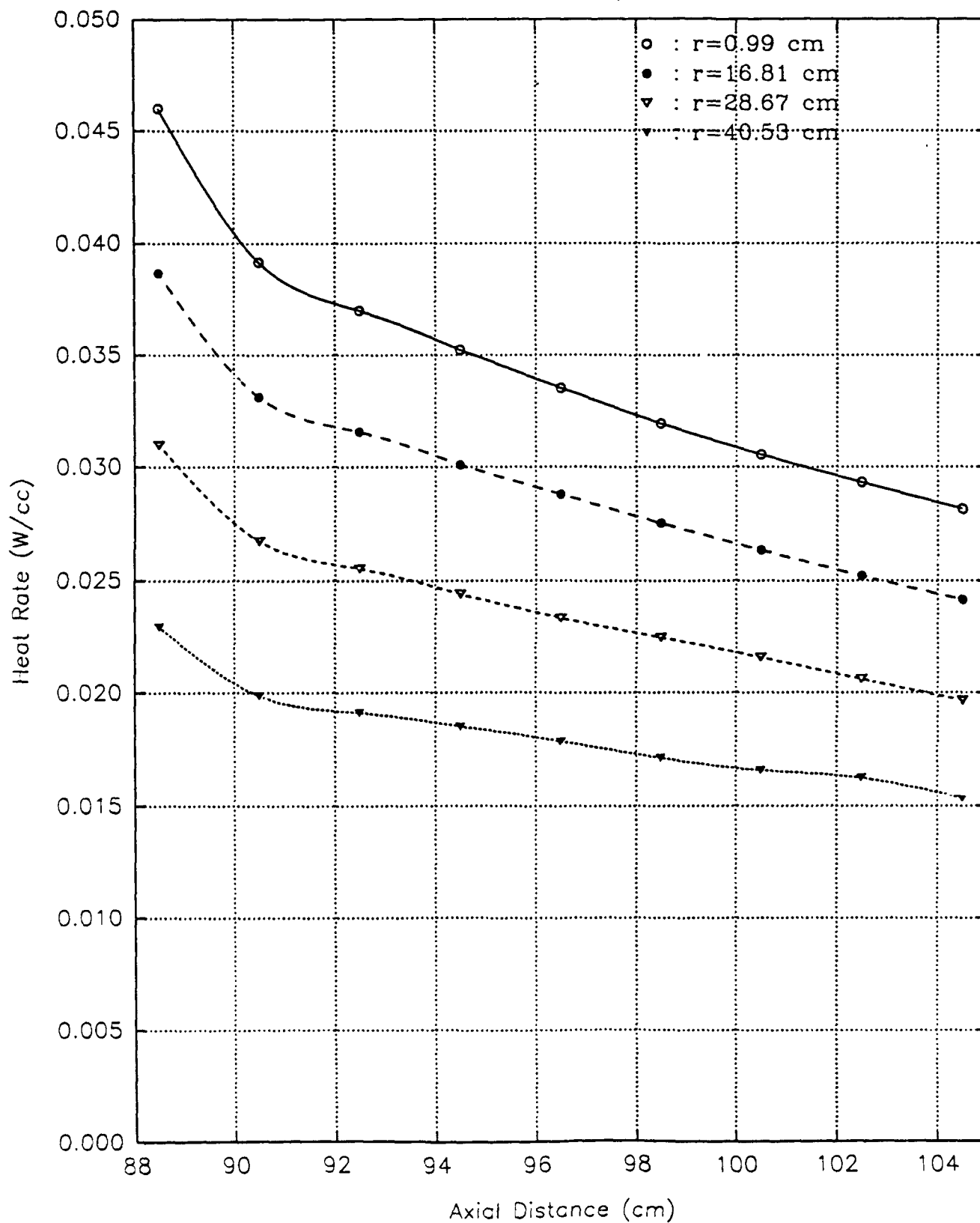
Graph #36

Silicon doses in the TPA/void region of a beryllium
moderated 400 MWt PBR with a lithium hydride/tungsten shield



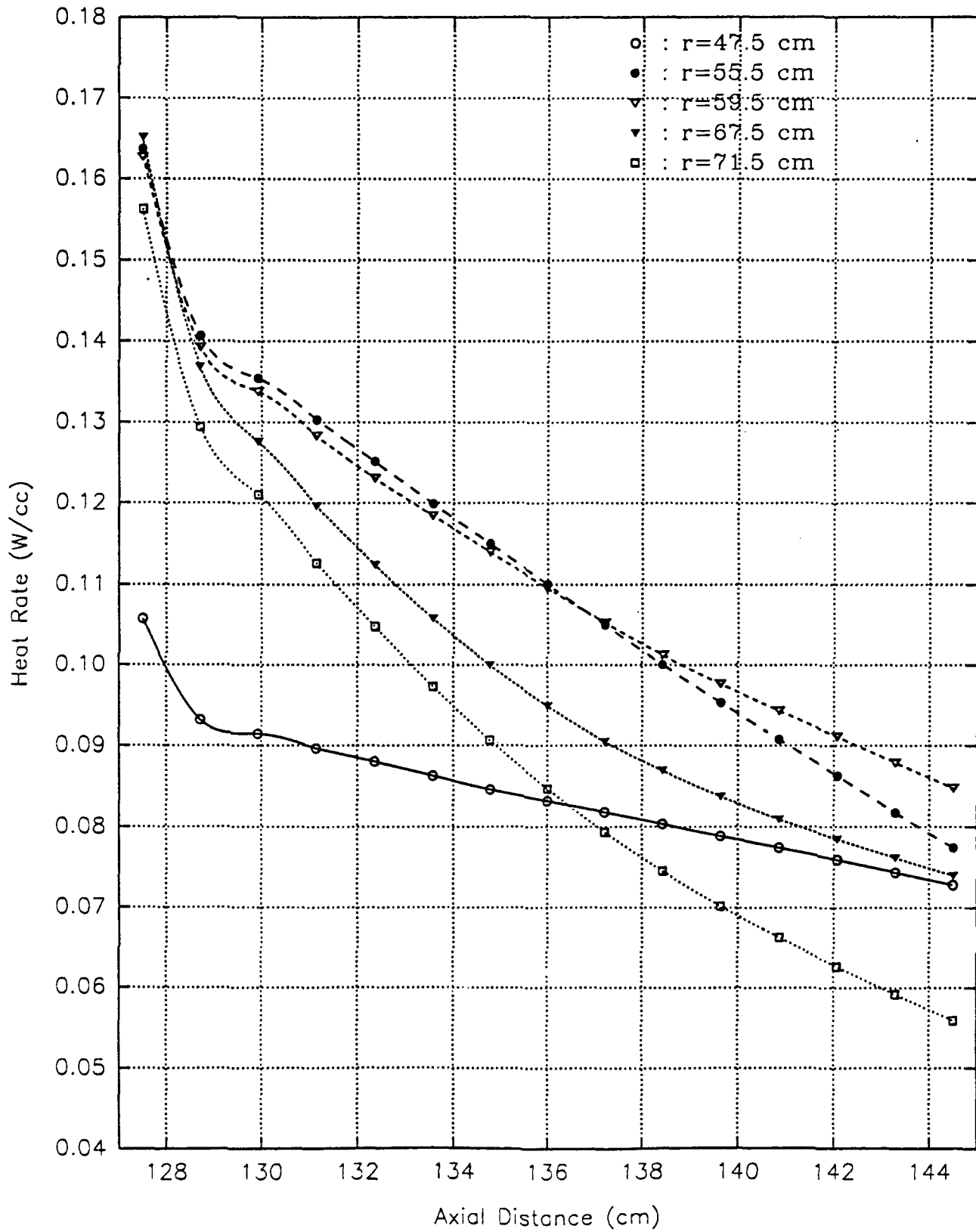
Graph #37

Hydrogen heating rates in the plenum region of a 2000 MW
PBR with a Beryllium moderated core and 35 cm LiH/2 cm W
on the reflector and 20 cm LiH/2 cm W on the vessel



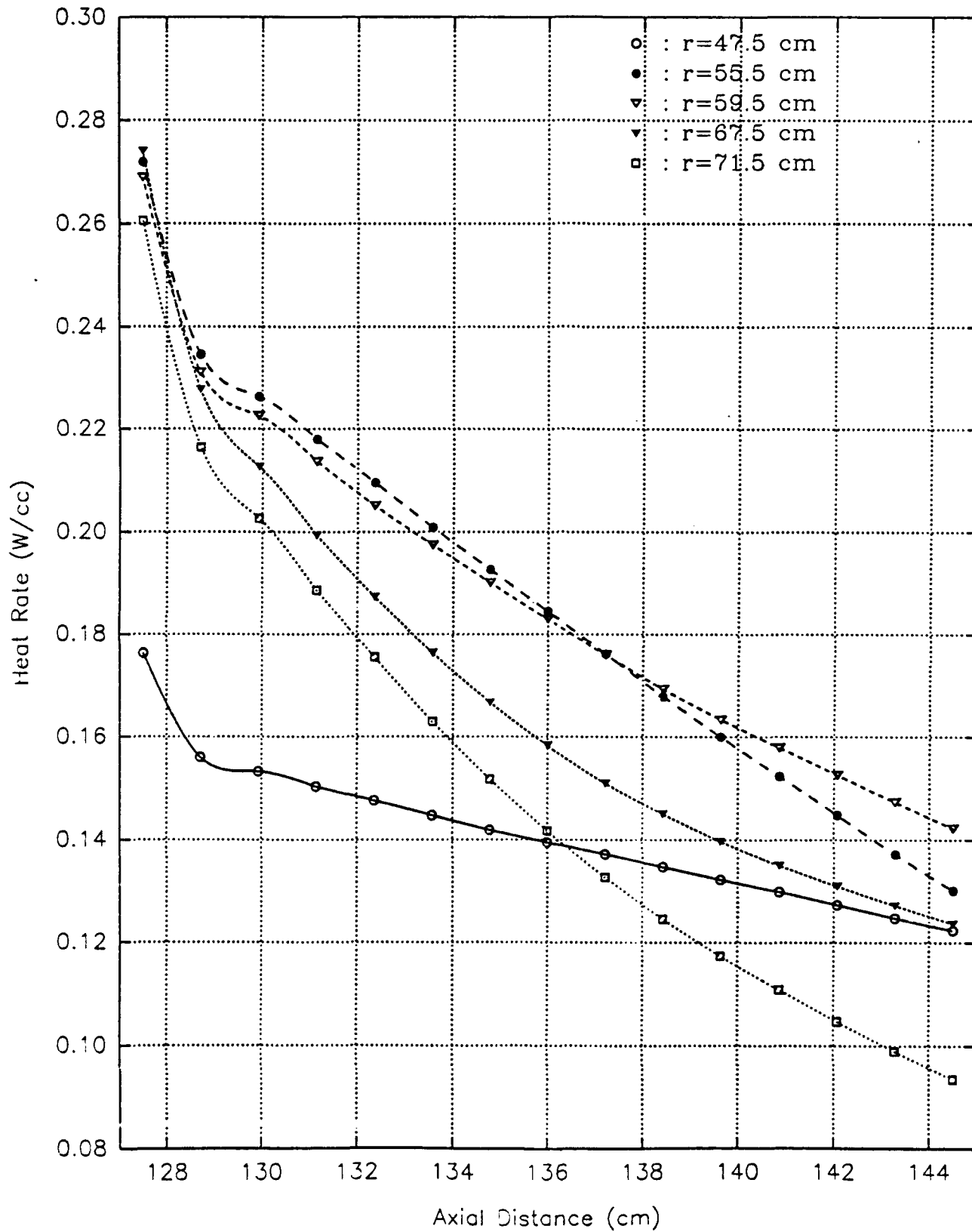
Graph #38

Carbon heating rates in the turbo-pump region of a 2000 MW
PBR with a Beryllium moderated core and 35 cm LiH/2 cm W
on the reflector and 20 cm LiH/2 cm W on the vessel



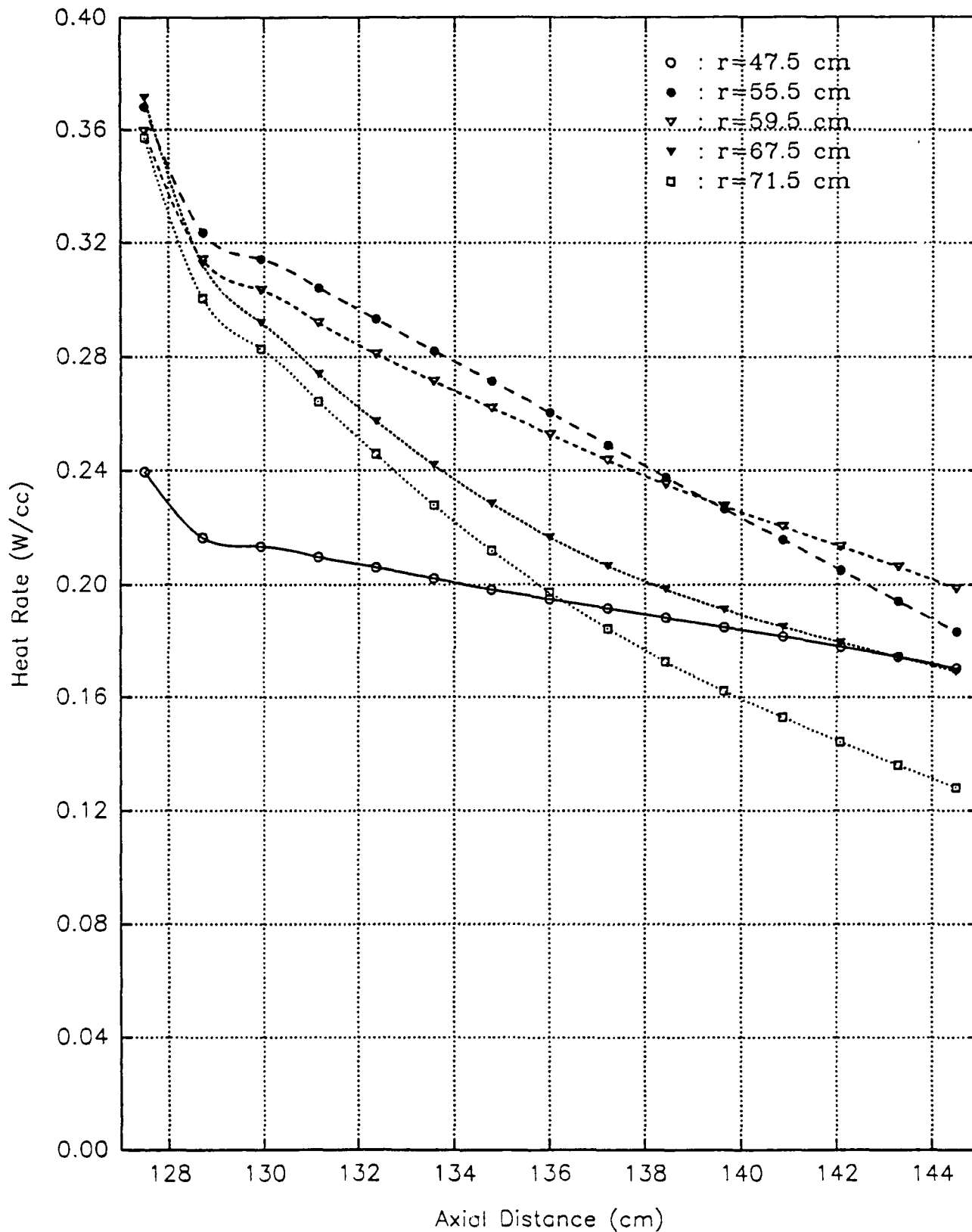
Graph #39

Aluminum heating rates in the turbo-pump region of a 2000 MW
PBR with a Beryllium moderated core and 35 cm LiH/2 cm W
on the reflector and 20 cm LiH/2 cm W on the vessel



Graph #40

Titanium heating rates in the turbo-pump region of a 2000 MW
PBR with a Beryllium moderated core and 35 cm LiH/2 cm W
on the reflector and 20 cm LiH/2 cm W on the vessel

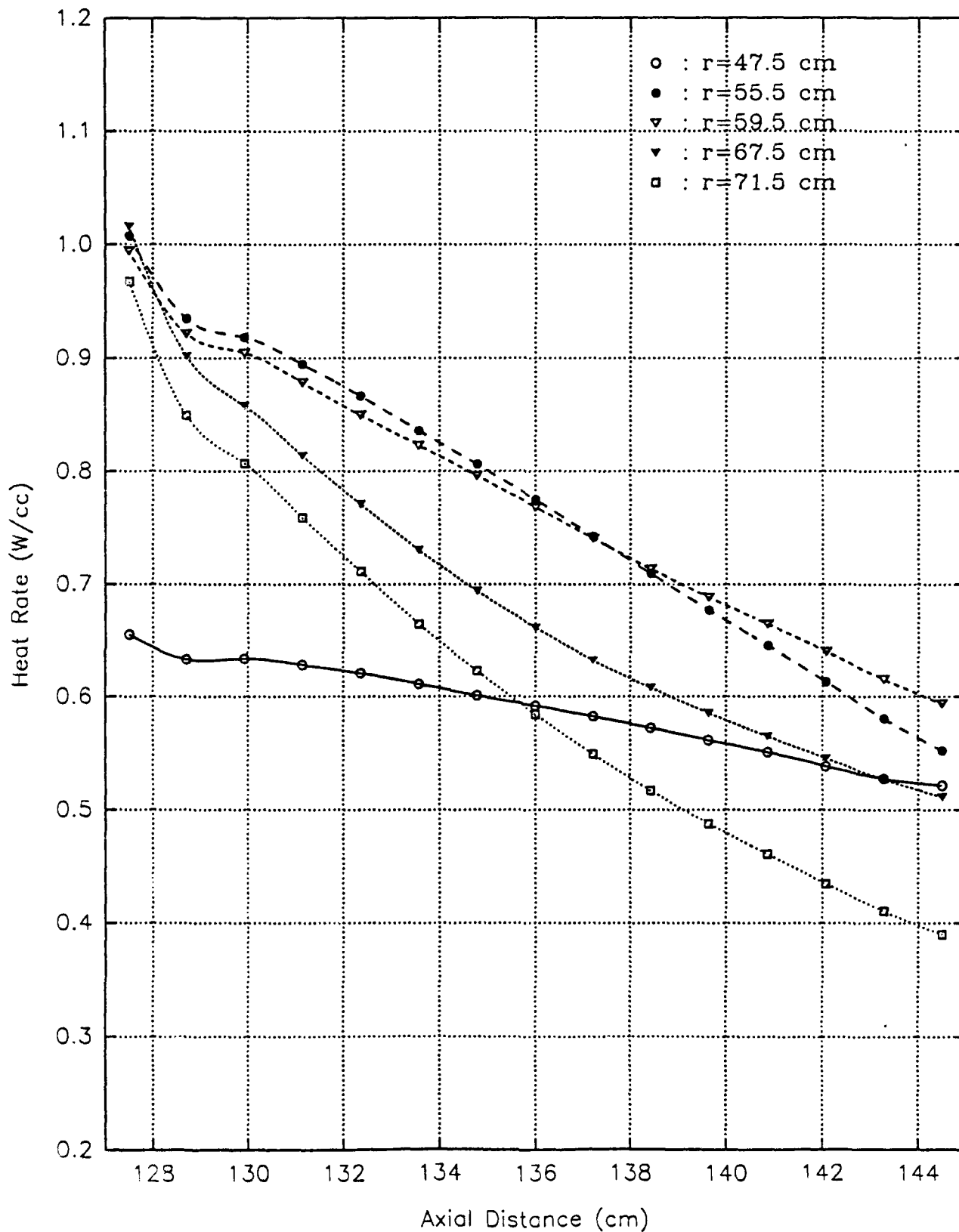


Graph #41

Stainless Steel heating rates in the turbo-pump region of a 2000 MW

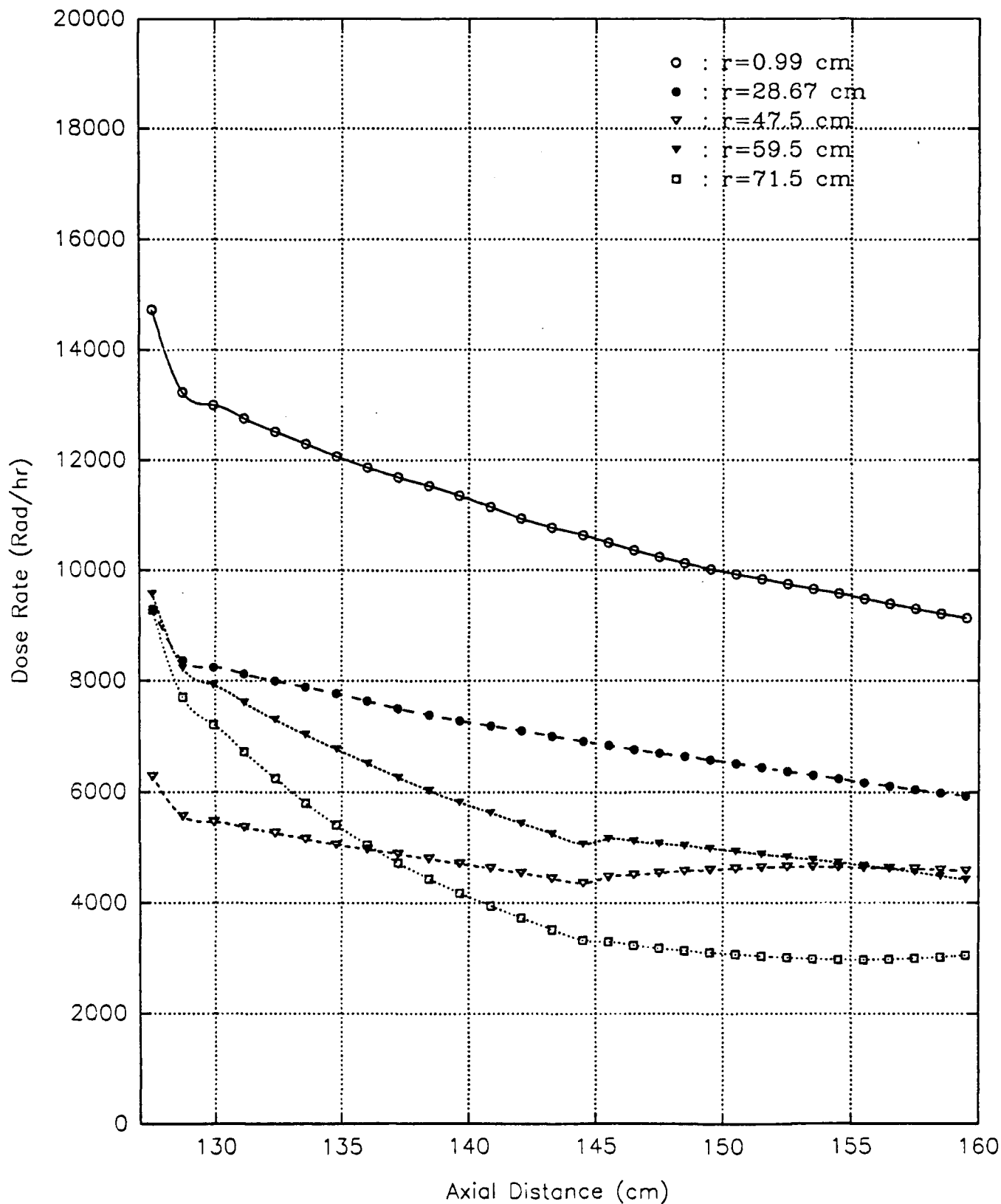
PBR with a Beryllium moderated core and 35 cm LiH/2 cm W

on the reflector and 20 cm LiH/2 cm W on the vessel



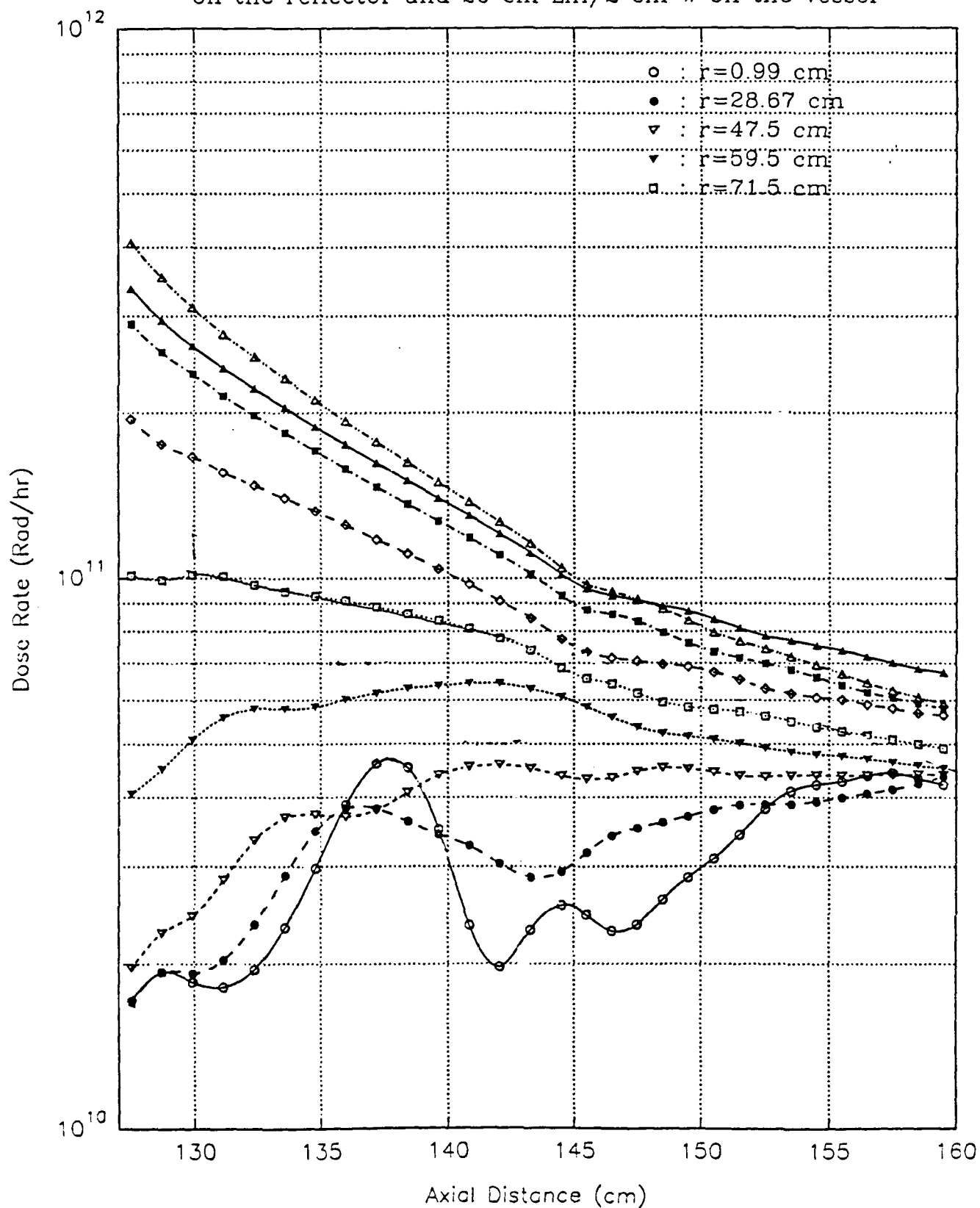
Graph #42

Silicon dose rates in the turbo-pump void region of a 2000 MW
PBR with a Beryllium moderated core and 35 cm LiH/2 cm W
on the reflector and 20 cm LiH/2 cm W on the vessel



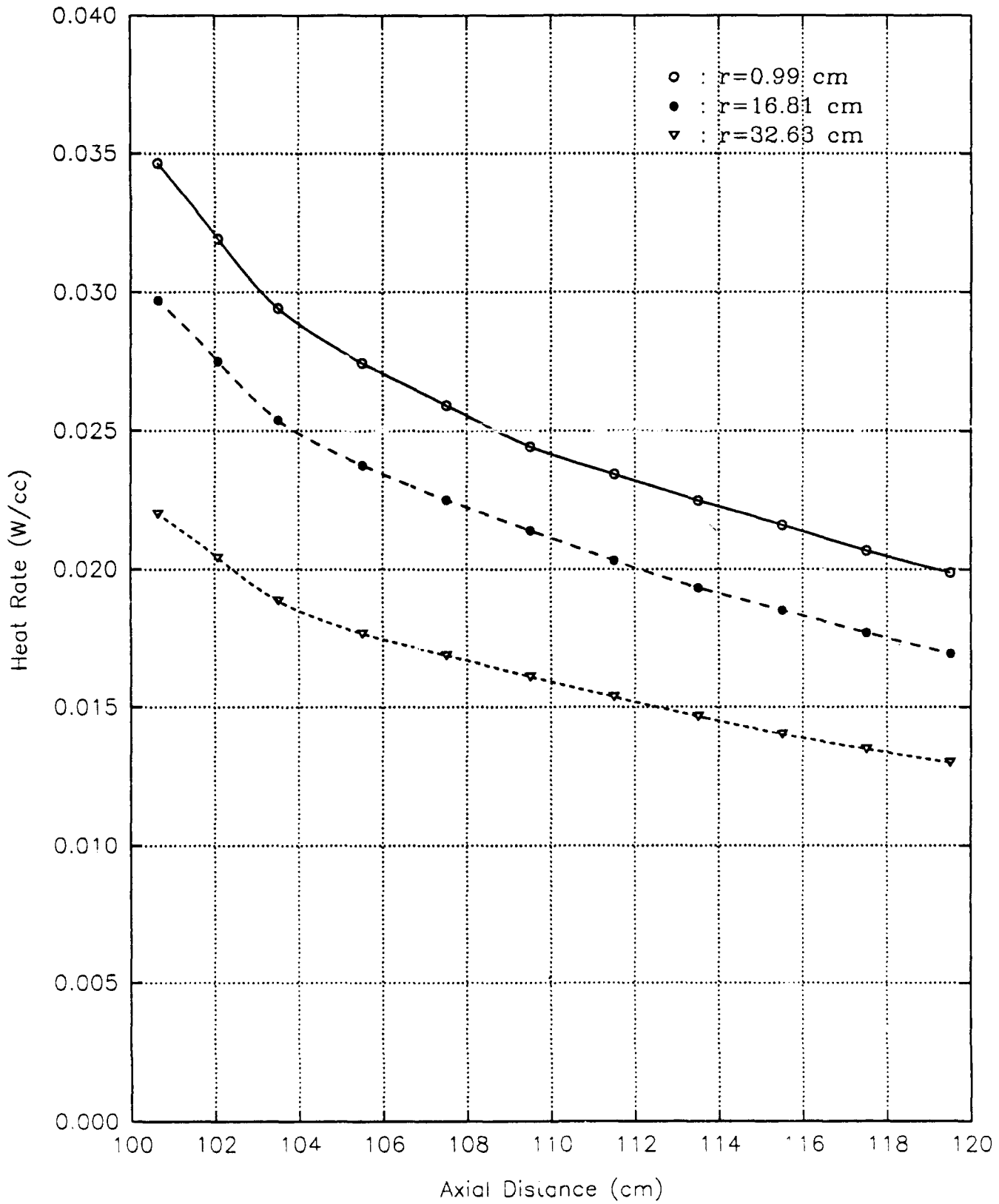
Graph #43

Fast neutron fluxes in the turbo-pump/void region of a 2000 MW
PBR with a Beryllium moderated core and 35 cm LiH/2 cm W
on the reflector and 20 cm LiH/2 cm W on the vessel



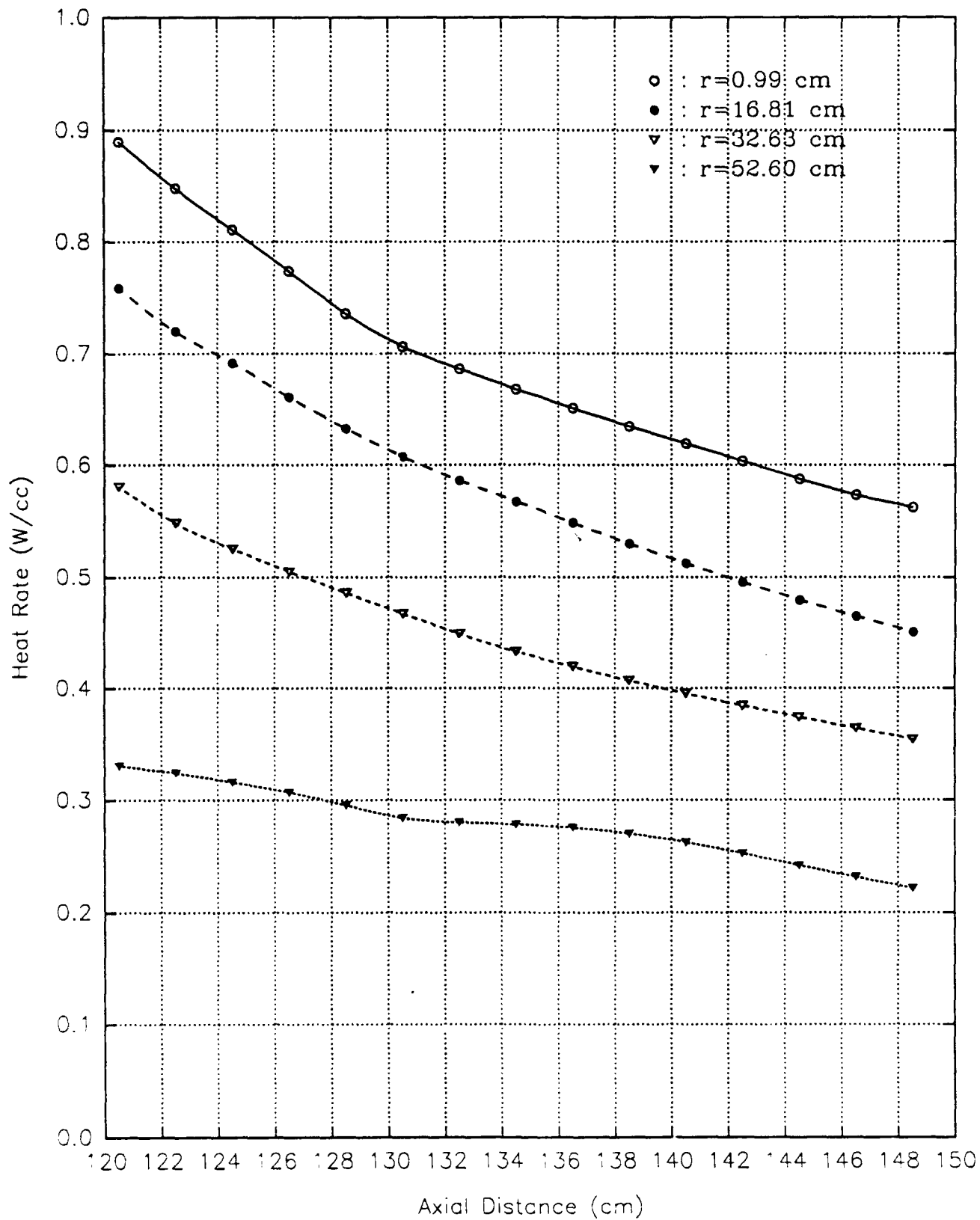
Graph #44

Hydrogen heating in the plenum region of a 2000 MWt
PBR with 50 cm LiH/2 cmW as an internal/collar shield



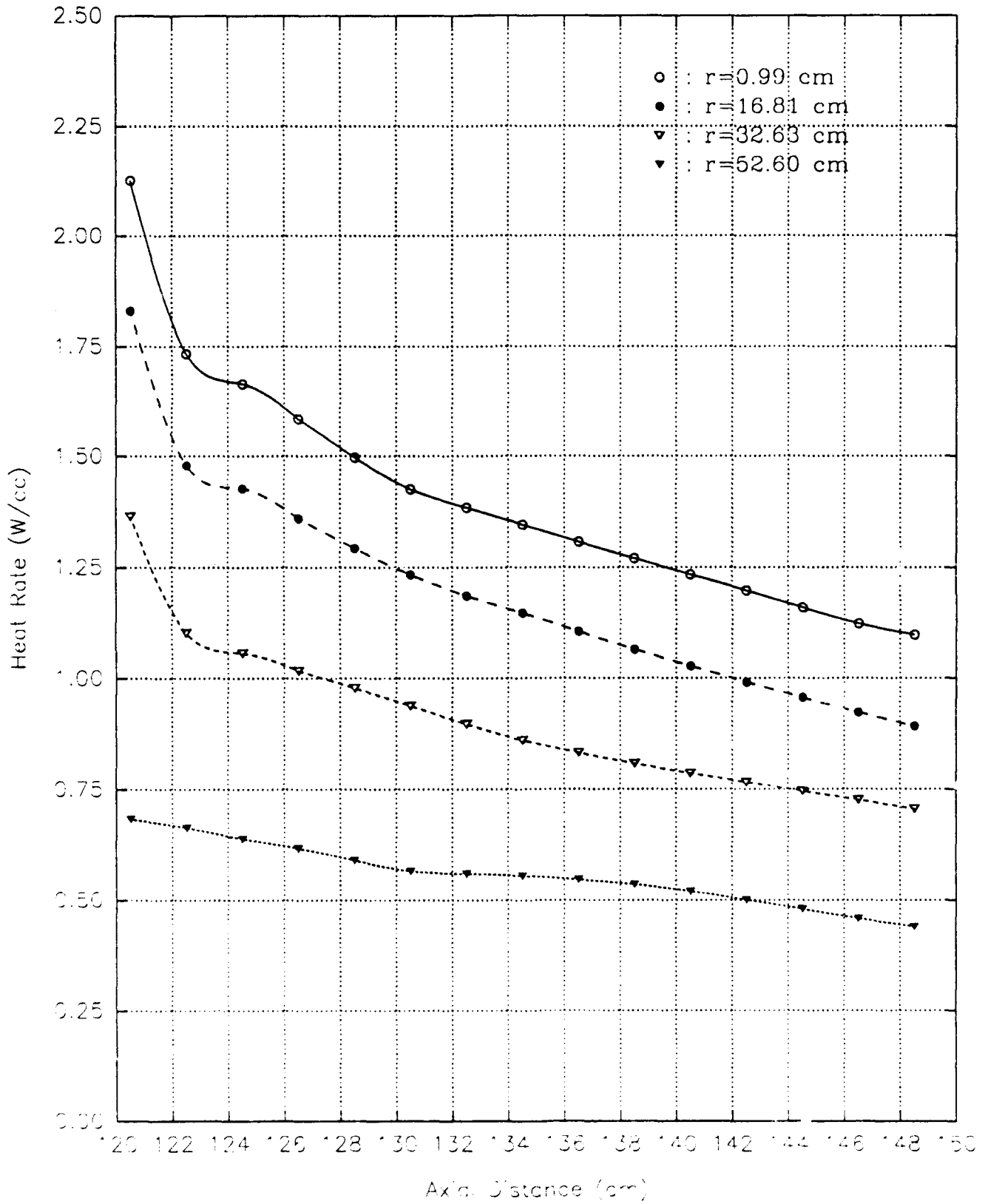
Graph #45

Carbon heating in the TPA/void region of a 2000 MWt
PBR with 50 cm LiH/2 cmW as an internal/collar shield



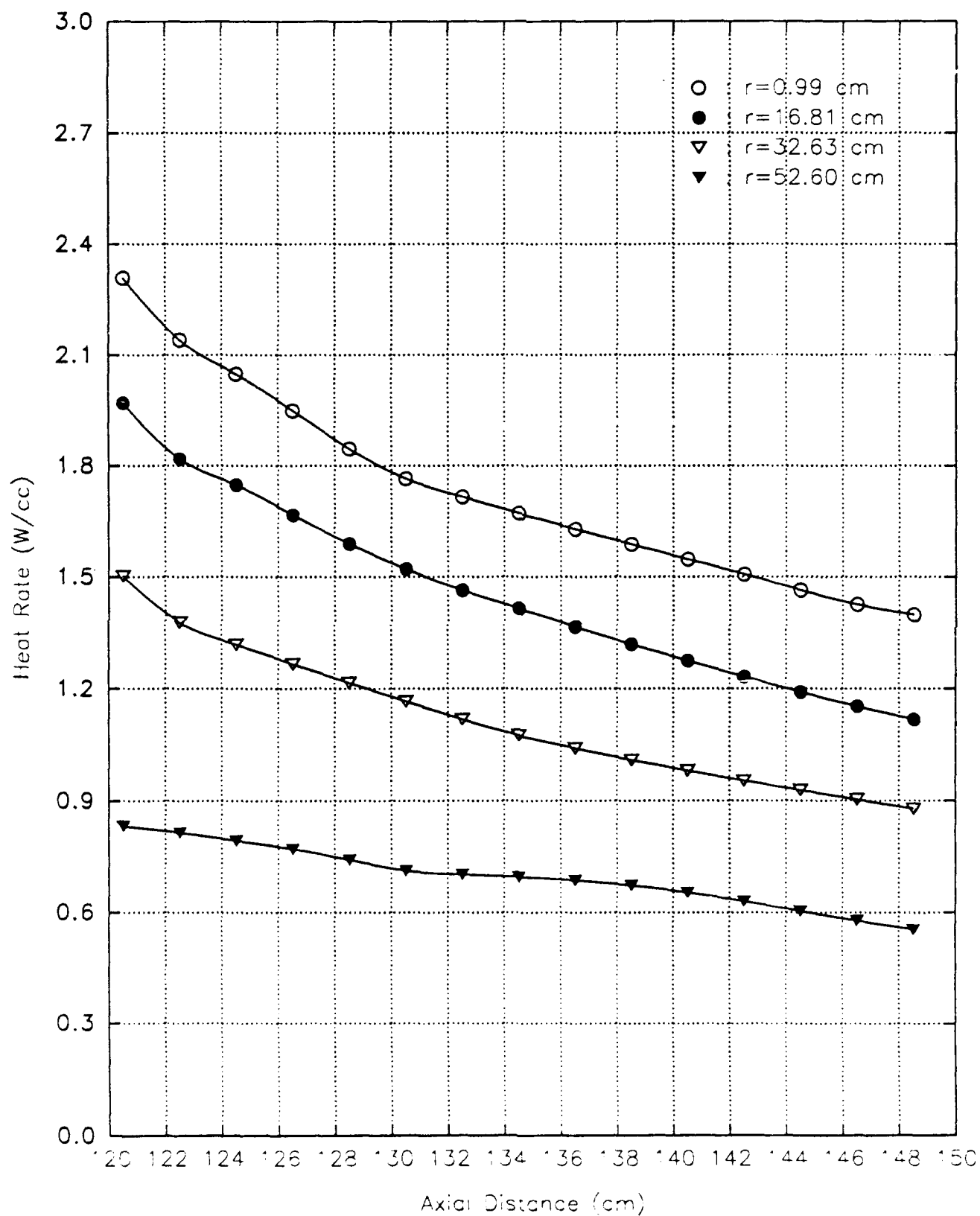
Graph #46

Aluminum heating in the TPA/void region of a 2000 MWt
PBR with 50 cm LiH/2 cmW as an internal/collar shield



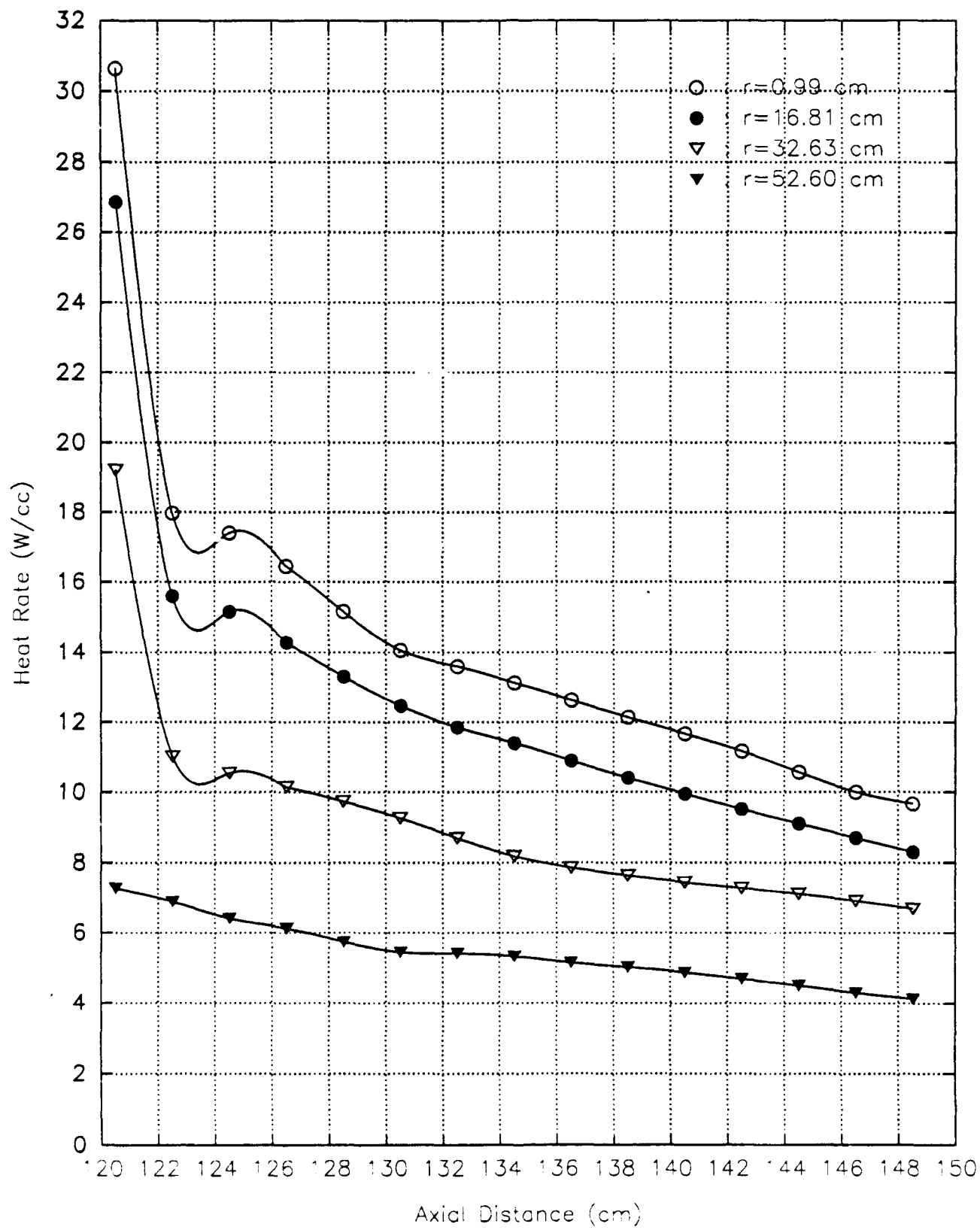
Graph #47

Titanium heating in the TPA/void region of a 2000 MWt
PBR with 50 cm LIH/2 cm W as an internal/collar shield



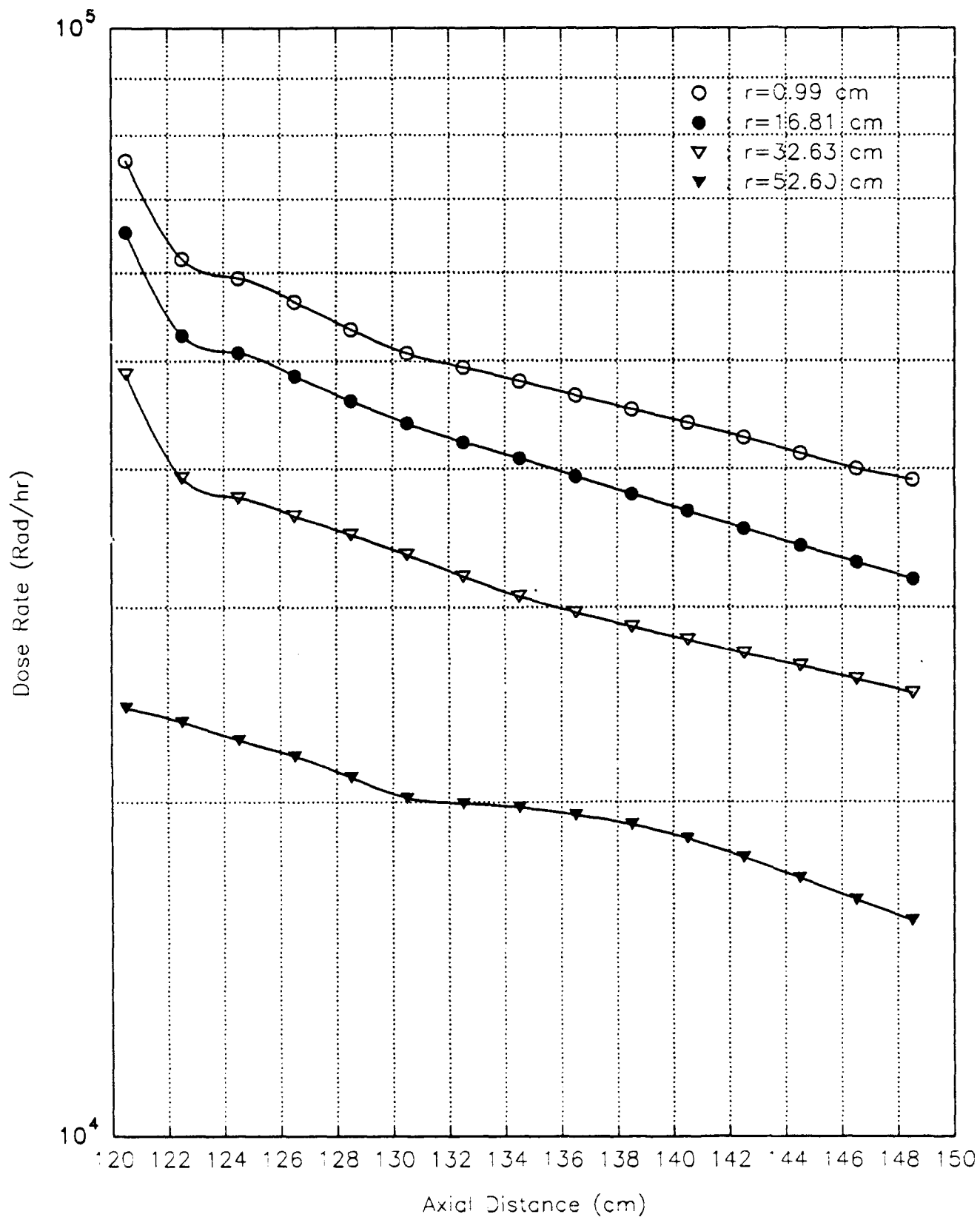
Graph #48

Stainless Steel heating in the TPA/void region of a 2000 MWt
PBR with 50 cm LIH/2 cm W as an internal/collar shield



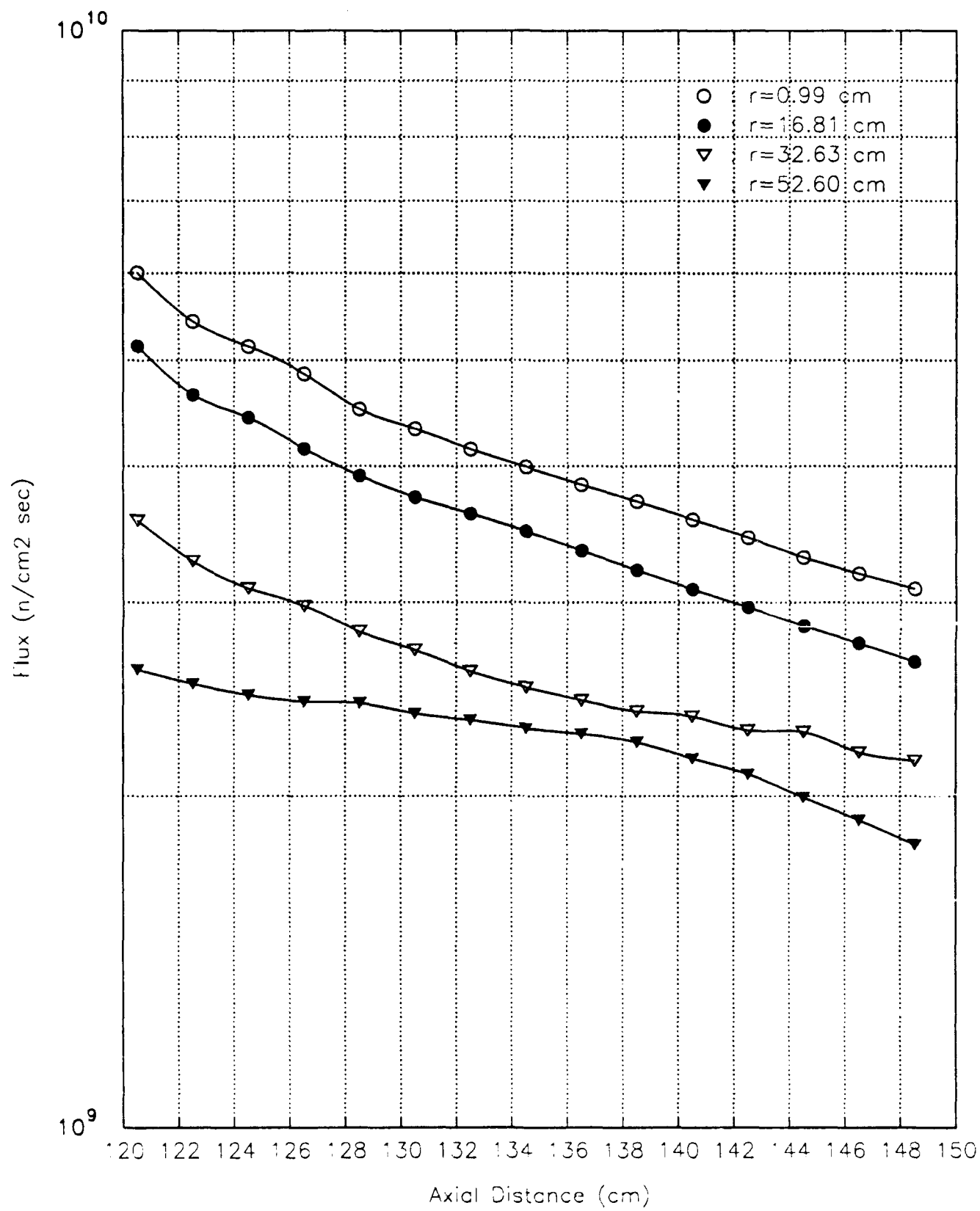
Graph #49

Silicon dose rates in the TPA/void region of a 2000 MWt
PBR with 50 cm LIH/2 cm W as an internal/collar shield



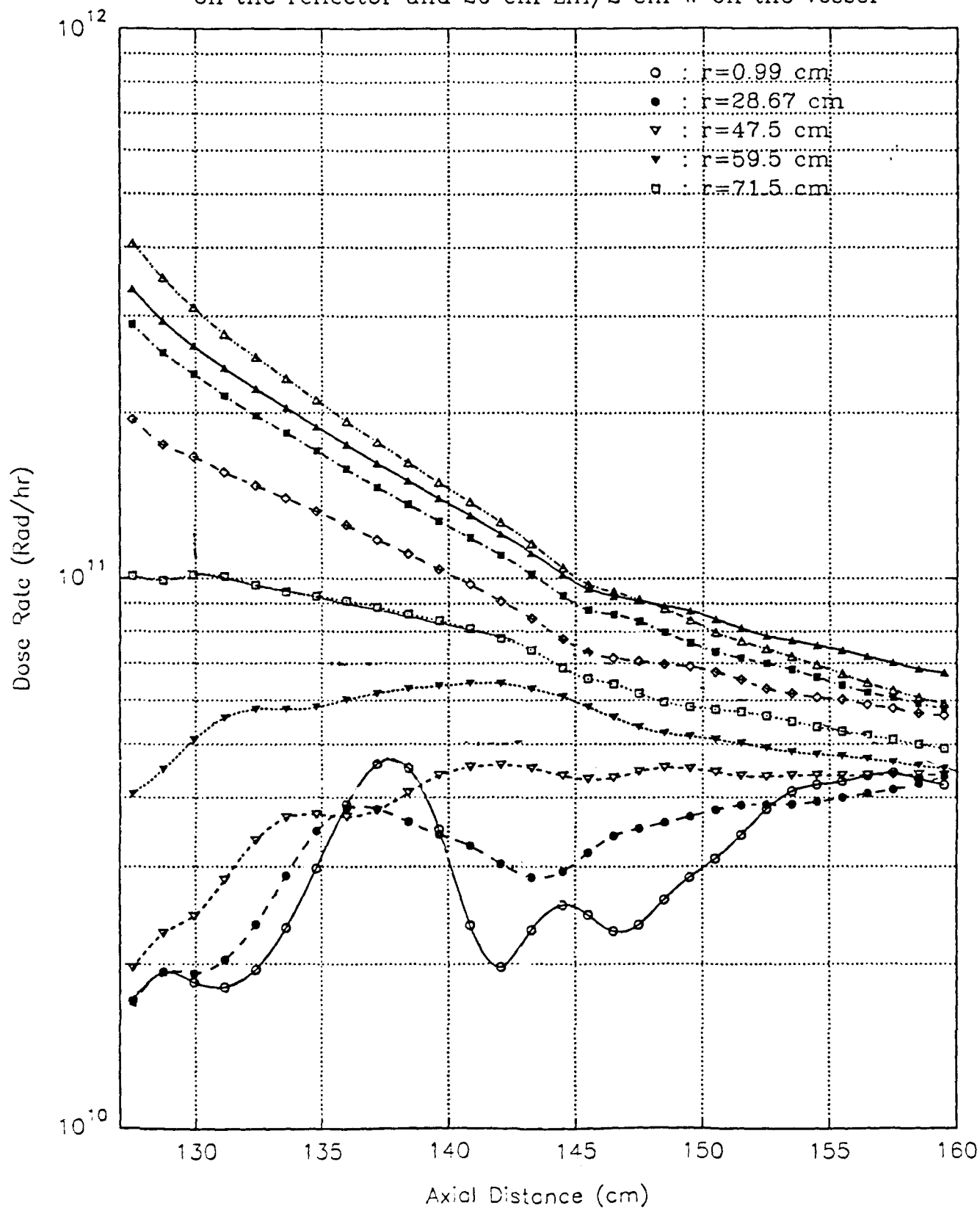
Graph #50

Fast neutron fluxes in the TPA/void region of a 2000 MWt
PBR with 50 cm LIH/2 cm W as an internal/collar shield



Graph #51

Fast neutron fluxes in the turbo-pump/void region of a 2000 MW
PBR with a Beryllium moderated core and 35 cm LiH/2 cm W
on the reflector and 20 cm LiH/2 cm W on the vessel



Graph #52